



Modeling performance of elite cyclists.

The effect of training on performance.

R. Rozendaal

Modeling performance of elite cyclists

The effect of training on performance.

by

R. Rozendaal

to obtain the degree of Master of Science
at the Delft University of Technology,
to be defended publicly on Wednesday November 1st, 2017 at 10:00 AM.

Student number: 4094255
Project duration: February 6, 2017 – November 1, 2017
Thesis committee: Prof. dr. ir. G. Jongbloed, TU Delft, supervisor
Dr. J. L. A. Dubbeldam, TU Delft
Dr. A. J. Cabo, TU Delft
T. van Erp, Msc, Team Sunweb

This thesis is confidential and cannot be made public until November 1, 2017.

An electronic version of this thesis is available at <http://repository.tudelft.nl/>.



Abstract

Both coaches and cyclists nowadays determine the training schedules for important races based on experience and gut-feeling. Data are available for the evaluation of training schedules, but a sound scientific method of accomplishing this does not yet exist. The biggest hurdle in developing such a method for cycling is the absence of an objective performance metric. This report uses the data of six cyclists in order to introduce and analyze a new performance metric: the cycled critical power. Subsequently, this metric is used to fit the parameters of the Fitness-Fatigue model; a model that is successfully applied in other sports to model the performance of an athlete. Several training attributes are included in the analysis, such as duration, intensity, and load; with which the performance of the cyclists is modeled. The model, applied to the data, leads to correlations for the six cyclists with R^2 -values within the range of 0.13 – 0.56. Compared to other scientific research, this range indicates that the Fitness-Fatigue model could be a valuable tool for elite cyclists and coaches when constructing their training schedules, but further research into the performance metric and the application of the Fitness-Fatigue model is still required.

Preface

Dear reader,

In front of you lies the result of a challenging and fruitful period that marks the end of my time as a student. The report has been written to fulfill the graduation requirements of the master Applied Mathematics at the Delft University of Technology and has kept me engaged from February until November 2017. The research is primarily concerned with applying several analytical models to real data and extending these models theoretically.

It all started more or less one year ago, somewhere far, far, away; Pisa in Italy to be exactly. I had contacted Geurt expressing the wish of graduating in sport analytics. In a Skype-meeting we quickly discussed the possibilities at Team Sunweb. Some weeks later, in another Skype-meeting, Teun proposed several data-related projects from which we decided to choose the one about optimizing training schedules.

The past nine months have been interesting, I was given room to pursue my own interests and construct my own time schedule. This required some self discipline, but the bi-weekly meetings with both Teun and Geurt were a useful big stick. In the beginning I did have a hard time to see where things were going, but in the end everything luckily fell into place.

Some words to express my gratitude are appropriate here, first of all for Geurt. Thank you for always being available for questions and coming up with a lot of ideas to improve my thesis. Sometimes there were too many of them, but you always gave me the freedom to choose which of them I wanted to pursue and which of them I left behind. Furthermore, your enthusiasm is contagious and was very helpful in motivating me.

I would also like to take some time to thank Teun, my daily supervisor from Team Sunweb. Our bi-weekly Skype meetings were always something to look forward to and every time it was exciting to see whether you would show up on time. I really appreciated your interest in my research. Although you did not always understand exactly what I was doing, you were very enthusiastic about the practical applications and could not wait to start using my algorithms. This gave me the feeling that my effort was being appreciated from a practical perspective as well. Furthermore, I am very grateful for the kick-start that you gave my project. The fact that the data were already clean and consistent and that you provided me all the appropriate literature from the start, really made my life so much easier.

Thanks as well to the two other members of my committee, Dr. A.J. Cabo and Dr. J.L.A. Dubbeldam for taking the time to read my report and attend the presentation.

Some last words of thanks are to my family; who made this all possible by supporting me through every step of life, my house-mates; who were there to get me through the last nine months, my room-mates at EWI; who unfortunately all left me during the course of my thesis; and everybody that made my student life the amazing, fantastic, and enlightening period that it was; you know who you are! Special thanks with regards to this report go out to Willem, Harry, Bart, Pim, and Joost, who took the time and effort to go through my report in search for errors and uncertainties.

With these last words, an era has ended, but new adventures are coming! I wish you a lot of fun reading my report.

*R. Rozendaal
Delft, October 2017*

Contents

1	Introduction	1
1.1	Context	1
1.2	Research goal	1
1.3	Outline	2
2	Background information	3
2.1	Team Sunweb	3
2.2	Energy supply systems	3
2.3	The power meter	4
2.4	Framework of Allen and Coggan	4
3	Data	7
3.1	Daily power meter data	8
3.2	Illustrations	8
3.2.1	Time trial - Cyclist 2	8
3.2.2	Climbing stage - Cyclist 3	8
3.2.3	Sprint - Cyclist 6	9
3.3	Summarized power meter data	10
3.4	Subjective data	10
4	Estimating critical power and anaerobic work capacity	13
4.1	Mathematical models	13
4.2	Data acquisition	16
4.2.1	Protocols	16
4.2.2	Extracting information from daily power meter data	17
4.3	Estimation	21
4.3.1	Measurement error	21
4.3.2	Linear-TW model	21
4.3.3	Curvilinear-P model	23
4.3.4	Relationship-CP model for a single cyclist	23
4.3.5	Relationship-CP model on multiple cyclists	25
4.4	Results	26
4.4.1	CP	26
4.4.2	W'	27
4.4.3	Trade-off	27
4.5	Accuracy of the estimators	28
4.6	Conclusion	28
5	Modeling the anaerobic work supply	29
5.1	Introduction	29
5.2	Mathematical assumptions and model derivation	29
5.3	Current model	30
5.4	Mismatch between assumptions and model	31
5.5	Proposed model	33
5.6	Model validation	35
5.7	Conclusion	36

6	Cycled critical power	37
6.1	Mathematical definition	37
6.1.1	Monotonicity and continuity of $f(CP)$	38
6.1.2	Specific model for $W'_{\text{bal}}(t)$	38
6.1.3	Visual example.	39
6.2	Dynamics of the cycled critical power.	39
6.3	Possible causes of volatility	40
6.4	Sensitivity analysis	40
6.5	Main cause for volatility.	42
6.6	Exercise intensity	42
6.7	Smoothing the cycled critical power	43
6.7.1	Local maxima	43
6.7.2	Curve fitting	44
6.8	Conclusion	45
7	Modeling performance	51
7.1	The fitness-fatigue model.	51
7.1.1	Interpretation of kernel parameters	53
7.2	Estimating the training parameters	54
7.2.1	Goodness of fit.	54
7.2.2	Relative training parameters	54
7.2.3	Kernel parameters	55
7.3	Implementation	55
7.3.1	Step by step analysis of training parameter estimation.	55
7.4	Results	55
7.4.1	The first step - Best predictor	56
7.4.2	The second step - Impact over time	56
7.4.3	The third step - Attribute selection.	58
7.4.4	The fourth step - Estimating both parameter sets simultaneously.	59
7.4.5	Fourth step for all cyclists	59
7.5	Conclusion	60
8	Conclusion and future work	61
8.1	Conclusion	61
8.2	Future research	62
8.2.1	Improving the CCP.	62
8.2.2	Improving the Fitness-Fatigue model	62
A	Proofs of lemmas and theorem of chapter 6.	65
A.1	Proof of Lemma 6.1	65
A.2	Proof of Lemma 6.2	66
A.3	Proof of Lemma 6.3	66
A.4	Proof of Theorem 6.1	67
B	Behaviour of LASSO-parameters.	69
C	Figures of final model.	71

Abbreviations and symbols

Table 1: List of Abbreviations

AP	Average power
AWC	Anaerobic work capacity
CP	Critical power
CCP	Cycled critical power
FTP	Functional threshold power
IF	Intensity factor
kJ	kilojoules
NLS	Non-linear least squares
NP	Normalized power
OLS	Ordinary least squares
TSS	Training stress score
TW	Total work
W	Watts
WLS	Weighted least squares

Table 2: List of symbols

CP	Critical power.
W'	Anaerobic work capacity.
$P(t)$	Power output at time t .
t_{exh}	Time to exhaustion.
n	Relationship parameter.
γ	Tolerance level or LASSO-penalty.
δ_{ij}	Measurement errors.
σ_{δ}	Standard error of measurement errors.
ϵ_i	Data point error.
I	Number of data points.
\hat{CP}	Estimate of CP .
\hat{W}'	Estimate of W' .
$\tau_{W'}$	Rate of reconstitution of anaerobic work capacity.
$W'_{\text{exp}}(t)$	Anaerobic energy expended at time t .
$W'_{\text{bal}}(t)$	Anaerobic energy still available at time t .
\overline{CCP}_t^i	Calculated cycled critical power for cyclist i on day t .
\widehat{CCP}_t^i	Estimated cycled critical power for cyclist i on day t .
CCP_t^i	Actual cycled critical power for cyclist i on day t .
M_d	Daily bound on CCP variation.
M_T	Total bound on CCP variation.
$Z_m(t)$	Training attribute m on day t .
$h(i)$	Kernel function.
$\lambda_{\text{fit}} = 1/\tau_{\text{fit}}$	Kernel parameter regarding fitness.
$\lambda_{\text{del}} = 1/\tau_{\text{del}}$	Kernel parameter regarding delay.
$\lambda_{\text{fat}} = 1/\tau_{\text{fat}}$	Kernel parameter regarding fatigue.
K	Respective impact of fatigue compared to fitness.
α_m	Relative training parameters

Introduction

“Far better an approximate answer to the right question, which is often vague, than an exact answer to the wrong question, which can always be made precise.” — J. Tukey,

It is the 28th of May 2017. Tom Dumoulin is warming up for a time trial; maybe the most important time trial of his entire career. It is the last stage of the 100th edition of the Giro d'Italia. Tom is in third place, 53 seconds behind Nairo Quintana and 14 seconds behind Vincenzo Nibali. Time trials are his specialty and he has been training for this moment for the entire season. However, doubts race through his mind. Has he been training hard enough? Is he not too fatigued after three long weeks of extreme climbing? He has no way to be sure.

1.1. Context

The questions raised in the previous paragraph are questions that are in the minds of elite cyclists and trainers all the time. In the past, they have been investigated from a physiological perspective, but recently a new scientific field has been flourishing: sports analytics. In sports analytics, historical data are used in order to construct descriptive and predictive models that can support decision makers to gain a competitive advantage. It has revolutionized how managers and coaches make their decisions in the sports of baseball, basketball, and football [22]. However, the use of sport analytics in cycling is still in its infancy.

The Fitness-Fatigue model [6] is a mathematical model that models and predicts the performance of an athlete based on past exercises. It has been successfully applied to a number of different sports, such as running [15], ice skating [9], and triathlons [2]. The Fitness-Fatigue model has yet not been widely applied to cycling due to difficulties in assessing performance that will be touched upon later in this introduction.

One of the most widely used information sources in sports analytics in elite cycling is the book 'Training and racing with a power meter' by Hunter Allen and Andrew Coggan [1]. It provides guidelines on how to use a power meter, a device that measures the power output of a cyclist, in order to optimize workouts and training schedules. In their book, the Fitness-Fatigue model is discarded in favor of a comparable, simplified model for various reasons. One reason is that to fit the model parameters to the actual data, multiple quantitative measurements of performance are required. The absence of this performance measure is one of the biggest difficulties in applying the Fitness-Fatigue model to cycling. Whereas in ice-skating or running the final time is a representative quantitative measure for performance, in cycling it is not. A cycling race or exercise is rarely held on the same track more than once and, furthermore, the weather conditions and competition have an enormous impact on the final time.

1.2. Research goal

The successful application of the Fitness-Fatigue model in elite cycling would mean a huge step forward in objectively validating and improving the training schedules of individual cyclists. Coaches and cyclists alike would then be able to time and tweak their training in order to reach their full potential during that one important race. Therefore, the main research goal of this report is:

"Adapt the Fitness-Fatigue model such that it can be used by elite cyclists to accurately model and predict their performance."

Two subgoals need to be completed before the main research goal can be achieved. The first subgoal is to find out which data are currently available in cycling that could quantify the performance of a cyclist and summarize different attributes of an exercise.

"Identify what data are available about performance and training attributes in cycling."

The second subgoal is to find an accurate performance metric that can be calculated on a frequent basis, such that the parameters of the Fitness-Fatigue model can be derived from it. This is done by studying the literature about current performance metrics and finally picking one of them. The picked performance metric is the cycled critical power (CCP), which was proposed by Vreugdenhil [18]. The quest for an accurate performance metric occupies a large part of this thesis.

"Identify an accurate performance metric that can be calculated on a frequent basis."

Using the results and conclusions from the two subgoals, the Fitness-Fatigue model can be adapted such that it might become a useful addition to the toolset of cyclists and coaches.

1.3. Outline

The report starts in Chapter 2 by introducing some terms and essential background information that are required to understand the rest of the report. Subsequently, in Chapter 3, the data available for this research are introduced. Chapter 4 illustrates the current state of sports analytics in cycling. In this chapter several methods from the current literature of estimating two important parameters (the critical power and anaerobic work capacity) are proposed and compared. In Chapter 5, a model is introduced to monitor the anaerobic work supply during an exercise. This model is required in the concept of the performance metric, cycled critical power, which is introduced and analyzed in Chapter 6. Finally, in Chapter 7, the Fitness-Fatigue model is applied to the data, analyzed, and evaluated. The report ends with a conclusion and prospects for future research in Chapter 8.

2

Background information

In this chapter, we introduce the background information that is required to understand the models and concepts in the rest of this report. It begins in Section 2.1 by introducing the partner in this research, Team Sunweb. Subsequently, in Section 2.2 the theory of different energy supply systems of the body is briefly touched upon. In Section 2.3, the measurement device with which to collect performance data is shown. In the last section, Section 2.4 the framework of Allen and Cogan [1], an important framework in optimizing training efficiency, is summarized. Some definitions of this framework are widely used in the cycling world and are therefore taken into account in the analyses in subsequent chapters.

2.1. Team Sunweb

Team Sunweb is a professional cycling team that consists of a men's and a women's division. The men's team has a German license. It was founded in 2005 as a Continental team, and received the World Tour license in 2013, the highest possible license available. The women's team was founded in 2011 and has a Dutch license. During their existence, both teams have used bicycles from Colnago, Koga, and Kelt, but since 2013 they have been riding Giant bicycles with Shimano components.

Team Sunweb has a focus on innovation, which might be the cause of the successful 2017 season in which they won the Giro d'Italia with Tom Dumoulin, four stages in the Tour de France along with the green and polka dot jersey for Michael Matthews and Warren Barguil respectively, and a fourth place for Wilco Kelderman in the Vuelta a Espana.



Figure 2.1: The logo of Team Sunweb

2.2. Energy supply systems

The body has several methods of supplying energy to its muscles and organs. A crude distinction of the energy supply systems is that of anaerobic versus aerobic energy supply.

Anaerobic energy supply is made available to fuel muscle contraction without the use of oxygen. This energy is stored in the body in the vicinity of the cells that consume the energy and is used in high intensity efforts such as sprints. It can provide large amounts of energy quickly, but also depletes in a short period of time. The supply that can be delivered by the anaerobic energy system is assumed to be bounded for an individual athlete, because it is bounded by the amount of energy that an athlete can accumulate in his or her body. The boundary for the amount of anaerobic energy supply is referred to as the anaerobic work capacity. Exhaustion occurs when the anaerobic energy supply is depleted.

Aerobic energy is created by a chemical process involving oxygen and it is the most important energy supply system in the body. It is used at medium and low intensity efforts and can be sustained for a longer

period of time. The amount of power at which the body starts using anaerobic energy is referred to as the aerobic threshold. The mathematical formulation of the aerobic threshold is referred to as the critical power.

The concepts of critical power and anaerobic work capacity have been formulated in order to model and estimate them through laboratory experiments. In these models, which we more thoroughly investigate in Chapter 4, critical power is denoted by CP and anaerobic work capacity by W' . The experiments that lead to the estimates of CP and W' are performed in a laboratory in which a subject is asked to hold a certain power output \bar{P} until exhaustion. The time to exhaustion t_{exh} for that particular power output \bar{P} is then registered. This experiment is repeated several times for different values of \bar{P} with at least one rest day in between each experiment. Afterwards, possible relations between \bar{P} and t_{exh} are investigated to find estimates for CP and W' . As of today, there are several relationships between \bar{P} and t_{exh} proposed in the literature. These relations are introduced, analyzed and compared among each other in Chapter 4

2.3. The power meter

The power meter is a device that measures different attributes of a cyclist during an exercise. The most important measurements are the power output in watts, the distance in kilometers, the cadence in rotations per minute, the speed in kilometers per hour, and the elevation in meters. The hardware available on the market differs from one company to the next. Where one company has a power meter that is installed in the crank, another offers a power meter that is installed in the chain. Over the years, Team Sunweb has used several power meters, starting from the SRM in '12, '13, and '14 and the Pioneer in '15 and '16. They are currently in a transition phase to the Shimano power meter. The data analyzed in this report have been collected with both the SRM and Pioneer power meters.

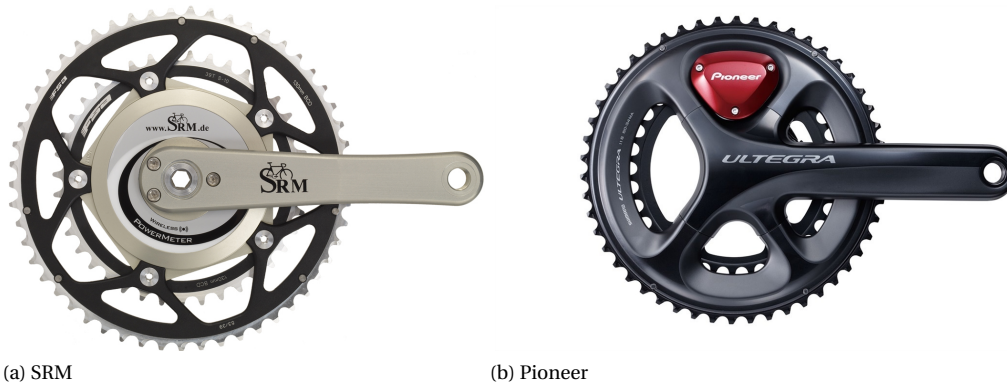


Figure 2.2: The SRM and Pioneer Power meter

2.4. Framework of Allen and Coggan

The book 'Training and racing with a power meter' [1] is widely used by coaches and cyclists alike to optimize their performance using the data from a power meter. In this book, some concepts are introduced that are widely used in elite cycling. These concepts are not supported by scientific research but because they are so intensively used in practice, they are incorporated in parts of this research. Below, we briefly touch upon the concepts of functional threshold power (FTP), normalized power (NP), the intensity factor (IF) and the training stress score (TSS). The FTP is a metric for the performance of a cyclist, whereas the NP, IF, and TSS are measures off the training load of an exercise.

Functional threshold power (FTP) The functional threshold power is defined as the highest power that a cyclist can maintain in a quasi-steady state for approximately one hour. The FTP is similar to the critical power (CP) concept, but the difference lies in the fact that the CP can theoretically be maintained infinitely.

Normalized power (NP) This definition is an extension on the average power (AP) as a measure of training load. It takes into account that a more variable power output is harder to maintain than a constant power output given that both have the same average power output. Normalized power is calculated as follows:

1. Calculate a 30-second rolling average for power;
2. Raise the values obtained in step 1 to the fourth power;
3. Take the average of all the values obtained in step 2;
4. Take the fourth root of the number obtained in step 3.

Mathematically we can write this as follows, where y_i is the 30-second rolling average for power.

$$NP = \left(\frac{1}{N} \sum_{i=1}^N y_i^4 \right)^{1/4}$$

Jensen's inequality tells us that $NP \geq AP$. When a cyclist delivers a constant power output P , then $NP = AP$. But if the power output of the cyclist is not constant, then $NP > AP$. If, for example, a cyclist rides half an hour at an output of 200W and half an hour at an output of 400W, the normalized power for that hour is $349.5 > 300 (= AP)$. Increasing the variance even more, such that the cyclist is performing half an hour at both 500W and 100W, the normalized power becomes 420.6W.

Intensity factor (IF) The intensity factor is an extension of normalized power as a measure of training load. It quantifies the training load respective to the fitness of a cyclist. The intensity factor is calculated by dividing NP by FTP. This way, it measures the intensity of an exercise respective to the cyclist his or her current performance level (the FTP).

$$IF = \frac{NP}{FTP}$$

Training stress score (TSS) In turn, the training stress score (TSS) is an extension on both NP and IF, since it also takes the duration of the exercise into account. The TSS is calculated as follows:

$$TSS = \left[\frac{T \times NP \times IF}{FTP} \right] \times 100 = T \times IF^2 \times 100 = T \times \left(\frac{NP}{FTP} \right)^2 \times 100 \quad (2.1)$$

with T is duration in hours. When a cyclist performs 1 hour at his FTP, the TSS of that exercise will be 100. The value of the TSS lies on a continuous scale that grades the intensity of an exercise. An exercise with a TSS of 100 is considered to be average.

The derivation of the formula for TSS is not strongly motivated, although the authors state that it is constructed to be a predictor for the amount of glycogen expended during the exercise. To our knowledge, this link has not been tested. However, TSS is used extensively in practice.

3

Data

“It is a capital mistake to theorize before one has data. Insensibly one begins to twist facts to suit theories, instead of theories to suit facts.” — Arthur Conan Doyle, Sherlock Holmes

In this chapter the available data are introduced and an exploratory data analysis is performed. The data are provided by Team Sunweb and contain six different cyclists; four men and two women. cyclists 1 through 4 are men, while cyclists 5 and 6 are women. For each cyclist there are three different data sets.

The first data set is a Matlab data file, obtained through a power meter which is incorporated in the crank and chain of the bicycle and records, at a given time interval, several metrics; speed, power, distance traveled, cadence, heart rate, and height. We call these daily power meter data. The second data set is also a Matlab data file and provides a summary of the daily power meter data. We call this the summarized power meter data. In the summarized power meter data set the following daily metrics are stored.

- Total distance.
- Average cadence.
- Average heart rate.
- Average power.
- Average speed.
- Normalized power.
- Intensity factor.
- Training load (TSS).
- Total elevation gain.
- Maximum power for 1, 5, 10, 15, 20, 30 seconds, 1, 2, 3, 5, 10, 20, 30, 60, 120, and 180 minutes.
- Respective average heart rate for the intervals above.
- Total time.
- Time in five different heart rate zones.
- Classification whether it was a race or training.
- Result of the day if it was a race (place in the ranking).
- Amount of energy (in kJ) used.

In the summarized power data set, mostly average values are stored. Sometimes, maximum values are necessary in the analyses. In that case the daily power meter data is used.

The third data set is an Excel document in which the cyclist personally collects subjective information, such as perceived intensity, fitness, and recovery. We call this the subjective data set.

In Sections 3.1, 3.3, and 3.4 the three different kinds of data sets are analyzed in more detail.

3.1. Daily power meter data

For every cyclist and for every day the cyclist exercised we have a daily power meter file, in which the following data is recorded; speed in km/h, power in watts, distance traveled in kilometers, cadence in rotations per minute, heart rate in heartbeats per minute, and height in meters. All these metrics are stored every second. This means that even if multiple exercises have been performed on a single day (i.e. a morning and evening exercise), only one daily power meter data set is saved. It is not common for cyclists to exercise more than once a day. In Table 3.1 some summarizing metrics of the daily power meter data are stated per cyclist. We notice that for all cyclists we have more than 250 daily power meter data sets and that the percentage of days we have data of is somewhere between 47% and 67%. The fact that this is not 100%, is caused by two reasons; the first is that a cyclist does not exercise every day, the second is that a cyclist needs to upload his/her data set in order for it to become available. As we will see later on in this chapter, the cyclists do not always upload their daily data sets. Furthermore, we notice that the average length of a daily power meter data set is around 10.000 seconds, which is a little less than 3 hours. The average power gives some indication about the power a cyclist is able to maintain.

Table 3.1: Summary information of daily power meter data

Cyclist	First day	Last day	# of daily files	Density ratio	Avg. length of daily files (in seconds)	Avg. power of daily files (in Watt)
Cyclist 1	21-03-2014	07-11-2016	640	0.67	11.626	182
Cyclist 2	24-11-2012	05-09-2016	882	0.64	11.712	205
Cyclist 3	10-11-2011	23-10-2016	856	0.47	16.765	196
Cyclist 4	15-04-2013	31-10-2016	603	0.47	11.847	221
Cyclist 5	04-06-2015	18-09-2016	266	0.56	8.329	152
Cyclist 6	13-12-2013	12-11-2016	550	0.52	11.800	146

There are some daily power meter data sets that need to be removed because of a wrongly calibrated power meter. This can be concluded from the average power applied on a given day. This is 0 for cyclist 2 on the 22nd and 23rd of May 2012 and 1.228 W during more than an hour for cyclist 1 on the 15th January 2016. These two files are removed from the analysis. No unusual data files were discovered by analyzing the average power output. Besides clear calibration errors, the power meter data is believed and thus assumed to be accurate.

3.2. Illustrations

In this section, three daily power meter data sets are analyzed and visualized to illustrate the data that are stored in the daily power meter data sets. Three different kinds of races for three different cyclists are given in the following subsections; a time trial for cyclist 2, a climbing stage for cyclist 3, and a sprint for cyclist 6.

3.2.1. Time trial - Cyclist 2

In this subsection a single data set is analyzed, specifically a time trial from cyclist 2 on the 23rd of May 2015, one of the stages of the 2015 Giro d'Italia. The time trial has a distance of 59.4 kilometers and is a flat race with some small climbs. In Figure 3.1 the power and speed during the warming up, cooling down, and time trial itself are plotted. We see that the power output of cyclist 2 is constant during the time trial at a power output of around 400W. The speed is constant in the beginning of the time trial and a bit more variable at the end, where there were some small climbs.

3.2.2. Climbing stage - Cyclist 3

In this subsection we take a closer look at a climbing stage and specifically the second stage of the 2014 Tour de Suisse for cyclist 3. The stage consisted of four climbs, two climbs of 'hors catégorie', i.e. the most difficult type of climb in a race, and two climbs of category two. The elevation is visualized in Figure 3.2 together with a rolling mean over 120 seconds of the speed in kilometers per hour and the power output in watts from cyclist 3. The rolling mean over 120 seconds at time t is the average power output over the 60 seconds before and after t , such that it smooths the time series. The rolling mean is plotted instead of the pure power and speed to make the graph better readable. At all four climbs the combination of high power and low velocity

is apparent due to the gravitational force that has to be overcome. The descents, on the other hand, show a power output close to zero combined with a high speed reaching levels of more than 80 kilometers per hour.

3.2.3. Sprint - Cyclist 6

Here we examine a stage that ended in a sprint; the sprint of cyclist 6 in the 2016 Boels Rental Ladies Tour. A rolling mean over 20 seconds of the power output and speed is plotted in Figure 3.3 for the last 20 minutes of the race. The data continue for some seconds after the actual finish when the cyclist is returning to her bus. As seen in the figure, the maximum for both power output and speed are reached in the final part of the race, as we would expect for a race that ends in a sprint.

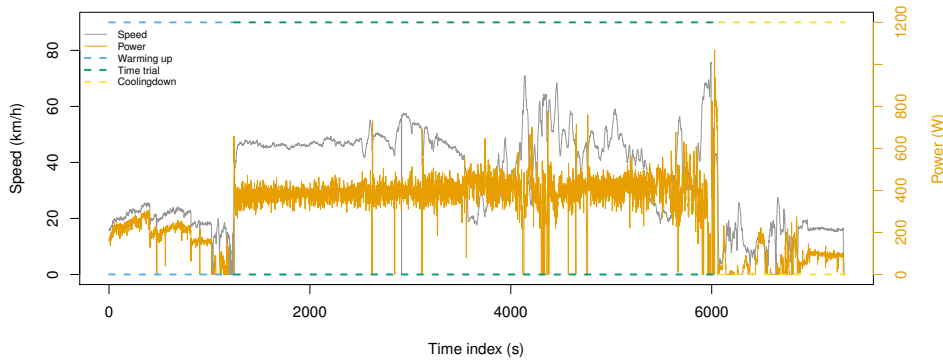


Figure 3.1: Power and speed of a time trial of Cyclist 2 divided in the warming up, actual time trial, and cooling down.

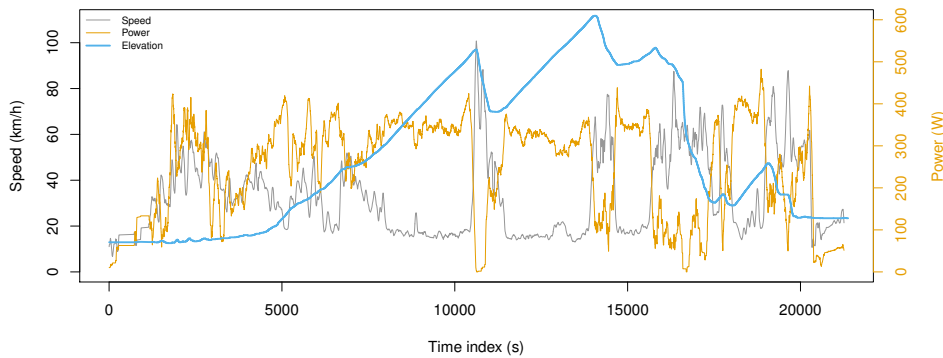


Figure 3.2: The rolling mean of power and speed over 120 seconds, and elevation of a climbing stage of Cyclist 3.

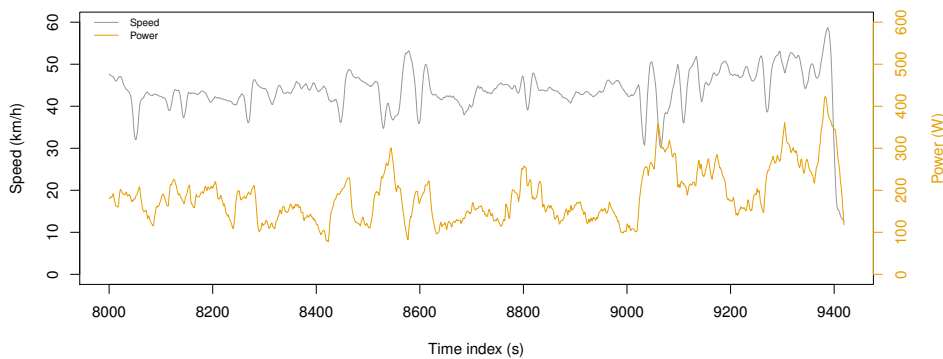


Figure 3.3: The rolling mean of power and speed of Cyclist 6 of the last 20 minutes of a race that ended in a sprint.

3.3. Summarized power meter data

The summarized power meter data set exists for each cyclist and is constructed by Team Sunweb to provide a better overview of how the daily power meter data evolves over time. The most important summary statistics used in the remainder of this report are the total distance, total time, average cadence, average heart rate, average power, average speed, normalized power and TSS. These data can be useful when we want to track the evolution of certain statistics over time or when want to compare two or more different statistics with each other, e.g. when we want to compare the correlation between average cadence and average power.

3.4. Subjective data

This data set is maintained by the cyclist, in which he or she, after the exercise enters values on a scale of 6-20 about his or her perceived fitness level, intensity of the training, and level of recovery. A scale of 6-20 has been chosen by the scientific experts at Team Sunweb, such that a cyclist always has the feeling he or she scored sufficient. Furthermore, the type of exercise and extra trainings are registered.

The cyclists register the following information in the subjective data set at the end of the days at which they exercised.

- The type of exercise (e.g. training, race, time trial, etc.)
- The fitness the cyclist felt during the training on a scale of 6-20.
- The intensity of the training according to the cyclist on a scale of 6-20.
- Whether the cyclist did another type of training (like running or going to the gym) and for how many minutes.
- How well recovered the cyclist felt before the training on a scale of 6-20.
- Extra remarks of the cyclist.

Figure 3.4 shows the histograms of the perceived rates of fitness, intensity, and recovery of cyclist 2. It is noticeable that the perceived rate of intensity of the exercises is evenly distributed, besides the peak at the value of 12, but that the cyclist seems to tend to the values of 15, 16, and 17 for the perceived rates of fitness and recovery.

The subjective data is gathered individually, thus it is unpractical to compare the subjective data of different cyclists among each other.

Especially the perceived intensity of an exercise is valuable information, because other research [9] has shown that this perceived intensity of an exercise influences the performance of an athlete. This can be explained by the fact that if an athlete considers an exercise intense, most likely he or she will gain extra muscle power from that exercise.

Unfortunately, the cyclists did not submit subjective data for all exercise days. Vice versa, also days exist for which the cyclist has provided subjective data, but no power meter data is available. In Figure 3.5 the total number of days for which data are submitted is visualized for all cyclists and divided into three subgroups; the number of days for which only power meter data is available, the number of days for which only subjective data is available, and the number of days for which both are available.

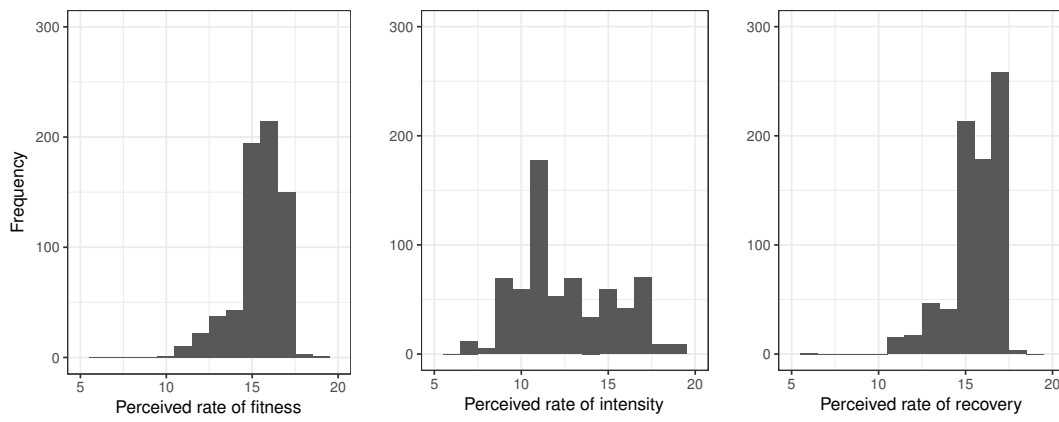


Figure 3.4: Histograms of the perceived rates of fitness, intensity, and recovery of cyclist 2

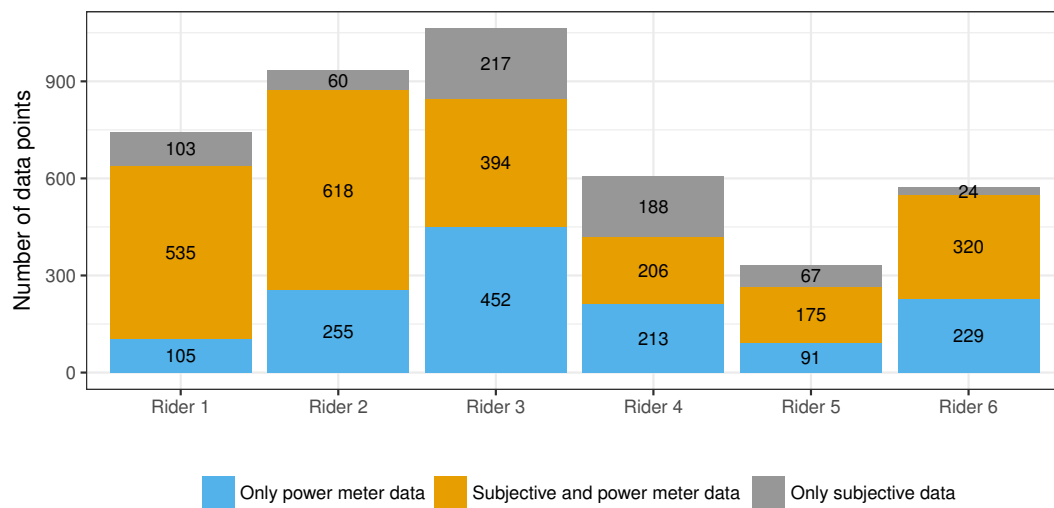


Figure 3.5: The number of available data sets for the different cyclists.

4

Estimating critical power and anaerobic work capacity

“A certain elementary training in statistical methods is becoming as necessary for everyone living in this world of today as reading and writing.” — H.G. Wells,

The goal of this chapter is plural. The chapter serves as a summary on the existing physiological models used in assessing the performance of a cyclist, which is represented by the critical power and anaerobic work capacity. Subsequently, it is investigated how the available data and existing models can be combined to assess the performance of a cyclist. This combination is found in a method to acquire specific data points from the data set, that can then be used in the existing physiological models. Afterwards, it is evaluated which model combined with the newly found data points leads to the most accurate estimates for the critical power and anaerobic work capacity.

The Chapter starts in Section 4.1 by studying the mathematical models that are proposed in the literature to estimate CP and W' . Afterwards, in Section 4.2 a method is proposed to acquire relevant information from the provided data sets. Section 4.3 states the statistical methods that are applied to the mathematical models and relevant data, to come up with estimations of CP and W' . Section 4.4 states the most important results of this chapter and compares the different statistical methods. In Section 4.5, the accuracy of estimates is investigated. Finally, Section 4.6 draws conclusions from the content of this chapter.

4.1. Mathematical models

This section summarizes the mathematical models proposed to model the dependency between the average power \bar{P} and time to exhaustion t_{exh} in existing literature. In the existing literature cyclists are tested in a laboratory on a bicycle ergometer. The subjects are asked to keep a certain power output (\bar{P}) as long as possible. Once they drop below this given power output, the time in seconds is recorded (t_{exh}). Researchers use these data points to come up with different mathematical models to describe the relation between \bar{P} and t_{exh} . Team Sunweb does not have this kind of data of their cyclists. Nonetheless, we try to acquire other data points from the data provided by the power meter that might be fitted to the same mathematical models. More on this data acquirement is explained in Section 4.2.

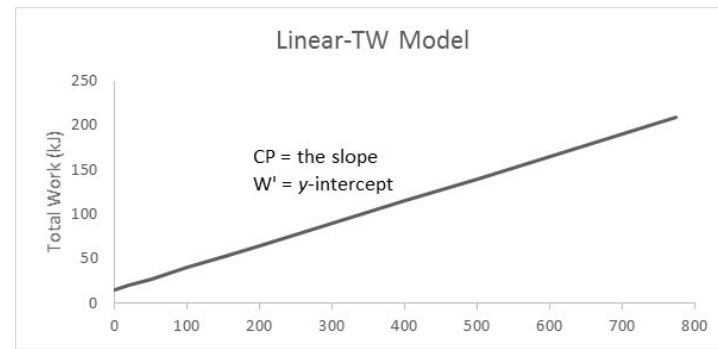
The first researchers that investigated the relationship between \bar{P} and t_{exh} are Monod and Scherrer [12]. They introduced the mathematical concept of critical power for a singular muscle. This concept is extended by Moritani et al. [13] to whole body exercise. Both papers discover a linear trend with a non-zero intercept in the data points between total work exercised ($TW = \bar{P} \times t_{\text{exh}}$) in kilojoule and time to exhaustion in seconds (t_{exh}) as shown in Equation (4.1). This model is called the linear-TW model.

$$TW = W' + CP \times t_{\text{exh}} \quad (4.1)$$

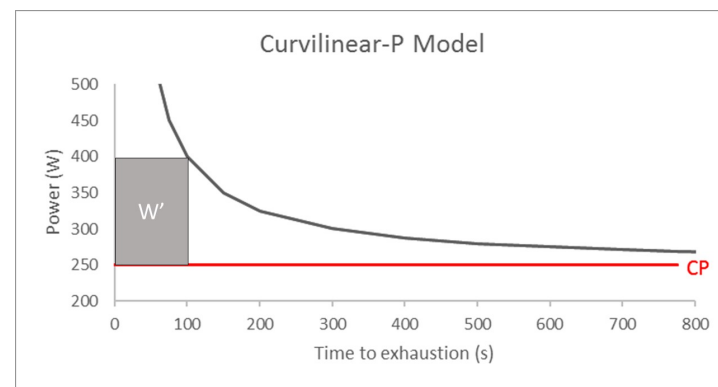
In this formula CP represents the critical power and W' represents a finite supply of energy that is used when performing at intensities above critical power. Moritani et al. [13] also show that CP is strongly correlated with the aerobic threshold and that W' is strongly correlated with the anaerobic energy capacity. The interpretation of CP and W' becomes more intuitive when both sides of Equation (4.1) are divided by t_{exh} . We notice

that the total work delivered (TW) divided by t_{exh} is the average power in joule applied per second (\bar{P}), i.e. the power in watts. This relationship is stated in Equation (4.2), which describes a curvilinear relationship between the average power output \bar{P} and time to exhaustion t_{exh} . This model is called the curvilinear-P model. In this equation the critical power is represented by the horizontal asymptote when \bar{P} is plotted against t_{exh} . In Figure 4.1 an example is visualized of the linear-TW model of Equation (4.1) and of the curvilinear-P model of Equation (4.2)

$$\bar{P} = \frac{W'}{t_{\text{exh}}} + CP \quad (4.2)$$



(a)



(b)

Figure 4.1: Linear-TW and curvilinear-P models visualized

Several extensions of models (4.1) and (4.2) are proposed in literature that improve the accuracy of the relationship between \bar{P} and t_{exh} for the data points found thus far. The first one we examine is the 3-parameter model [14] that tackles the unlikely assumption of both models that \bar{P} can approach infinity as t_{exh} goes to zero, i.e. an infinite amount of power is possible for a small enough period of time. Therefore, Morton et al. [14] propose a model in which a new parameter k is added such that the curvilinear-P model transforms into a 3-parameter model, given in Equation (4.3). This new parameter shifts the (t_{exh}, P) graph to the left on the t_{exh} -axis such that a maximal instantaneous power is obtained at $t_{\text{exh}} = 0$. This maximal instantaneous power P_{max} is given by the equation $P_{\text{max}} = CP - \frac{W'}{k}$ from which we can deduce that $k < 0$. Furthermore, Morton et al. [14] show that k is significantly different from zero and their model leads to significantly smaller estimates of CP and larger estimates of W' .

$$\bar{P} = \frac{W'}{t_{\text{exh}} - k} + CP \quad (4.3)$$

Tsai [24] proposes another adjustment to the base models. He highlights a flaw in the models using the following mathematical argument. Starting with Equation (4.2) we assume that multiplying by t_{exh} would lead to Equation (4.1), but this is under the assumption that $P(t)$ is a discrete process. In reality, $P(t)$ is a

continuous process, thus to go from $P(t)$ to TW integration over t is necessary, which leads to the calculation as in Equation (4.4). In this equation the parameters CP and W' are substituted by a and b ; parameter estimates.

$$\begin{aligned}
 TW(t_{\text{exh}}) &= \int_1^{t_{\text{exh}}} P(t) dt \\
 &= \int_1^{t_{\text{exh}}} \frac{a}{t} + b dt \\
 &= [a \ln(t) + bt]_1^{t_{\text{exh}}} + C \\
 &= a \ln(t_{\text{exh}}) + bt_{\text{exh}} - b + C
 \end{aligned} \tag{4.4}$$

We take the start time to be 1 to overcome problems with the $\ln(t)$ and assume the total work at $t = 1$ to be 0. Thus, if we consider b to be CP and $-b + C$ to be W' , an extra term $a \ln(t_{\text{exh}})$ is left out of the linear-TW model. For large t_{exh} , this term $a \ln(t_{\text{exh}})$ is dominated by bt_{exh} such that the relation looks linear, but zooming in on low values of t_{exh} shows a curvilinear relationship caused by the term $a \ln(t_{\text{exh}})$. Tsai emphasizes the pitfall that with only a couple of data points the trend might be considered linear while it is not. This is illustrated in Figure 4.2 where the total work is plotted together with the two components of $a \cdot \ln(t_{\text{exh}})$ and $b \cdot t_{\text{exh}}$ for some arbitrary values of a and b . This figure emphasizes the pitfall that for $t_{\text{exh}} > 40$ the relationship between total work and time to exhaustion is regarded linear while for small t_{exh} this is not the case. Later in this chapter this behavior is also observed in the data acquired from the daily power meter data.

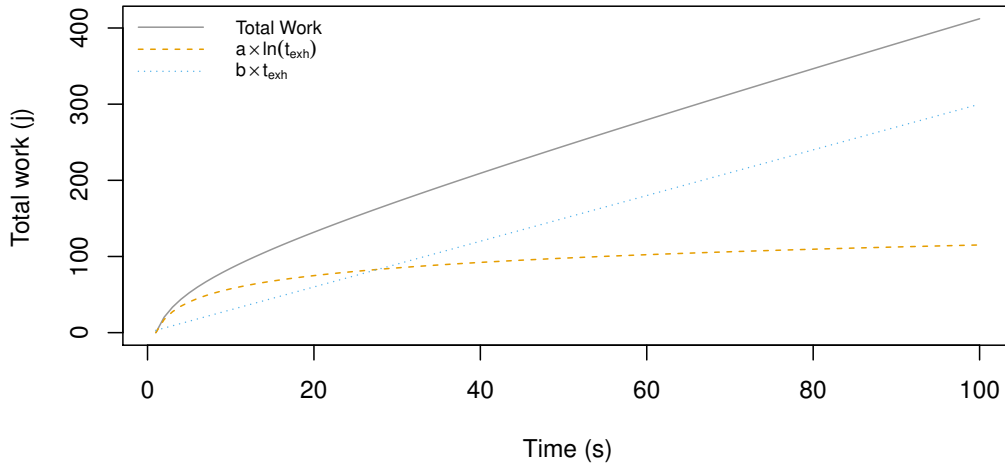


Figure 4.2: An example of the curvilinear relationship between TW and t .

In order to take the logarithmic trend into account for small t_{exh} , Tsai introduces a new parameter n , $0 < n < 1$, called the relationship constant. The model is stated in Equation (4.5).

$$\bar{P} = \frac{a}{t_{\text{exh}}^n} + b \tag{4.5}$$

In this model b is equal to CP but a is not equal to W' , because W' is the amount of energy performed above CP , thus $W' = (\bar{P} - CP) \cdot t_{\text{exh}}$. Substituting (4.5) yields $W' = (\frac{a}{t_{\text{exh}}^n} + CP - CP) \cdot t_{\text{exh}} = a \cdot t_{\text{exh}}^{n-1}$. In order to estimate W' for the relationship-CP model, Tsai suggests to use 90 seconds for t_{exh} when evaluating W' , because several studies [7], [11] show that W' can be predicted from one all-out exercise test lasting 90-120 seconds.

Tsai also shows for several sports that n is significantly different from 1 and that for cycling $n = 0.48 \pm 0.15$ (mean \pm standard deviation). He performed his experiments on a group of 27 competitive cyclists to acquire the required data points. This model is called the relationship-CP model.

4.2. Data acquisition

The consensus within (cycling) sports, according to Team Sunweb, is that CP and W' are good metrics to quantify the fitness of an athlete, thus they are widely used in practice. The problem however, lies in estimating the values of CP and W' for specific cyclists at specific times. Several testing protocols are used in order to gather data with which CP and W' can be estimated. Subsection 4.2.1 states the protocols currently used to acquire data points. Subsection 4.2.2 introduces a way to acquire comparable data points from the daily power meter data.

4.2.1. Protocols

The standard scientific protocol of acquiring data to estimate CP and W' is by performing multiple tests on an ergo-meter with at least a 24 hour rest inbetween to remove the influence of fatigue [13]. During such a test, the subject is asked to maintain a fixed given level of power output. When the subject is exhausted and thus not able to maintain the prescribed level of power the elapsed time t_{exh} is recorded. Thus, a data point is a couple (t_i, \bar{P}_i) which represents the time t_i that the cyclist can maintain the power output \bar{P}_i .

In order to be able to estimate CP and W' at least three data points, but preferably more, and thus three or more tests are needed for the linear-TW and curvilinear-P model. For the 3-parameter model and relationship-CP model a minimum of four data points is required. The data collection makes it a time consuming protocol that is hard to execute on regular basis and that interferes with normal training. Furthermore, the data points are not acquired on the same day, so another disadvantage is that the daily form of the subject causes noise in the data points. To address these shortcomings, Vanhatalo et al. [25] propose a protocol of a 3-minute all-out test in which CP is estimated as the average power in the last 30 seconds of this test. This test however, yields no estimation of W' .

At Team Sunweb a testing protocol proposed by Allen and Cogan [1] is used to estimate the functional threshold power (FTP), which is the power a cyclist is able to maintain for one hour. In this protocol there is a warm-up and a main set, in which there is an all-out effort of 20 minutes. The estimate for the FTP is then calculated by taking the average power in the 20 minutes all-out effort and subtracting 5% to compensate that the all-out effort is only over 20 minutes instead of an hour. The 5%-value is frequently used by professional cycling teams but for which there is no scientific support. The disadvantages of this method are that there is no scientific evidence how the estimations of the FTP behave and that it yields no estimation of CP and W' . The data acquired through this latest protocol for our six cyclists are listed in Table 4.1. Cyclist 1 did not perform this protocol.

Table 4.1: Average power obtained through the 20-min-all-out test.

Information not stated due to confidentiality reasons.

4.2.2. Extracting information from daily power meter data

Currently, Team Sunweb only performs the 20 minutes all-out protocol, from which an estimation of the FTP is determined. In order to be able to estimate CP and W' in the mathematical models, we require data points (t_i, \bar{P}_i) that represent the maximum time t_i that a cyclist can maintain an average power \bar{P}_i . In this subsection, two methods are proposed to extract similar data from the daily power meter data. Although, we do not know if and when a cyclist becomes exhausted during a race, we try to extract t_i and the corresponding \bar{P}_i from the daily power meter data that represent the data points used in the original models. The first method takes the maximum normalized power in a given time interval. The second method uses pronounced maxima, a concept that is introduced later on in this report.

Maximum normalized power in a given time interval

The standard protocol tests how long a cyclist can maintain a given power output. Turning this question around, we can ask what the maximum average power a cyclist can apply for a fixed time interval is. A lower bound for this maximum average power can be gathered from the data, looking at the cyclist's maximum average power ridden in the given time interval in the available data set. This yields a lower bound because in case the cyclist has not gone all out during the time interval, which is likely if the time period is part of a longer exercise or race, the actual power he or she could achieve is higher. This method has the advantage that for all six cyclists there are enough data available to have reliable lower bounds to estimate a base value of CP . But there are also multiple disadvantages: first of all, the maximum average power for different time intervals are reached on different days, therefore the fact that CP might have changed over time, causes noise in the data. Secondly, the power that is applied during such a time interval does not have to be constant, worse still, it probably is not. Lastly, the time intervals at which the maximum average power is taken, have to be chosen. This is an arbitrary process and has a strong impact on the final values of CP and W' .

In order to overcome the disadvantage of variability in the data, Allen and Cogan [1] have proposed the so-called normalized power, see Chapter 2. This metric smooths the time series and takes into account the fact that many critical physiological responses are curvilinearly related to exercise intensity. Therefore, we use the NP instead of the AP.

The considerations to take into account when selecting the time intervals are the following: we should pick time intervals that prevent overlapping measurements. Furthermore, we should not take too short or too long time intervals into account. Short intervals are prone to measurement errors and say more about the maximum power a cyclist can apply and not so much about the time he or she can maintain this power. Long time intervals should be avoided because they give no good lower bound, due to the fact that during actual trainings and races cyclists never go all out for more than for 30 minutes.

Following these considerations, we use the following time intervals and corresponding maximum normalized power from the data for each cyclist to estimate his or her CP and W' in the next section; 5 seconds, 10 seconds, 15 seconds, 30 seconds, 1 minute, 2 minutes, 3 minutes, 5 minutes, 10 minutes, 20 minutes and 30 minutes.

Pronounced maxima

One of the biggest disadvantages of the method proposed in the previous subsection, is the fact that the time intervals are fixed. To see why this is a disadvantage, take a look at Figure 4.3 and assume that the cyclist has maintained an average power over 10 seconds of 880 watts, but the one second before that interval (on index 5) he was also able to push 800 watts. Because the time interval is fixed, we approximate that the cyclist can maintain 880 watts for 10 seconds, while in reality he can maintain a comparable average power for 11 seconds. Thus, the data point with $t_i = 11$ and $\bar{P}_i = 873$ is a data point that represents the required interpretation better than the data point with $t_i = 10$ and $\bar{P}_i = 880$.

To overcome this disadvantage, we introduce the concept of pronounced maxima. In the following definition we use the notation $\bar{P}_{[r,s]}$ for the average of the time series $P_i(t)$ over the interval $[r, s]$.

Definition 4.1. A **pronounced maximum** is a finite and compact subset $[r, s]$ of the discrete indices of a time series P_i which satisfies the following four properties:

1. $\bar{P}_{[r-k, r-1]} \leq (1 - \gamma) \bar{P}_{[r, s]}$ where $k = \lceil \frac{s-r+1}{50} \rceil$.
2. $\bar{P}_{[s+1, s+k]} \leq (1 - \gamma) \bar{P}_{[r, s]}$ where $k = \lceil \frac{s-r+1}{50} \rceil$.
3. $\bar{P}_{[r, r+k-1]} \geq (1 - \gamma) \bar{P}_{[r+k, s]}$ where $k = \lceil \frac{s-r+1}{50} \rceil$.
4. $\bar{P}_{[s-k+1, s]} \geq (1 - \gamma) \bar{P}_{[r, s-k]}$ where $k = \lceil \frac{s-r+1}{50} \rceil$.

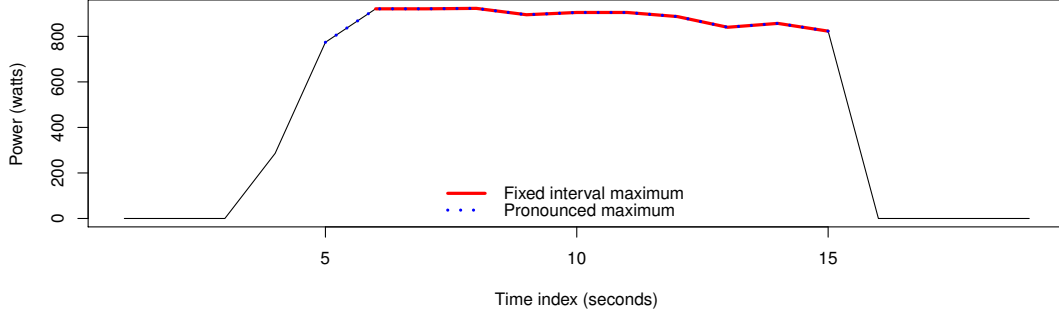


Figure 4.3: The advantage of a pronounced maximum explained

The constant $0 < \gamma < 1$ is called the **tolerance level**. In Figure 4.4 the concept of a pronounced maxima is schematically visualized on an interval.



Figure 4.4: Schematic visualization of the definition of pronounced maxima. The blue area is the pronounced maximum.

In summary, this definition states that a pronounced maxima is a subset $[r, s]$ of the indices of a time series P_i with the following properties. The k points directly in front of or behind the subset $[r, s]$ have an average value of P_i lower than $(1 - \gamma)$ times the average of P_i over $[r, s]$. Furthermore, the first and last k points of the subset $[r, s]$ have an average value of P_i at least $(1 - \gamma)$ times the average of P_i over the remaining indices of $[r, s]$. This means that for the boundary points r and s the time series outside the interval $[r, s]$ is 'significantly lower' than inside the interval.

The value of k determines the size of the intervals at the boundaries of the pronounced maximum. In case of a small pronounced maximum, say $s - r < 50$, it is important to look at the single points just in- and outside the interval. But in case of a large pronounced maximum, say $s - r = 600$, we would like to add or remove larger chunks of the pronounced maximum such that an incidental low value does not influence the pronounced maximum. Therefore, it is chosen that k should be a fraction of the length of the interval, with a minimum value of 1, i.e. $k = \lceil \frac{s-r+1}{50} \rceil$. The fraction $\frac{1}{50}$ is arbitrary and could be chosen differently.

Thus, a pronounced maximum on the time series P_i is a subset $[r, s]$ on which the average applied power is at least a factor $\frac{1}{1-\gamma}$ larger than the two adjacent intervals of length $k = \lceil \frac{s-r+1}{50} \rceil$. From such a pronounced maximum a data point (t_i, \bar{P}_i) can be acquired that represents an interval of length t_i in which the cyclist maintained an average power output of \bar{P}_i . In this case $t_i = r - s + 1$ and $\bar{P}_i = \frac{1}{r-s+1} \sum_{i=r}^s P(i)$. The question that remains is how to choose the level γ , but this is hard to say beforehand. Different tolerance levels are tried experimentally later in this report.

The algorithm to find pronounced maxima in the entire data set is as follows. A loop is executed for each cyclist and every daily data set. In this daily data set, the time intervals of the last subsection are used and for each of these time intervals the maximum average power on that given time interval is computed for the specific cyclist on the given day. Then we check whether it is necessary to remove data points at the beginning of the interval $[r, s]$ as follows. The power output of indices $[r, r+k-1]$ relative to the average power output of the interval $[r+k, s]$ is compared to the tolerance level γ as stated in Equation (4.6). If this ratio is larger than the tolerance level γ , then property 3 of Definition 4.1 does not hold, thus it is necessary to remove the points $[r, r+k-1]$ from the pronounced maximum $[r, s]$. This comparison is performed iteratively until Equation (4.6) does not hold anymore. The same procedure is followed to check whether the end points of the interval $[r, s]$ should be removed.

$$\frac{\frac{1}{s-r-k+1} \sum_{i=r+k}^s P(i) - \frac{1}{k} \sum_{j=r}^{r+k-1} P(j)}{\frac{1}{s-r-k+1} \sum_{i=r+k}^s P(i)} > \gamma \quad (4.6)$$

For the part (beginning or end) where no points are removed, it is then checked whether extra data points should be added to the pronounced maximum in a similar manner. E.g. at the left endpoint of the interval, it is checked whether $[r - k, r - 1]$ should be added to the pronounced maximum by calculating the relative difference between the average power output at time $[r - k, r - 1]$ and the average power output over $[r, s]$ which is then compared to the tolerance level γ as stated in Equation (4.7). If this ratio is lower than γ , then property 1 of Definition 4.1 does not hold, thus it is necessary to add the points $[r - k, r - 1]$ to the pronounced maximum. This procedure is performed iteratively until Equation (4.7) does not hold anymore. If there were no points removed at the end of the interval, it is also checked whether it is necessary to add points at the end of the pronounced maximum.

$$\frac{\frac{1}{s-r+1} \sum_{i=r}^s P(i) - \frac{1}{k} \sum_{j=r-k}^{r-1} P(j)}{\frac{1}{s-r+1} \sum_{i=r}^s P(i)} < \gamma \quad (4.7)$$

The output of this algorithm is a long list of pronounced maxima for each cyclist. However, within this list there are some entries that need to be removed, because these entries do not represent an interval in which the cyclist has gone all out. First, the entries for which there are other entries that have an equal or longer time span and higher average power can be removed. This is because these entries do not represent a maximum possible applied power, because other entries have a higher average power over the same time interval or longer. Secondly, all entries with a time interval longer than 30 minutes are removed, because experience shows that no cyclist will go all out longer than 30 minutes during a race or training. Thirdly, in order to prevent correlation between the data points, from the entries that have overlapping time periods only the entry with the largest time interval is kept.

Comparison

Thus far, we have two methods to acquire data points of (t_i, \bar{P}_i) that can be interpreted as the data points obtained by the laboratory experiments; maximum normalized power and pronounced maxima. Figure 4.5 shows the acquired data of both methods for a given cyclist. First of all, we notice that both methods result in similar data, as the data points seem to be scattered on the same curvilinear relationship. However, we also notice that the pronounced maximum method leads to more data points, which in turn leads to a more accurate estimation of CP and W' . Furthermore, with the pronounced maximum method we are also certain that there are no overlapping intervals yielding multiple data points, which might be possible in the method of maximum normalized power. Therefore, from now on we continue with data points acquired by the method of pronounced maxima and assume that these data points represent time intervals in which the cyclist has gone all out. This way, we assume the data can be described by the models stated in Section 4.1.

Tolerance level

An important question remains what tolerance level should be used. A low tolerance level γ means that points at the side of the interval are removed when they have a power output only just below the average of the other points in the pronounced maximum and points are not added to the pronounced maximum unless their power output is almost equal to the average of the current pronounced maximum. This has the benefit that the power during the pronounced maximum has less variation and thus gives more stable power outputs. The danger of a low tolerance level is that it only leads to data points with small time intervals because it easily removes points at either side of the pronounced maximum. Table 4.6a compares the average amount of data points per cyclist and average length of the time interval of the data for multiple tolerance levels and Figure 4.6b shows a scatter plot of the data points for different tolerance levels. The table shows no apparent trend between the tolerance level and important metrics and the figure confirms this observation. Thus, a tolerance level of $\gamma = 0.05$ does not lead to a small data set or only data points with relatively small time intervals. Because the tolerance level of $\gamma = 0.05$ does have the advantage that it leads to more stable data points, we continue with the data set of pronounced maxima with $\gamma = 0.05$.

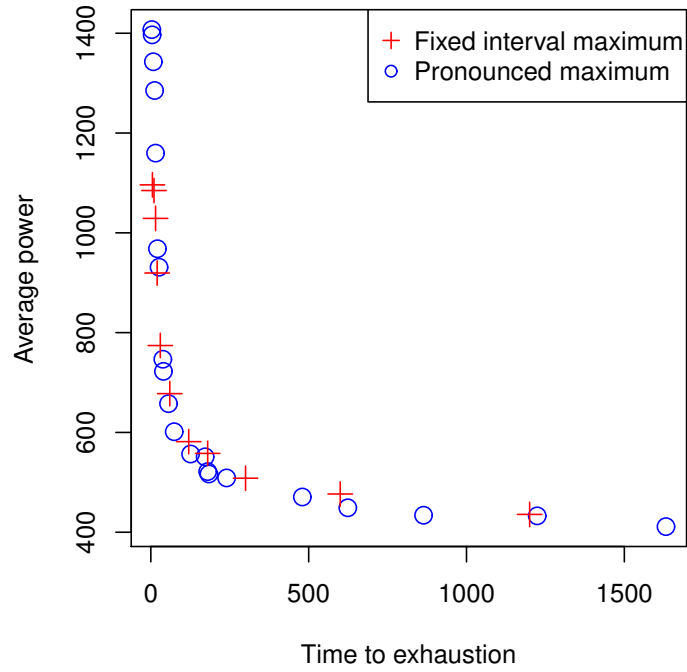
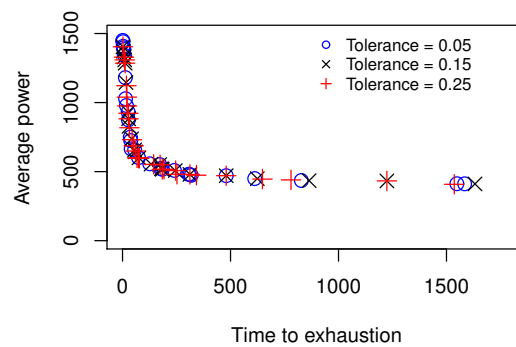


Figure 4.5: Plot of the data obtained by the two different methods of data acquisition

Tolerance level	Avg. # data points per cyclist	Avg. length of time interval
0.05	22.0	303.2
0.10	21.7	310.1
0.15	21.3	314.3
0.20	23.3	289.7
0.25	23.5	300.4
0.30	23.8	309.6

(a) Metrics for different tolerance levels



(b) Scatter plot for different tolerance levels

Figure 4.6

4.3. Estimation

Departing from the mathematical models stated in Section 4.1, there are three statistical methods that are simple and easily applicable; ordinary linear least squares (OLS), weighted linear least squares (WLS), and non-linear least squares (NLS). In the subsections below we cover the combinations of the different mathematical models and statistical methods. The data of cyclist 2 is used to visualize the results.

A comparison of the estimators acquired by performing OLS on the linear-TW, the curvilinear-P and NLS on the 3-parameter model is made by Bergstrom et al. [4]. They also includes the estimation of CP of the 3-minute all-out test. In their paper, Bergstrom et al. [4] analyze how the estimates relate to each other, but not which estimates are the most accurate. We, however, in Section 4.4, pick a combination of a mathematical model and a statistical method from those proposed in the following subsections, that according to us provides the most accurate estimates when using pronounced maxima as data input.

4.3.1. Measurement error

Like every measuring device, the power meter has a measurement error. We assume these measurement errors δ_{ij} to be independently and normally distributed with a mean of 0 and variance of σ_δ^2 . The indices i represent the different data points, (the pronounced maxima). The indices j represent the time points of the respective pronounced maxima i . Thus, the power P_{ij} measured at time j is the sum of the actual applied power ϕ_{ij} plus a normally distributed error $\delta_{ij} \stackrel{\text{iid}}{\sim} N(0, \sigma_\delta^2)$. We show that this error has more influence on the pronounced maxima with a low t_i than those with a high t_{exh} . The average power over a time interval of length t_{exh} is equal to

$$\bar{P}_i = \frac{1}{t_i} \sum_{j=1}^{t_i} P_{ij} = \frac{1}{t_i} \sum_{j=1}^{t_i} (\phi_{ij} + \delta_{ij}) = \frac{1}{t_i} \sum_{j=1}^{t_i} \phi_{ij} + V_i \quad (4.8)$$

$$V_i \stackrel{\text{iid}}{\sim} N\left(0, \frac{\sigma_\delta^2}{t_i}\right) \quad (4.9)$$

These calculations show that the measurement error of \bar{P}_i is normally distributed with a mean of 0 and variance of $\frac{\sigma_\delta^2}{t_i}$, thus a larger t_i leads to less variability in the value of \bar{P}_i and thus a more accurate estimation of $\bar{\phi}_i$.

4.3.2. Linear-TW model

In the Linear-TW model a linear relationship is assumed between the explanatory variable t_{exh} and the response variable $TW = \bar{P} \cdot t_{\text{exh}}$ as in Equation (4.10). Furthermore, we assume that the data points extracted with the method of pronounced maxima have an error term of ϵ_i which are independently and normally distributed with a mean of 0 and variance of σ_ϵ^2 . Thus, we assume that the data points can be described as in Equation (4.10).

$$\begin{aligned} TW_i &= CP \cdot t_i + W' + \epsilon_i \\ \bar{P}_i \cdot t_i &= CP \cdot t_i + W' + \epsilon_i \end{aligned} \quad (4.10)$$

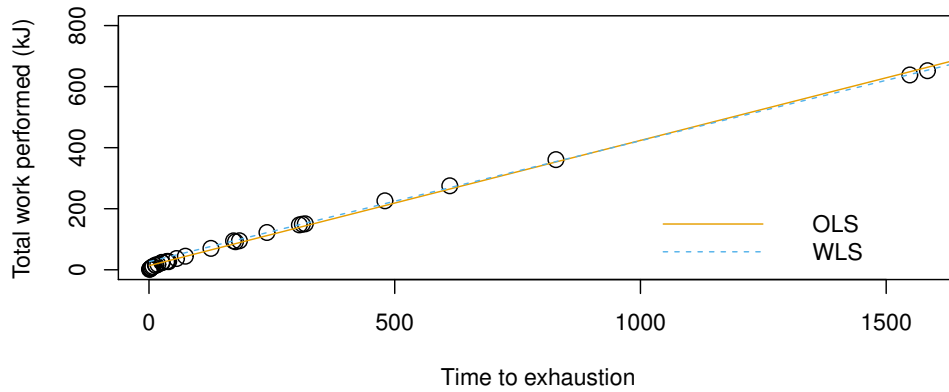
For this model both an ordinary and weighted least squares regression are performed on the explanatory variable t_i and response variable $TW_i = \bar{P}_i \cdot t_i$. The estimated values of CP and W' , i.e. \hat{CP} and \hat{W}' , are calculated as in Equation (4.11), where w_i are the weights of the data points and I is the number of available data points.

$$(\hat{CP}, \hat{W}') = \operatorname{argmin} \sum_{i=1}^I (\bar{P}_i \cdot t_i - \hat{CP} \cdot t_i - \hat{W}')^2 \cdot w_i \quad (4.11)$$

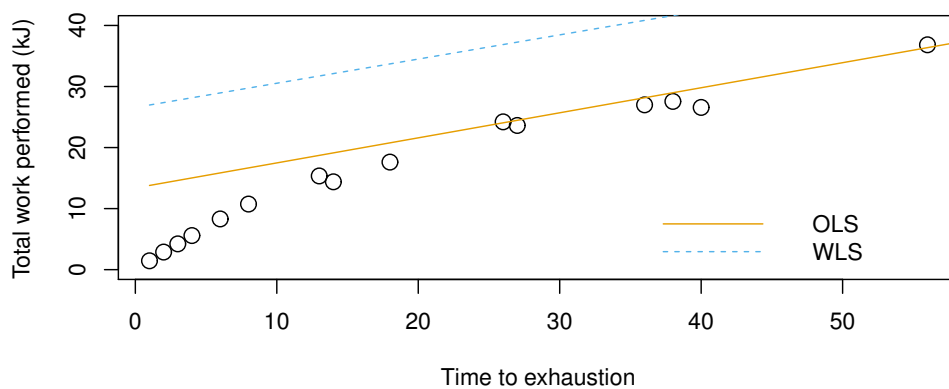
For OLS we choose the weights to be constant, i.e. $w_i = 1$. For WLS we choose the weights to be equal to the length of the time interval of the data point, i.e. $w_i = t_i$. This way, the data points with longer time intervals have more impact on the estimation of CP and W' , compensating for the measurement error. This method is equivalent to using the maximum likelihood estimator for heteroscedastic data. The disadvantage of WLS is that the data points with longer time intervals have more variation in the applied power and that in long time intervals it is more probable that a cyclist did not go all out.

$\hat{C}P$ and \hat{W}' are calculated in the same way for both OLS and WLS: the argument of the argmin function of Equation (4.11) is differentiated to both $\hat{C}P$ and \hat{W}' . This leads to the normal equations in which the derivatives are set equal to zero. The two normal equations lead to a linear system which can be used to solve for $\hat{C}P$ and \hat{W}' .

In Figure 4.7a the regression lines of both the OLS and WLS are plotted for cyclist 2. The figure shows that both methods lead to varying results with for OLS that $\hat{C}P = 410$ W and $\hat{W}' = 13.381$ j, and for WLS that $\hat{C}P = 396$ W and $\hat{W}' = 26.571$ j. Taking a closer look at the data points for which $t_{\text{exh}} < 60$ in Figure 4.7b reveals a logarithmic trend as foreseen by the argument of Tsai [24], stated in Section 4.1, where he claims that there is a logarithmic relationship between TW and t_{exh} for small values of t_{exh} . This explains the large differences in \hat{W}' between OLS and WLS, because the data points with small t_{exh} impact the WLS less, the effect of the logarithmic term has the least effect on the estimators for WLS. Later, in the relationship-CP model, this effect is incorporated in the model.



(a) OLS and WLS regression on the pronounced maxima of cyclist 2 using the linear-TW model.



(b) Pronounced maxima of cyclist 2 with time to exhaustion below 60 seconds. This figure shows the logarithmic trend that is present for low t_{exh} .

Figure 4.7: OLS and WLS performed on the linear-TW model. The lower plot shows the beginning interval of the upper to show the logarithmic trend for small t_{exh}

4.3.3. Curvilinear-P model

To the Curvilinear-P model the two regression methods OLS and WLS are applied as well. Once more it is assumed there is a linear relationship, this time between the explanatory variable $1/t_{\text{exh}}$ and response variable \bar{P} such that a linear relation is expected between them. Furthermore, we assume the data points have an error term of $\epsilon_i \stackrel{\text{iid}}{\sim} N(0, \sigma_\epsilon^2)$, such that the data is described as in Equation (4.12).

$$\bar{P}_i = \frac{W'}{t_i} + CP + \epsilon_i \quad (4.12)$$

Once more, the estimates of OLS and WLS are calculated by the procedure as stated in Equation (4.13), where the weights for OLS are $w_i = 1$ and for WLS $w_i = t_i$ for the same reasons as in the previous subsection.

$$(\hat{CP}, \hat{W}') = \operatorname{argmin} \sum_{i=1}^I \left(\bar{P}_i - \hat{CP} - \frac{\hat{W}'}{t_i} \right)^2 \cdot w_i \quad (4.13)$$

The calculations of \hat{CP} and \hat{W}' are performed as in the last subsection by taking derivatives and using the normal equations.

The estimates for OLS are $\hat{CP} = 673\text{w}$ and $\hat{W}' = 1.265\text{j}$ and for WLS are $\hat{CP} = 450\text{w}$ and $\hat{W}' = 3.575\text{j}$. Both these results represent relatively high values of CP and low values of W' . In Figure 4.8 the results of OLS and WLS on the pronounced maxima of cyclist 2 are plotted. In Figure 4.8a the OLS clearly overestimates the data points with relative high t_{exh} and thus leading to an overestimation of CP . However, the WLS seems to have found a more accurate fit. In Figure 4.8b \bar{P} is plotted against $1/t_{\text{exh}}$, because these are the variables between which a linear relationship is sought. From this figure we notice that the relation between the two variables $1/t_{\text{exh}}$ and \bar{P} is not linear, thus the estimators are not useful. This is another reason Tsai [24] proposed the relationship constant, to transform the relation between $1/t_{\text{exh}}$ and \bar{P} to a linear relation.

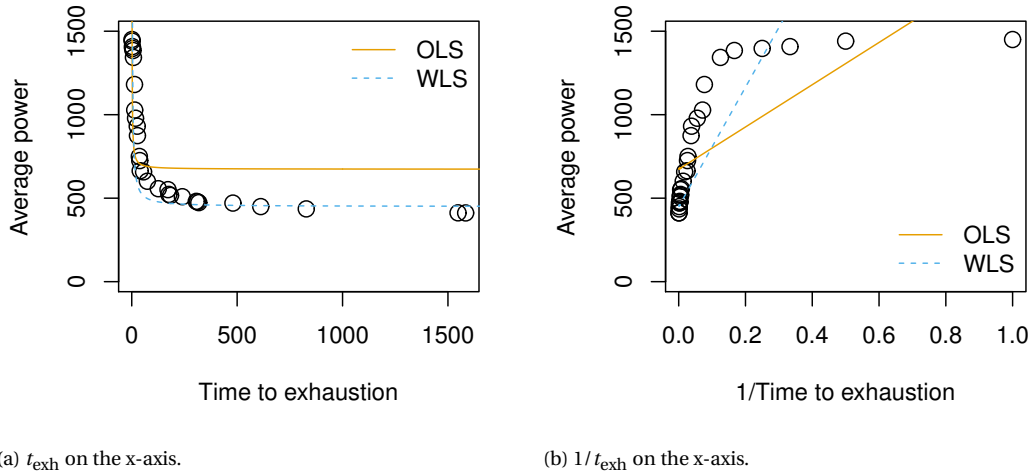


Figure 4.8: Regressions of the curvilinear-P model on the pronounced maxima.

4.3.4. Relationship-CP model for a single cyclist

In the relationship-CP model of Tsai [24] a relationship parameter n is added to the explanatory variable; $1/t_{\text{exh}}^n$. This is done to transform the relation between the explanatory variable and the response variable \bar{P} to a linear relation. Independently and normally distributed errors $\epsilon_i \stackrel{\text{iid}}{\sim} N(0, \sigma_\epsilon^2)$ are again assumed to be present in the data. Thus, the data is described as stated in Equation (4.14).

$$\bar{P}_i = \frac{a}{t_i^n} + b + \epsilon_i \quad (4.14)$$

In [24] it is found that $n = 0.48$ for cyclists, thus using this value we can perform OLS and WLS on the data to calculate \hat{a} and \hat{b} through the following equation.

$$(\hat{a}, \hat{b}) = \operatorname{argmin} \sum_{i=1}^I \left(\bar{P}_i - \frac{\hat{a}}{t_i^{0.48}} - \hat{b} \right)^2 \cdot w_i \quad (4.15)$$

After calculating \hat{a} and \hat{b} the estimates of CP and W' are calculated as proposed in Section 4.1, i.e. $\hat{CP} = \hat{a}$ and $\hat{W}' = \hat{b} \cdot 90^{1-0.48}$.

The transformation of $\frac{1}{t_{\text{exh}}}$ to $\frac{1}{t_{\text{exh}}^{0.48}}$ is shown in Figure 4.9b, which indeed shows a stronger linear relationship between the two variables. However, the OLS visualized in Figure 4.9a still overestimates the CP while the WLS seems to have found a good fit. The estimations of OLS are $\hat{CP} = 474$ W and $\hat{W}' = 15.029$ j and of WLS are $\hat{CP} = 348$ W and $\hat{W}' = 22.671$ j.

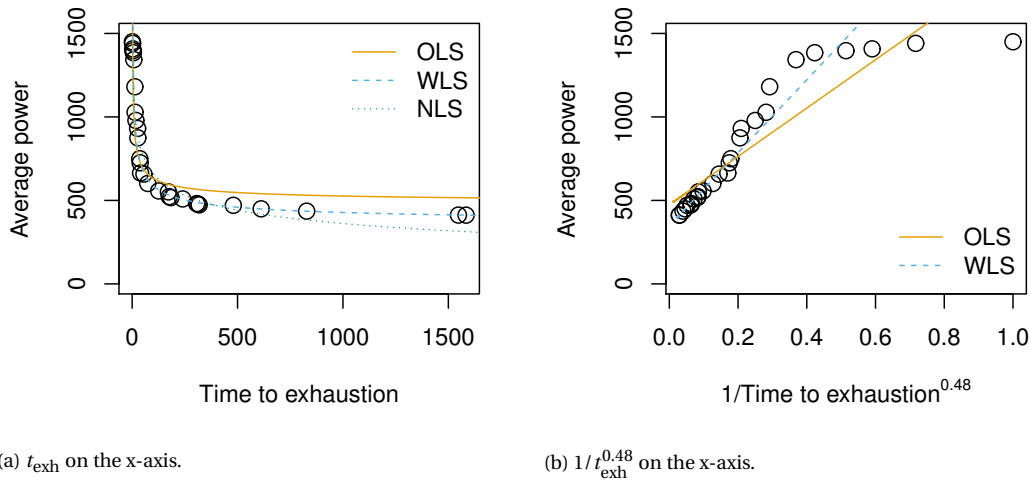


Figure 4.9: OLS, WLS, and NLS performed on the relationship model. The right plot shows the x-axis transformation of the left plot.

A non-linear regression is also performed on the relationship model, this time without fixing n , but including it into the regression. Thus, the data is described as stated in Equation (4.14), but this time n is assumed to be an unknown parameter for every single cyclist. This way, the regression tries to transform the data such that it can be approximated by a linear regression, i.e. calculating the following values.

$$(\hat{a}, \hat{b}, \hat{n}) = \operatorname{argmin} \sum_{i=1}^I \left(\bar{P}_i - \frac{\hat{a}}{t_i^{\hat{n}}} - \hat{b} \right)^2 \cdot w_i \quad (4.16)$$

These values can not be computed by solving a linear system of normal equations as is the case for OLS and WLS. The normal equations of the NLS for this model are stated here:

$$\begin{aligned} -2 \sum_{i=1}^I \frac{w_i}{t_i^{\hat{n}}} \left(\bar{P}_i - \frac{\hat{a}}{t_i^{\hat{n}}} - \hat{b} \right) &= 0 \\ -2 \sum_{i=1}^I w_i \left(\bar{P}_i - \frac{\hat{a}}{t_i^{\hat{n}}} - \hat{b} \right) &= 0 \\ -2 \sum_{i=1}^I \hat{a} t_i^{-\hat{n}} \ln(t_i) w_i \left(\bar{P}_i - \frac{\hat{a}}{t_i^{\hat{n}}} - \hat{b} \right) &= 0 \end{aligned} \quad (4.17)$$

As can be seen, these equations are not linear in \hat{n} and therefore the algorithm of Gauss-Newton is used to find the values for \hat{a} , \hat{b} and \hat{n} [5]. The Gauss-Newton approximation requires starting values for \hat{a} , \hat{b} , and \hat{n} . We

use $\hat{n} = 0.48$ and for \hat{a} and \hat{b} the estimated values of WLS as starting values. After running the approximation we calculate $\hat{C}P = \hat{a}$ and $\hat{W}' = \hat{b} \cdot 90^{1-\hat{n}}$.

The regressions yields a value of $\hat{n} = 0.15$ such that the transformation is performed as visualized in Figure 4.10. The estimations of NLS are $\hat{C}P = -390$ W, $\hat{W}' = 96.143$ j and $\hat{n} = 0.15$. It is remarkable that the NLS value of $\hat{n}(0.15)$ is significantly lower than the value claimed by Tsai [24], which was 0.48 ± 0.15 . This may be due to the fact that Tsai estimated his value of n on the data of competitive cyclists, where our data comes from elite cyclists. In Table 4.2, we see the different estimators of \hat{n} for the different cyclists. From this table it looks like \hat{n} is always lower than 0.48. Even more remarkable is that the method of NLS leads to negative values for $\hat{C}P$ for four out of six cyclists as can be seen in Table 4.3.

Cyclist	Cyclist 1	Cyclist 2	Cyclist 3	Cyclist 4	Cyclist 5	Cyclist 6
\hat{n}	0.13	0.15	0.13	0.34	0.34	0.23

Table 4.2: Values of \hat{n} for the different cyclists

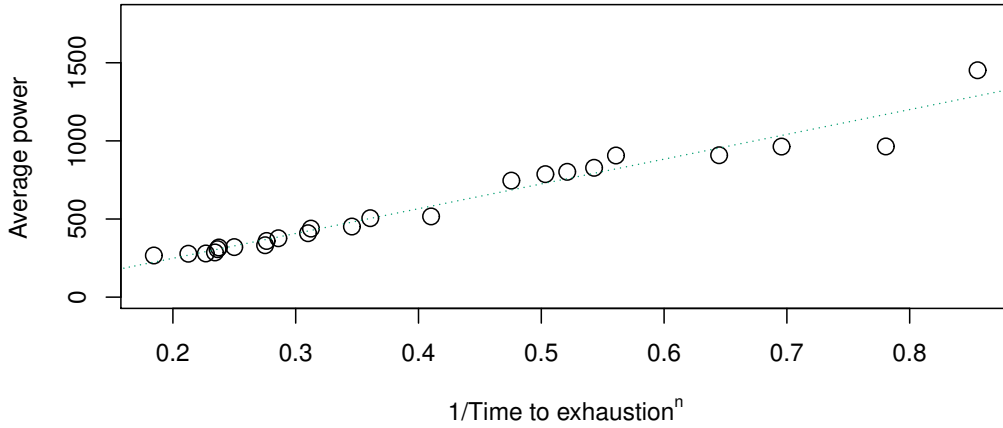


Figure 4.10: Relationship transformation with $n = 0.15$ and the corresponding NLS for cyclist 2

4.3.5. Relationship-CP model on multiple cyclists

In this section we assume that the relationship parameter n is equal for all cyclists and perform NLS on the data set of the pronounced maxima of all six cyclists. We assume the data is described as in Equation (4.18) where the index $i \in [1, I_r]$ are the data points for cyclist $r \in [1, 6]$ and $\epsilon_{ri} \stackrel{\text{iid}}{\sim} N(0, \sigma_\epsilon^2)$.

$$\bar{P}_{ri} = \frac{a_r}{t_{ri}^n} + b_r + \epsilon_{ri} \quad (4.18)$$

NLS is performed to find the values of \hat{n} , \hat{a}_r and \hat{b}_r for $r \in [1, 6]$ that satisfy the following equation.

$$(\hat{n}, \hat{a}_r, \hat{b}_r) = \operatorname{argmin} \sum_{r=1}^6 \sum_{i=1}^{I_r} \left(\bar{P}_{ri} - \frac{a_r}{t_{ri}^n} - b_r \right)^2 \cdot w_{ri} \quad (4.19)$$

This leads to $2 \cdot 6 + 1 = 13$ equations similar to those in Equation (4.17). In these equations w_{ri} can be chosen to be equal to 1 such that all data points are weighted equally or $w_{ri} = t_{ri}$ such that measurement errors are taken into account. The normal equations are again solved by Gauss-Newton with starting values $n = 0.48$ and a_r, b_r equal to the estimated values \hat{a} and \hat{b} of Equation (4.15).

For weights all equal to 1 the estimator $\hat{n} = 0.16$ and all six $\hat{C}P_r$ values are negative. Taking the weights of $w_{ri} = t_{ri}$ and thus taking the measurement errors into account, the estimator $\hat{n} = 0.38$ and the values of $\hat{C}P_r$ are all positive. They are discussed in detail in the next section, but we can already conclude that the

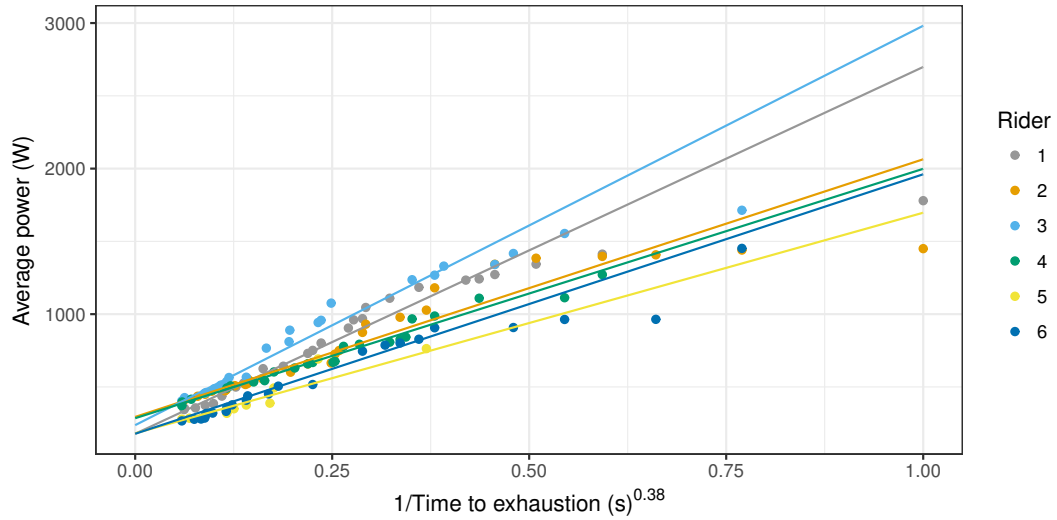


Figure 4.11: Regression of NLS on the relationship-CP model with a single value of n for all cyclists.

weights w_{r_i} are important in this setting. The linear regression lines of \bar{P} versus $1/t_{\text{exh}}^{0.38}$ are shown in Figure 4.11 together with the data points of all cyclists. The accuracy of these regression lines is hard to judge visually, because the points with a high weight, thus a high t_i have a small $1/t_i^{0.38}$ and are close together in the plot. Despite this, a linear relationship between \bar{P} and $1/t_{\text{exh}}^{0.38}$ seems justifiable from this plot.

4.4. Results

In this section the estimations of the different models and statistical methods are stated and compared. The critical power estimates are compared in Subsection 4.4.1, the W' estimates in Subsection 4.4.2. Finally, one combination of mathematical model and statistical method is picked.

4.4.1. CP

In Table 4.3 the values of the estimates of CP are stated for the different mathematical models and statistical methods. First of all, we notice that the estimates of OLS on the curvilinear-P model are unrealistically high, thus this combination of model and method does not lead to practical results. This is in accordance with the conclusions drawn from Figure 4.8a. Furthermore, NLS on the relationship model with a different value of \hat{n} for every cyclist leads to negative values for the critical power, therefore this combination of method and model does also not lead to realistic results. The estimates of CP when \hat{n} is assumed to be constant for all cyclists are low and another unexpected result surfaces; cyclist 1 has a lower estimated CP than cyclist 5. This is unexpected since there is a gender difference between the two cyclists and elite male cyclists are in general believed to have a higher CP than elite female cyclists, as is supported by the results of Table 4.1.

Table 4.3: Estimations of CP in watts for the different cyclists and methods.

	Linear-TW		Curvilinear-P		Relationship-CP model			
	OLS	WLS	OLS	WLS	OLS	WLS	NLS single	NLS all
Cyclist 1	340	330	735	389	480	253	-757	178
Cyclist 2	410	396	673	450	473	348	-390	294
Cyclist 3	406	387	727	461	482	318	-713	237
Cyclist 4	382	367	567	410	281	331	253	285
Cyclist 5	271	269	343	282	217	215	117	181
Cyclist 6	265	251	434	302	280	205	-68	149

From Table 4.1 we would expect the order of estimated CP from highest to lowest to be: cyclist 4, cyclist 2/cyclist 3, cyclist 5, cyclist 6 (cyclist 1 has not performed 20 minutes all out tests yet). It is remarkable that

in the remaining 6 combinations cyclist 4 has a lower estimated CP than cyclist 2 and in four of the six combinations also lower than cyclist 3. In OLS performed on the relationship model, cyclist 4 even has an equal estimated CP as cyclist 6. Additionally, we concluded from Figure 4.9a that this combination of model and method does not yield good results, so we do not consider it an accurate combination.

4.4.2. W'

In Table 4.4 the estimated values of W' are stated for the different models. According to the literature and experience within Team Sunweb the range of W' for elite cyclists is 10.000 - 40.000j thus the OLS and WLS on the curvilinear-P model and NLS on the relationship-CP model do not lead to realistic estimations of W' . Furthermore, OLS leads to low values of W' on both the linear-TW and relationship-CP model. Therefore, the two most accurate combinations of model and method are WLS on the linear-TW and relationship-CP model. For the remainder of this report, the estimations of WLS on the relationship-CP model are used in order to avoid the pitfall indicated by Tsai [24], described in Section 4.1 and visualized in Figure 4.7b.

Table 4.4: Estimations of W' in joule for the different cyclists and methods.

	Linear-TW		Curvilinear-P		Relationship-CP model			
	OLS	WLS	OLS	WLS	OLS	WLS	NLS single	NLS all
Cyclist 1	17.965	28.534	1.369	5.487	17.921	32.271	132.303	82.223
Cyclist 2	13.382	26.571	1.265	3.574	15.029	22.671	96.144	57.755
Cyclist 3	24.033	43.289	2.826	7.276	23.000	35.552	137.425	89.530
Cyclist 4	14.206	33.255	3.390	6.774	19.059	22.659	31.628	55.903
Cyclist 5	16.397	17.979	6.778	11.150	22.178	21.987	32.680	49.450
Cyclist 6	15.417	28.078	2.210	4.283	16.561	22.682	51.743	58.166

4.4.3. Trade-off

It is interesting to see how the estimates of CP and W' relate to each other. A cyclist with a high CP needs less anaerobic energy to maintain a high power, while a cyclist with low CP requires more anaerobic energy to maintain the same power. Therefore, we would expect high values of CP to go with low values of W' and vice versa. In Figure 4.12 the pairs of estimates of CP and W' are plotted, clustered on the model and method that leads to the estimates. In this figure the relationship-CP model with NLS on each single cyclist is left out due to the negative values of its CP estimates. This plot confirms our believe that high values of CP pairs with low values of W' and vice versa. It also shows which methods lead to relatively high or low values of CP .

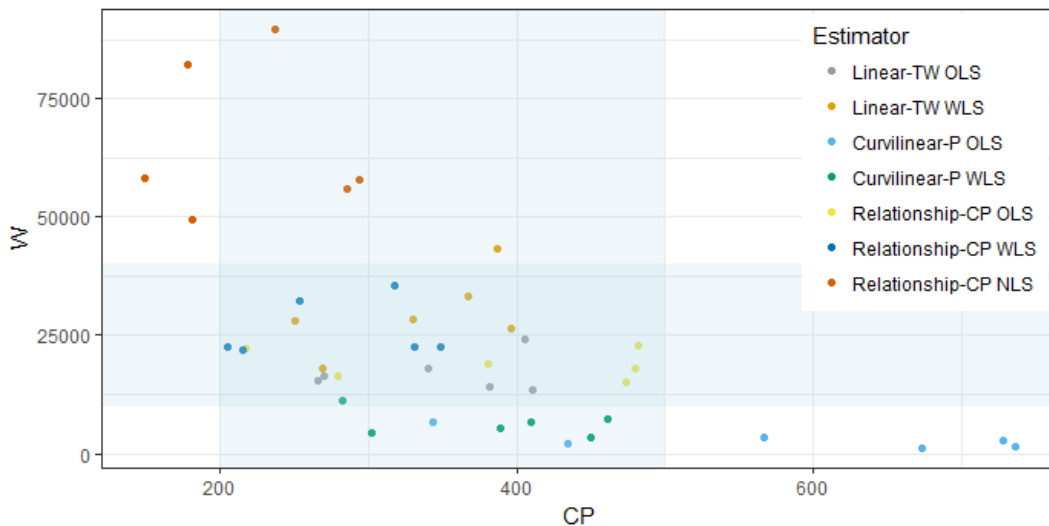


Figure 4.12: The trade off between CP and W' for the different estimators. The blue bands represent the range within we expect the estimates of CP and W' .

4.5. Accuracy of the estimators

Now that we have chosen a model with which to estimate the values of CP and W' , we want to quantify the accuracy of these estimators. Under the law of large numbers, we assume a normal distribution and calculate 95% confidence intervals by adding and subtracting 1.96 (the 97.5 percentile point of the normal distribution, leading to a symmetrical 95% confidence interval) times the value of standard error divided by the square root of the number of observations of the estimate. The resulting values are stated in Table 4.5.

Table 4.5: 95%-confidence intervals for the estimators of the WLS relationship-CP model.

	CP	W'
Cyclist 1	253 ± 4	32.271 ± 637
Cyclist 2	348 ± 3	22.671 ± 380
Cyclist 3	318 ± 6	35.552 ± 935
Cyclist 4	331 ± 2	22.659 ± 369
Cyclist 5	215 ± 10	21.987 ± 1.973
Cyclist 6	205 ± 3	22.682 ± 532

The table shows that the estimations have small confidence intervals. Do keep in mind that the estimates are based on the assumption that the relationship-CP model on a single cyclist is correct with a relationship parameter of 0.48 and on the assumption that pronounced maxima are a good representation of intervals in which the cyclist goes all out.

4.6. Conclusion

Although critical power (CP) and anaerobic work capacity (W') are considered to yield good indicators of the performance level of an athlete, their estimation procedures based on experimental data can not be performed on a regular basis. The daily power meter data can be used to obtain estimates of CP and W' , but since multiple daily power meter data sets are required to obtain these estimates, the estimates can only be obtained over a longer period of time. Therefore, the models and methods of this chapter do not yield a frequent performance metric.

Without a frequent performance metric the impact of training attributes on the performance of a cyclist can not be modeled as thoroughly as we would like to. To be able to do this, we need to be able to monitor the performance of a cyclist on a more frequent basis (e.g. daily) and it is practically impossible to perform a daily 3-minute or 20-minute all-out test. In Chapter 6, a performance metric is proposed that is less rigorous than the critical power and anaerobic work capacity, but can be calculated on a more frequent basis. Before this performance metric can be introduced, we need to be able to model the dynamics of the anaerobic work supply. Therefore, the next chapter, Chapter 5 dives into the question how to model the anaerobic work supply.

5

Modeling the anaerobic work supply

“Life is like riding a bicycle. In order to keep your balance, you must keep moving” — Albert Einstein

In the next chapter, we introduce a concept to quantify the performance of a cyclist. Before that is possible, another part of the existing physiological models needs to be introduced; models that can monitor the anaerobic work supply based on power output data. This chapter starts by introducing the mathematical assumptions of this model in Section 5.2. Subsequently, in Sections 5.3 and 5.4 the existing models are evaluated and flaws in these models are highlighted. To overcome these flaws, a new model is proposed in Section 5.5 and its validity is evaluated in Section 5.6.

5.1. Introduction

The W' estimated in the previous chapter represents the anaerobic work capacity, i.e. the number of kilojoules the body can expend above critical power. Skiba et al.[21] propose a dynamic model in which the anaerobic energy supply is also reconstituted when a cyclist performs below his or her critical power. To make this model more tangible, we will therefore refer to the anaerobic work supply as a battery, where W' is the capacity of the battery. The remaining energy in the battery is referred to as the anaerobic work supply. This model is based on the following assumptions;

1. The expenditure of W' begins the moment a cyclist exceeds CP ,
2. The reconstitution of W' begins the moment the subject falls below CP , and
3. The reconstitution follows a deterministic exponential time course.

These assumptions correspond to the battery that is draining when the cyclist is exceeding his or her CP and recharging at an exponential rate when the cyclist is performing below his or her CP . In [19] the model is improved by testing for various lengths of recovery intervals and in [20] the validity of the W'_{bal} model is tested in the field with power meter data. Skiba et al. [19] conclude that the calculated W'_{bal} was significantly different between two different conditions: a cyclist claiming to be exhausted, and a cyclist claiming not to be.

5.2. Mathematical assumptions and model derivation

The model proposed in the paper of Skiba et al. [21] is lacking the mathematical justification. Therefore, in this section, we state the underlying mathematical assumptions that are required for this model.

The balance of W' at a certain time t is denoted by $W'_{\text{bal}}(t)$ and represents the number of kilojoules of anaerobic work supply available at time t . In other words, $W' - W'_{\text{bal}}(t)$ is the number of kilojoules that is missing from the initial supply W' at time t . The value of $W'_{\text{bal}}(t)$ can thus be interpreted as the amount of energy stored in the battery at time t . Notice that it is required that $0 \leq W'_{\text{bal}}(t) \leq W'$ for every t . In this section the dynamics of $W'_{\text{bal}}(t)$ are translated to differential equations, which are solved afterwards in order to be able to calculate $W'_{\text{bal}}(t)$. A distinction is made between times t at which $P(t) \geq CP$ and $P(t) < CP$ where $P(t)$ is the power output at time t of the cyclist. In the case that $P(t) \geq CP$ we assume that the balance of W' decreases with a rate of $P(t) - CP$, which is linear when $P(t)$ is constant over a given time interval. When

the cyclist is performing below CP , i.e. $P(t) < CP$, we assume that the balance of W' increases with a rate proportional to two values; 1) the difference between CP and $P(t)$, and 2) the difference between W' and $W'_{\text{bal}}(t)$. The former is because we assume energy is reconstituted faster when the cyclist is performing at a lower power. The latter indicates that the rate of reconstitution depends positively on how much energy is missing. Notice that we choose a rate proportional to $(CP - P(t))$ multiplied with $W' - W'_{\text{bal}}(t)$. This is a specific choice and other options could be explored in future research.

Consider the time interval $[t, t + \Delta t]$ with Δt sufficiently small such it holds for the entire interval that $P(t) > CP$ and that $P(t)$ is constant. Then we have that during the interval $[t, t + \Delta t]$ the amount of energy of $\Delta t \cdot (CP - P(t))$ is expended. Thus, we make the following derivation to find the dynamics of $W'_{\text{bal}}(t)$:

$$\begin{aligned} W'_{\text{bal}}(t + \Delta t) &= W'_{\text{bal}}(t) - \Delta t \cdot (P(t) - CP) \\ \lim_{\Delta t \rightarrow 0} \frac{W'_{\text{bal}}(t + \Delta t) - W'_{\text{bal}}(t)}{\Delta t} &= -(P(t) - CP) \\ \frac{dW'_{\text{bal}}(t)}{dt} &= -(P(t) - CP) \end{aligned} \quad (5.1)$$

Thus, at points in time that $P(t) > CP$ we have that $W'_{\text{bal}}(t)$ is decreasing linearly with respect to the difference between $P(t)$ and CP .

Now consider once more the time interval $[t, t + \Delta t]$, but this time with Δt sufficiently small such that in the entire interval it holds that $P(t) < CP$ and $P(t)$ is constant. Now, we assume that $W'_{\text{bal}}(t)$ is increasing at a rate proportional to the values of $CP - P(t)$ and $W' - W'_{\text{bal}}(t)$. The product of the two terms is divided by a constant $\tau_{W'}$, which represents the rate of recovery for a cyclist, i.e. how fast does a cyclist recharges his or her battery. Now we can make the following derivation to find the dynamics of $W'_{\text{bal}}(t)$.

$$\begin{aligned} W'_{\text{bal}}(t + \Delta t) &= W'_{\text{bal}}(t) + \Delta t \cdot (CP - P(t)) \cdot (W' - W'_{\text{bal}}(t)) / \tau_{W'} \\ \lim_{\Delta t \rightarrow 0} \frac{W'_{\text{bal}}(t + \Delta t) - W'_{\text{bal}}(t)}{\Delta t} &= (CP - P(t)) \cdot (W' - W'_{\text{bal}}(t)) / \tau_{W'} \\ \frac{dW'_{\text{bal}}(t)}{dt} &= (CP - P(t)) \cdot (W' - W'_{\text{bal}}(t)) / \tau_{W'} \end{aligned} \quad (5.2)$$

Combining the Equations (5.1) and (5.2) yields the dynamics of $W'_{\text{bal}}(t)$ as stated in Formula (5.3).

$$\frac{dW'_{\text{bal}}(t)}{dt} = \begin{cases} -(P(t) - CP) & \text{if } P(t) \geq CP \\ (CP - P(t)) \cdot (W' - W'_{\text{bal}}(t)) / \tau_{W'} & \text{if } P(t) < CP \end{cases} \quad (5.3)$$

5.3. Current model

The current model, as proposed by Skiba et al. in [19], [20], and [21] is based on the three assumptions stated in the introduction of this chapter, and according to us also on the mathematical assumptions stated in the previous subsection. Their model is summarized in the Equation stated in (5.4).

$$W'_{\text{bal}}(t) = W' - \int_0^t W'_{\text{exp}}(u) \cdot e^{-(t-u)/\tau_{W'}} du \quad (5.4)$$

In this equation, $W'_{\text{bal}}(t)$ is the amount of kilojoules available at time t , $W'_{\text{exp}}(u)$ is the expended energy at time u , i.e. $W'_{\text{exp}}(u) = \max(P(u) - CP, 0)$, and $\tau_{W'}$ is a constant that determines the rate of reconstitution of W' . In [19], [20], and [21] the constant $\tau_{W'}$ is calculated through Equation (5.5) in which the recovery power (RP) is used. The recovery power is the average power of the exercise below critical power, i.e. $RP = \int_0^T (CP - P(t)) \mathbb{1}_{\{P(t) < CP\}} dt$.

$$\tau_{W'} = 546 \cdot e^{-0.01 \cdot (CP - RP)} + 316 \quad (5.5)$$

It was recently shown that this equation does not hold for elite cyclists, such as we are investigating. Bartram et al. [3] propose another formula for $\tau_{W'}$ that is suited to elite cyclists, which is used in this report and stated in Equation (5.6).

$$\tau_{W'} = 2287.2 \cdot (CP - RP)^{-0.688} \quad (5.6)$$

The current implementation of monitoring $W'_{\text{bal}}(t)$ is done by an approximation of the integral in Equation (5.4) as proposed in [10]. The interval $[0, T]$ is discretized into N time steps of length h , i.e. $0 = t_0 < t_1 < \dots < t_N = T$. The length h is assumed to be constant, which is a justifiable assumption since most power meters store data on equidistant time intervals. In Equation (5.7) the integral of (5.4) is approximated by a summation. This is possible under the assumption that $\tau_W \gg h$.

$$\begin{aligned} I_t &= \int_0^t W'_{\text{exp}}(u) \cdot e^{-(t-u)/\tau_{W'}} du \\ &\approx \sum_{j=0}^i W'_{\text{exp}}(j) \cdot e^{-(i-j) \cdot h/\tau_{W'}} \end{aligned} \quad (5.7)$$

Rewriting the formula for I_t , it can be calculated recursively, as stated in the following equation.

$$\begin{aligned} I_t &\approx W'_{\text{exp}}(i) + \sum_{j=0}^{i-1} W'_{\text{exp}}(j) \cdot e^{-(i-j) \cdot h/\tau_{W'}} \\ &= W'_{\text{exp}}(i) + e^{-h/\tau_{W'}} \sum_{j=0}^{i-1} W'_{\text{exp}}(j) \cdot e^{-(i-1-j) \cdot h/\tau_{W'}} \\ &= W'_{\text{exp}}(N) + e^{-h/\tau_{W'}} I_{t-h} \end{aligned} \quad (5.8)$$

Using Equation (5.8) the integral of Equation (5.4) can be approximated for every time step and $W'_{\text{bal}}(t)$ can be easily calculated by $W'_{\text{bal}}(t) = W' - I_t$ where $t = N \cdot h$.

5.4. Mismatch between assumptions and model

One of the assumptions in the model of [21] is that W' is not recovered during the period in which a cyclist is performing above CP . But technically this assumption does not hold in Expression (5.4). We illustrate this by using a suitable artificial example. Let us have a cyclist with a CP of 200 Watt and a W' of 10.000 joule. Now assume this cyclist has a power output of 300 for the first 100 seconds and a power output of 100 for the next 100 seconds of an exercise. According to the assumptions, he should be expending $300 - 200 = 100$ joule every second the first 100 seconds and not recovering any of the expended energy because he is performing above CP . Thus, after 100 seconds W'_{bal} should be $10.000 - 100 \cdot 100 = 0$. But, the model of Equation (5.4) yields the anaerobic energy supply at $t = 100$ is equal to 3.781 as in Equation (5.9). Notice that $RP = 200$ and therefore $\tau'_W = 96.23$ according to Equation (5.6).

$$\begin{aligned} W'_{\text{bal}}(100) &= W' - \int_0^{100} W'_{\text{exp}}(u) \cdot e^{-(100-u)/\tau_{W'}} du \\ &= 10.000 - \int_0^{100} 100 \cdot e^{-(100-u)/96.23} du \\ &= 3.781 \end{aligned} \quad (5.9)$$

The sketched situation is visualized in Figure 5.1 where we see the power output, critical power and dynamic values of W'_{bal} . This figure illustrates that the current implementation does not correspond with the assumptions because the remaining energy at $t = 100$ is approximately 3.800, where it should have been zero. This can also be seen from the curve of W'_{bal} between $t = 0$ and $t = 100$ which is not a linear line as it should be, but an exponential decay.

Furthermore, the simplification of calculating RP as the average power of all power output below CP is in our opinion an oversimplification. In addition to the mismatch stated above it leads to an unrealistic situation while the power output in the second half has influence on the reconstitution rate in the first half. We find it more plausible that reconstitution of W' depends on the power performed at that exact moment, i.e. reconstitution is faster when a small wattage is used compared to a high wattage. This means the recovery rate should depend on the difference between CP and $P(t)$ and not on the difference between CP and RP .

Another example shows the problem of taking the recovery power over the entire ride. Again, we look at a cyclist with a CP of 200 watts and W' of 10.000 joule. This time, he rides 100 seconds with a power output

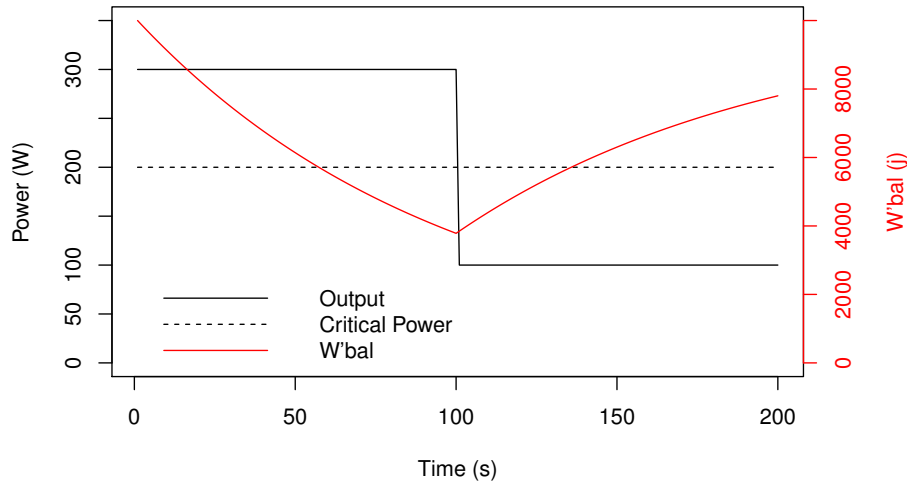


Figure 5.1: The dynamic value of W'_{bal} for the current implementation in an artificial setting.

of 300, then rides 100 seconds with a power output of 199 watts and then 1.000 seconds with a power output of 10 watts, see Figure 5.2 for a visualization of this exercise. As before, we would expect $W'_{bal}(100)$ to be equal to zero, but in this case it is even above 4.500. This is due to the fact that the cyclist is already restoring while performing above CP and the speed of recovery during this period depends on the power output in the subsequent rest-period. Furthermore, in the period in which the cyclist is performing just below his CP at 199 watts, he is restoring almost all expended joules. Both unexpected results are due to the fact that recovery power at that point is taken over the average of the entire period from $t = 201$ to $t = 1200$ at which the cyclist is performing below CP . Therefore, $RP = (100 \cdot 199 + 1000 \cdot 10) / 1100 = 27$ such that $\tau_{W'} = 2287.2 \cdot (200 - 27)^{-0.688} = 66$. Because of this low value of $\tau_{W'}$ the recovery of W' during the entire exercise is fast, even during the period in which the cyclist is performing above or just below CP .

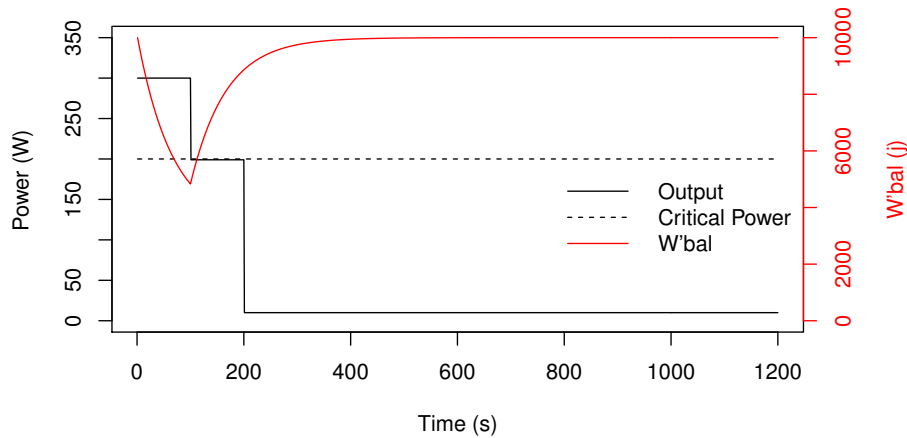


Figure 5.2: The dynamic value of W'_{bal} for the current implementation in an artificial setting.

5.5. Proposed model

The new model proposed in this section is based on the dynamics of $W'_{\text{bal}}(t)$ derived in Equation (5.3). Furthermore, it is shown that the model complies with the assumptions made by Skiba et al. [21], which are stated in the introduction of this chapter. Notice that the proposed model is our interpretation of the given assumptions and that other models can also be investigated further in future research.

Because the power at time t , $P(t)$, is stored discretely instead of continuously, the dynamics stated in Equation (5.3) are translated to a discrete setting. Assume that we use an equidistant grid for the time differentiation, which is justifiable because a power meter stores data every second, with a time step of length h . Thus, we divide the interval $[0, T]$ into equidistant time steps $0 = t_0 < t_1 < \dots < t_N = T$ where $t_i = i \cdot h$ and $N = T/h$. Now Equation (5.3) yields the following translation in the discrete setting.

$$W'_{\text{bal}}(t_i) = \begin{cases} W'_{\text{bal}}(t_{i-1}) - h \cdot (P(t_{i-1}) - CP) & \text{if } P(t_{i-1}) \geq CP \\ W'_{\text{bal}}(t_{i-1}) + h \cdot (CP - P(t_{i-1})) \cdot (\hat{W}' - W'_{\text{bal}}(t_{i-1})) / \tau_{W'}(t) & \text{if } P(t_{i-1}) < CP \end{cases} \quad (5.10)$$

In this model we use the $\tau_{W'}$ of Equation (5.6), but instead of the recovery power RP we use $P(t_i)$, such that the rate of recovery depends directly on the applied power at time t instead of the average recovery power. Thus, $\tau_{W'}(t)$ now depends on $P(t)$ and thus indirectly on t , i.e.

$$\tau_{W'}(t) = 2287.2 \cdot (CP - P(t))^{-0.688} \quad (5.11)$$

This way, the rate of reconstitution of $W'_{\text{bal}}(t)$ does not depend on the average recovery power, which can give a distorted view, but rather on the difference between CP and $P(t)$ at a particular time point t . Using $\tau_{W'}(t)$ dependent on $P(t)$ instead of RP tackles the problem stated in Section 5.4 and Figure 5.2, in which a cyclist has a high rate of recovery while he is performing just below CP since he has a low RP .

The three assumptions of Skiba et al. [21] are now shown to be satisfied by the proposed model of Equation (5.10). The first assumption is that the expenditure of W' begins the moment a cyclist exceeds CP . In Equation (5.10) it is clear that at time t_i a cyclist exceeds CP , i.e. $P(t_i) > CP$, then one time step later t_{i+1} , W'_{bal} is expended by an amount of $h \cdot (P(t_i) - CP)$. The second assumption states that the reconstitution begins the moment the subject falls below CP . If, at time t_i the cyclist falls below CP , i.e. $P(t_i) < CP$, then one time step later W'_{bal} is recovered with an amount of $h \cdot (CP - P(t_{i-1})) \cdot (W' - W'_{\text{bal}}(t_{i-1})) / \tau_{W'}$. The only mismatch is that the expenditure and reconstitution do not start directly when a cyclist respectively exceeds or falls below CP , but one time step later. We believe that with a small value of h , the impact of this inaccuracy is negligible. The third assumption is the hardest one to show and define mathematically. Our interpretation is as follows; during a time interval $[t_i, t_j]$ for which $P(t)$ is constant and below CP , the rate of reconstitution is negatively exponential in the elapsed time since the beginning of the recovery interval, i.e. t_i , as in Equation (5.4).

In order to show that the proposed model satisfies this assumption, we assume that during the time interval $[t_i, t_j]$ $P(t)$ is constant, i.e. for all $t \in [t_i, t_j] : P(t) = P$ for a fixed $P < CP$, such that Equation (5.2) results in:

$$\begin{aligned} \frac{d}{dt} W'_{\text{bal}}(t) &= (CP - P)(W' - W'_{\text{bal}}(t)) / \tau_{W'}(t) \\ \frac{d}{dt} (W' - W'_{\text{bal}}(t)) &= -(CP - P)(W' - W'_{\text{bal}}(t)) / \tau_{W'}(t) \\ W' - W'_{\text{bal}}(t) &= c_1 \cdot e^{-(CP-P)(t-t_i)/\tau_{W'}(t)} \\ W'_{\text{bal}}(t) &= W' - c_1 \cdot e^{-(CP-P)(t-t_i)/\tau_{W'}(t)} \end{aligned} \quad (5.12)$$

Now introducing the boundary condition at $t = t_i$ where $W'_{\text{bal}}(t_i) = W' - W'_{\text{exp}}(t_i)$. Here $W'_{\text{exp}}(t_i)$ is the amount of energy expended at time t_i , i.e. $W'_{\text{exp}}(t_i) = W' - W'_{\text{bal}}(t_i)$, the amount of energy depleted. This boundary condition yields that $c_1 = W'_{\text{exp}}(t_i)$ thus

$$W'_{\text{bal}}(t) = W' - W'_{\text{exp}}(t_i) \cdot e^{-(CP-P)(t-t_i)/\tau_{W'}(t)} \quad t \in [t_i, t_j] \quad (5.13)$$

Comparing the new and current model, i.e. Equations (5.4) and (5.13), we notice two differences. The first difference is the integral that is present in the second term of Equation (5.4) which is absent in Equation (5.13), the second one is the term $(CP - P)$ which is present in the exponent in Equation (5.13) and absent in

Equation (5.4). The absence of the integral in the proposed model is explained by the fact that in Equation (5.13) we assume that $P < CP$ in the interval $[t_i, t]$. Making the same assumption in Equation (5.4) yields that $W'_{\text{exp}}(u) = 0$ for $u \in [t_i, t]$ because $P < CP$ indicates that no energy is expended. Therefore, Equation (5.4) becomes $W' - W'_{\text{exp}}(t_i) \cdot e^{-(t-t_i)/\tau_{W'}}$. The explanation for the second difference is found in the definition of $\tau_{W'}$. Taking the formula for $\tau_{W'}$ of Equation (5.6) in which RP is substituted by $P(t)$, the presence of the term $(CP - P(t))$ in the exponent of Equation (5.13) can be incorporated in the formula of $\tau_{W'}$ by increasing the exponent of $(CP - P(t))$ in Equation (5.11) by one.

Finally, we need to show that $0 \leq W'_{\text{bal}}(t) \leq W'$. The fact that $0 \leq W'_{\text{bal}}(t)$ does not follow directly from Equation (5.13), but the values of CP and W' should be chosen in such a way that a negative W'_{bal} is impossible. This is because a negative W'_{bal} is practically impossible as well and would thus indicate an error in the values of either CP or W' .

The fact that $W'_{\text{bal}}(t) \leq W'$ does follow directly from Equation (5.13) and we prove this by induction. First of all, at time $t = 0$ we have that $W'_{\text{bal}}(0) = W'$, thus $W'_{\text{bal}}(0) \leq W'$. Now assume that $W'_{\text{bal}}(t_{i-1}) \leq W'$, we show that also $W'_{\text{bal}}(t_i) \leq W'$. In the case that $P(t_{i-1}) \leq CP$ it follows from Equation (5.10) that $W'_{\text{bal}}(t_i) = W'_{\text{bal}}(t_{i-1}) - h \cdot (P(t_{i-1}) - CP)$ which is less than or equal to W' because $W'_{\text{bal}}(t_{i-1}) \leq W'$ and $h \cdot (P(t_{i-1}) - CP) \geq 0$.

The case that $P(t_{i-1}) \geq CP$ is harder. Now we need to show that $W'_{\text{bal}}(t_i) \leq W'$ which is equivalent with showing that $W'_{\text{bal}}(t_i) - W'_{\text{bal}}(t_{i-1}) \leq W' - W'_{\text{bal}}(t_{i-1})$. Substituting the value of $W'_{\text{bal}}(t_i)$ from Equation (5.10), results in the following inequality:

$$\begin{aligned} h \cdot (CP - P(t)) \cdot (W' - W'_{\text{bal}}(t)) / \tau_{W'}(t) &\leq W' - W'_{\text{bal}}(t) \\ h \cdot (CP - P(t)) / \tau_{W'}(t) &\leq 1 \\ \frac{h}{2287.2 \cdot (CP - P(t))^{-0.688}} &\leq 1 \\ h \cdot (CP - P(t))^{0.688} &\leq 2287.2 \\ h^{1.5} (CP - P(t)) &\leq 76,332 \end{aligned} \quad (5.14)$$

So under the assumptions that $h = 1$ and $P(t) \geq 0$ this leads to the condition that $CP \leq 76,332$ in order for $W'_{\text{bal}}(t_{i-1}) < W'$. In reality this condition always holds, as the range of realistic values of CP is approximately $[200, 500]$.

Figures 5.3 and 5.4 are the situations from the beginning of this paragraph to which the proposed model of W'_{bal} is added as the dashed red line. In these cases the course of $W'_{\text{bal}}(t)$ behaves as expected, it decreases linearly at the interval $0 < t < 100$ when $P(t) > CP$ and recovers exponentially at the interval $t > 100$ when $CP < P(t)$. Furthermore, $W'_{\text{bal}}(100) = 0$ as it should be. Lastly, in Figure 5.4 it is clear that the rate of recovery is higher when the difference between CP and $P(t)$ is larger.

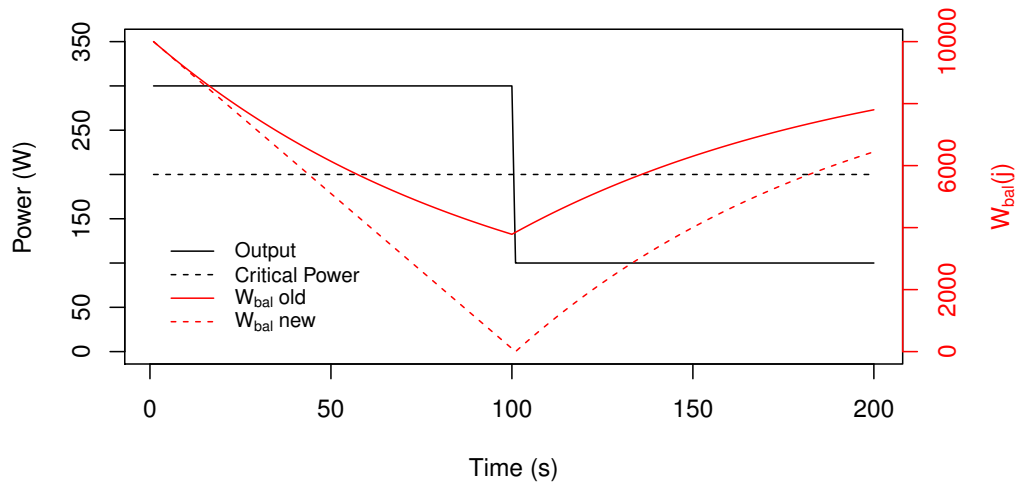


Figure 5.3: The dynamic value of W'_{bal} for the current and proposed implementation in an artificial setting.

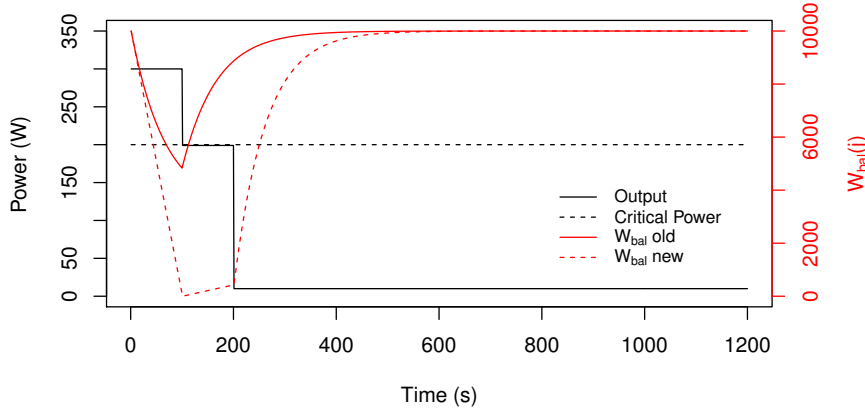


Figure 5.4: The dynamic value of W'_{bal} for the current and proposed implementation in an artificial setting.

5.6. Model validation

In order to validate the model we apply it to the time trial of cyclist 2 of Subsection 3.2.1. We use this time trial because it provides us with a clean data set in which we can assume that the cyclist’s anaerobic work supply was depleted to ride a good time. In Figure 5.5 the results of the calculations of $W'_{bal}(t)$ are plotted in three different situations. The gray and orange line are respectively the new and old method of calculating W'_{bal} for the estimated values of Tables 4.3 and 4.4 with $\hat{C}P = 348$ and $\hat{W}' = 22.671$. Both models do not behave as we expect. The old implementation of the model reaches a minimum of $W'_{bal}(t)$ of 7.475 joule, which is 33% of the capacity. Our assumption was that the cyclist gave his all during the time trial and thus would have reached a minimum of $W'_{bal}(t)$ closer to zero. This is because [20] has shown that $W'_{bal}(t)$ at exhaustion has a 95% confidence interval of 0 – 900 joule.

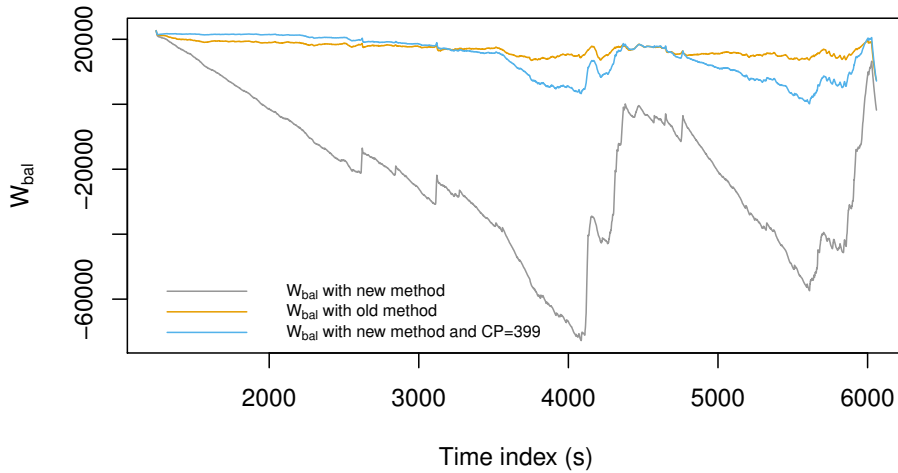


Figure 5.5: The modeled $W'_{bal}(t)$ in the old and new implementation for the time trial of cyclist 2.

However, the new method of calculating W'_{bal} achieves a minimum value of -72.759 joule, which is impossible due to the fact that a cyclist cannot expend energy it does not possess. This could indicate four flaws; firstly the model is not realistic, secondly the estimation of $\tau_{W'}$ is not accurate, thirdly the estimation of CP is incorrect, and finally the estimation of W' is incorrect.

We assume the newly proposed model to be correct and try to find the problem in one of the other flaws indicated. The effect of $\tau_{W'}$ is negligible because in the first 45 minutes of the race, after which the minimum W'_{bal} is reached, the cyclist performs only 6% of the time under his estimated CP . At the time points he is

performing above CP $\tau_{W'}$ does not influence the dynamics of W'_{bal} , thus changing $\tau_{W'}$ would only have a minimal influence on the minimum of W'_{bal} . W' is probably not the problem either. Because it is merely the begin point of $W'_{\text{bal}}(t)$ at $t = 0$, it would need to be increased by 72.759 joule in order to make sure the minimum of $W'_{\text{bal}} = 0$. This would mean the initial estimations has to be multiplied by a factor of 4.2. Therefore, the most plausible conclusion is that the estimation of CP is too low. A minimal CP of 399 is required in order to make sure that the minimum of $W'_{\text{bal}}(t)$ is above zero. The dynamics of $W'_{\text{bal}}(t)$ for $CP = 399$ are also plotted in Figure 5.5.

5.7. Conclusion

Models exist in which the dynamics of the anaerobic work supply are modeled based on the critical power and power output of a cyclist. These models have also been validated in a field test [20], but some mathematical flaws are present in the models. Therefore, a new model is proposed that hopefully provides a more accurate model of the anaerobic work supply. This new model has not been objectively validated yet, thus no claims can be made on its accuracy. In the next chapter, a performance metric will be introduced in which the anaerobic work supply model plays a large role. Therefore, it would be valuable if more research was performed to improve the accuracy of the anaerobic work supply model. This could be achieved by further research in the function of $\tau_{W'}$, the model equations, and by field tests to validate the model.

6

Cycled critical power

“Good morale in cycling comes from good legs” — S. Yates

In order to quantify the performance level of a cyclist, a metric for the performance of a cyclist is required. At the end of the day, a cyclist is judged on his performance during races, so his or her classification in a race appears to be a natural quantification of performance. However, the race result is an incomplete measure for performance, since a cyclist his or her effort during the race is not always captured by it, as a result of tactics, competitors, and the type of stage. Therefore, the results of a race do not quantify the absolute performance of an individual cyclist. Passfield et al. [17] summarize the studies that have been executed in analyzing power meter data to quantify a performance metric. They investigate the methods of 'mean power output', 'binning of training data', and 'the concept of critical power', but conclude that there is no single reference measurement of performance yet. They highlight the need for new methods to quantify performance. Vreugdenhil [18] proposes a new metric called the cycled critical power (CCP) that measures performance. In this chapter, the concept of cycled critical power is explained and thoroughly investigated.

The concept of CCP is based on the assumption that a cyclist, due to his or her fanatic attitude, goes all out during an exercise. Translated to the mathematical model this means that W'_{bal} reaches zero at least once every day, i.e. $\min_t W'_{\text{bal}}(t) = 0$. This might be at the end of the day, during a sprint for example, or somewhere during the day at, for example, a particular hard climb. With a given and fixed W' , the power output of an exercise $P(t)$ and a system of equations to model the dynamics of $W'_{\text{bal}}(t)$, the value of CP for which this assumption holds, i.e. $\min_t W'_{\text{bal}}(t) = 0$, can be acquired. This value of CP is called the cycled critical power (CCP).

This chapter starts in Section 6.1 by stating the mathematical definition of CCP and proving that it is well-defined. Subsequently, in Section 6.2, the results for cyclist 2 are illustrated and it is found that the values of CCP are more volatile than expected. Three possible causes for this volatility are identified in Section 6.3. In Section 6.4 the first two causes are investigated, but they do not seem to cause the volatility. In Sections 6.6 and 6.7 multiple methods are proposed to tackle the cause of the volatility. Finally, in Section 6.8 the various methods are compared and conclusions are drawn.

6.1. Mathematical definition

In this section the mathematical definition of cycled critical power (CCP) is introduced and it is proven that the CCP is well defined, i.e. for every exercise there is one, unique value for the CCP. The mathematical definition for the CCP is as follows.

Definition 6.1. Given fixed $W' > 0$ and power output $P(t) \geq 0$ for $t \in [0, T]$ during a specific exercise. The time interval $[0, T]$ is discretized in an equidistant grid of $0 = t_0 < t_1 < \dots < t_N = T$ with an intermediate distance h . Furthermore, a recursive function $W'_{\text{bal}}(i) : [0, N] \rightarrow \mathbb{R}$ is given to model the dynamics of W'_{bal} .

$$\begin{aligned} W'_{\text{bal}}(0) &= W' \\ W'_{\text{bal}}(i) &= \begin{cases} W'_{\text{bal}}(t_{i-1}) - h_1(P(t_{i-1}) - CP) & \text{if } P(t_{i-1}) \geq CP \\ W'_{\text{bal}}(t_{i-1}) + h_2(CP - P(t_{i-1})) & \text{if } P(t_{i-1}) < CP \end{cases} \end{aligned} \quad (6.1)$$

in which $h_1(x)$ and $h_2(x)$ are continuous functions that satisfy the following constraints: for $x \geq 0$: $h_j \geq 0$, for $j = 1, 2$, $h_j(0) = 0$ for $j = 1, 2$, $0 < \frac{dh_1}{dx} < M$, and $0 \leq \frac{dh_2}{dx} < M$ for an arbitrary M . Furthermore, the dynamics of $W'_{\text{bal}}(t)$ are restricted by the constraint that for all $t \in [0, T]$: $W'_{\text{bal}}(t) \leq W'$.

Then, the **cycled critical power (CCP)** is the value of CP for which $\min_t W'_{\text{bal}}(t) = 0$, i.e. the value of CP for which the function $f(CP) := \min_t \{W'_{\text{bal}}(t)|_{CP}\} = 0$. The notation $W'_{\text{bal}}(t)|_k$ is used to denote the value of $W'_{\text{bal}}(t)$ calculated with $CP = k$.

In physiological terms, the CCP is the implicit critical power of a cyclist, within a given training or race, assuming that during this exercise the cyclist depleted his anaerobic work supply at least once.

Note that in this definition the recursive function to model the dynamics of W'_{bal} is stated generally. It is restricted in three ways; 1) by requiring that $h_j \geq 0$ for $x > 0$ and $h_j(0) = 0$ we ensure that $W'_{\text{bal}}(t)$ is decreasing when performing above critical power, increasing when performing below critical power, and constant when performing on critical power, 2) the constraints $0 < \frac{dh_1}{dx} < M$ and $0 \leq \frac{dh_2}{dx} < M$ are needed in order for the function $f(CP)$ to be continuous and monotonic, and 3) the constraint that for all $t \in [0, T]$: $W'_{\text{bal}}(t) \leq W'$, ensures that the unrealistic case in which there is more anaerobic energy available than capacity is prevented.

Now we show that these general constraints on the model of $W'_{\text{bal}}(t)$ suffice for the CCP to be well defined. Later on, we show that the dynamic of $W'_{\text{bal}}(t)$ stated in the previous chapter in Equation (5.10) satisfies the given constraints.

6.1.1. Monotonicity and continuity of $f(CP)$.

The function $f: \mathbb{R} \rightarrow \mathbb{R}$ with $f(CP) = \min_t \{W'_{\text{bal}}(t)|_{CP}\}$ is monotone for all values of $CP \in \mathbb{R}$, and strictly increasing for $CP < \max_{t \in [0, T]} \{P(t)\}$. This is proven in the Lemmas 6.1 and 6.2. Afterwards it is also proven that the function $f(CP)$ is continuous. The continuity and monotonicity of $f(CP)$ are finally used to show that the value for CCP is well defined. The proofs of the following lemma's and theorem are stated in appendix A.

Lemma 6.1. *The function $f: \mathbb{R} \rightarrow \mathbb{R}$ with $f(CP) = \min_t \{W'_{\text{bal}}(t)|_{CP}\}$ is monotone.*

Lemma 6.2. *The function $f: \mathbb{R} \rightarrow \mathbb{R}$ with $f(CP) = \min_t \{W'_{\text{bal}}(t)|_{CP}\}$ is strictly increasing for $CP < \max_{t \in [0, T]} \{P(t)\}$*

Now lastly we show that the function $f(CP)$ is also continuous.

Lemma 6.3. *The function $f: \mathbb{R} \rightarrow \mathbb{R}$ with $f(CP) = \min_t \{W'_{\text{bal}}(t)|_{CP}\}$ is continuous.*

With these building blocks we can finally show that the value of CCP is well defined.

Theorem 6.1. *The definition of CCP is well defined, i.e. there is a unique value CCP for which $f(CCP) = \min_{t \in [0, T]} \{W'_{\text{bal}}(t)|_{CCP}\} = 0$.*

6.1.2. Specific model for $W'_{\text{bal}}(t)$

In the previous subsection, a general definition for the model of $W'_{\text{bal}}(t)$ is used and for this general definition, it is proven that the definition of CCP is well-defined. In the remainder of this report we use the recurrent formula for $W'_{\text{bal}}(t)$ of Equation (5.10). Therefore, we first show that these equations satisfy the constraints of Definition 6.1. For readability the Equation (5.10) is stated here once more:

$$W'_{\text{bal}}(t_i) = \begin{cases} W'_{\text{bal}}(t_{i-1}) - h \cdot (P(t_{i-1}) - CP) & \text{if } P(t_{i-1}) \geq CP \\ W'_{\text{bal}}(t_{i-1}) + h \cdot (CP - P(t_{i-1})) \cdot (\hat{W}' - W_{\text{bal}}(t_{i-1})) / \tau_{W'}(t) & \text{if } P(t_{i-1}) < CP \end{cases} \quad (6.2)$$

Note that $h_1(x)$ and $h_2(x)$ from Definition 6.1 are in this case $h_1(x) = h \cdot x$ and $h_2(x) = h \cdot x \cdot (W' - W'_{\text{bal}}(t_{i-1})) / (2287.2 \cdot x^{-0.688})$ where h is the distant between two points in the discretized grid of $[0, T]$. First of all, it is already shown in Section 5.5 that $W'_{\text{bal}}(t_i) \leq W'$ for all $i \in [1, N]$. Additionally, it is trivial to show that $h_1(x)$ and $h_2(x)$ are continuous, greater or equal to zero for $x > 0$, and $h_1(0) = h_2(0) = 0$. Lastly, the derivatives of $h_1(x)$ and $h_2(x)$ are given by:

$$\begin{aligned} \frac{dh_1}{dx} &= h \\ \frac{dh_2}{dx} &= \frac{h \cdot (W' - W'_{\text{bal}}(t_{i-1}))}{3860.8} (CP - P(t_{i-1}))^{0.688} \end{aligned} \quad (6.3)$$

It is trivial to see that $\frac{dh_1}{dx}$ is strictly positive and bounded. Furthermore, for $h_2(x)$, we know that $h > 0$, $0 \leq P(t_{i-1}) < CP$, $W'_{\text{bal}}(t_{i-1}) \leq W'$, and that $W'_{\text{bal}}(t_{i-1})$ is bounded from below because it is a finite subtraction from W' . With this information we can also conclude that $\frac{dh_2}{dx}$ is positive and bounded.

6.1.3. Visual example

In this subsection we provide a visual example of the concept of the CCP for which we use the validation of Section 5.6. The CCP for that given day under the dynamics of $W_{\text{bal}}(t)$ of Equation (5.10) is 399. The interpretation of this value is the following. Under the assumption that the cyclist has gone all out during that day, the CCP is the minimal value for the critical power that is required in order to have for all $t \in [0, T]$: $W'_{\text{bal}}(t) \geq 0$, i.e. for the model to be correct. Figure 6.1 visualizes this explanation. In the figure we see the dynamics of $W'_{\text{bal}}(t)$ over time of the time trial of Section 3.1. For $CP = 380$ and $CP = 390$, we see that W'_{bal} reaches levels below 0, which is in contradiction with the definition of W'_{bal} . For $CP = 410$ and $CP = 420$ we see that W'_{bal} reaches a minimum of respectively 7.4 and 8.5 kJ, which is inconsistent with the assumption that the cyclist has gone all out and completely depleted his anaerobic energy. In the case that $CP = 399$ we see that the minimum of the $W'_{\text{bal}}(t) = 0$, thus the CCP of this specific day for this cyclist is 399.

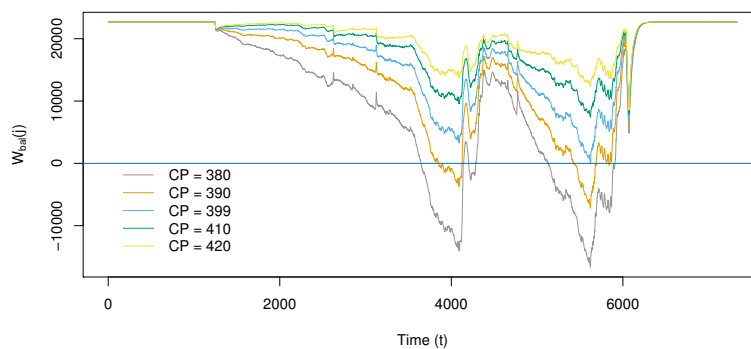


Figure 6.1: The dynamics of $W'_{\text{bal}}(t)$ for five different values of CP in the time trial of Section 3.1.

6.2. Dynamics of the cycled critical power

Figure 6.2 shows the value of the calculated cycled critical power over multiple years for cyclist 2, this calculated value is denoted by \overline{CCP}_t^i . In this notation the indices t and i denote the day and cyclist respectively. As the data are highly variable, a rolling mean over 21 days is plotted as well to make the graph better readable. The rolling mean shows a drop to zero around October of each year, which is the seasonal break. Afterwards, during every season a positive trend is visible together with two or three peaks. This is as expected, because a regular cyclist improves during the season and peaks at two or three big races. A disappointing observation is that the CCP is so volatile, because that contradicts the expectation that the performance level does not change too much over time; the volatility is unrealistic. This volatility can be caused by several problems, that are explained in more detail in the following section.

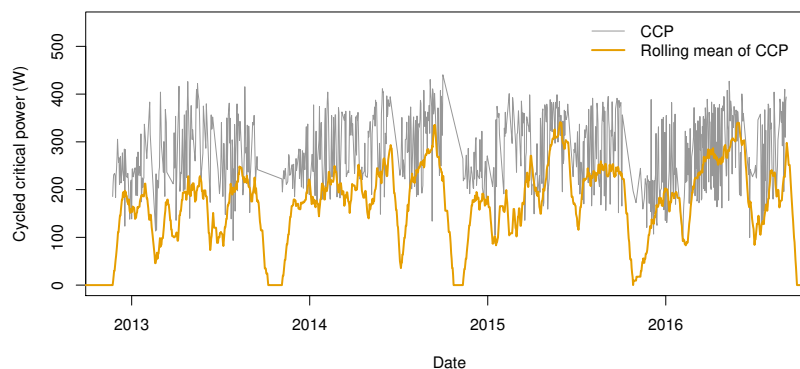


Figure 6.2: The calculated cycled critical power and its rolling mean over 21 days of cyclist 2.

6.3. Possible causes of volatility

Three reasons are identified that could cause the unrealistic volatility in the obtained values of the CCP. They are stated in the list below.

1. The general model of equation (6.1) does not correctly calculate the amount of anaerobic energy left in the body at time t .
2. The value of W' is incorrect or not constant over time.
3. A cyclist does not deplete his or her anaerobic work supply each exercise.

Validating the first cause is beyond the scope of this report, but could and should be performed on basis of experimental data in the laboratory. In practice, it would be difficult to find a model that satisfies the first assumption, but every improvement in the model to correctly calculate the supply of anaerobic energy left in the body, would mean an improvement in accuracy for the \overline{CCP} . In the remainder of this report we assume the model of Equation (5.10) to be correct, but we question the formula of $\tau_{W'}(t)$. Because two different formulas for $\tau_{W'}(t)$ are proposed in literature, we will analyze both of them in the next section. For the second cause, we know that the values of W' are uncertain, so in the next section a sensitivity analysis is performed to analyze the influence on the CCP of the uncertainty of both the value of W' and the formula of $\tau_{W'}(t)$. This analysis will show that the volatility of the calculated \overline{CCP} values is not caused by the value of W' or $\tau_{W'}$. Therefore, the most probable cause for the volatility is the incorrect assumption that a cyclist depletes his or her anaerobic work supply each exercise.

For exercises in which the cyclist did deplete his anaerobic work capacity, the model returns a good approximation for the CCP, but in exercises where his anaerobic work supply was not depleted, the CCP is underestimated, as we will see later in this chapter. The data obtained on days that the cyclist did deplete his or her anaerobic work supply, do contain valuable information. In order to take these data points into account, two possible methods are proposed to tackle this problem. In Section 6.6 an approach is proposed in which the subjective fitness and intensity are used. In Section 6.7 two mathematical smoothing methods are investigated that selectively choose the days at which the cyclist did go all out and try to estimate the value of the CCP in between these days using bounds that come from the values of \overline{CCP} at the intermediate points.

6.4. Sensitivity analysis

The value of the \overline{CCP} depends on the value of W' and on the function $\tau_{W'}(t)$. This section investigates the influence of W' and $\tau_{W'}(t)$ on the value of the \overline{CCP} . In Figure 6.3 the value of CCP for three exercises are plotted; the time trial, sprint and climbing stage of Section 3.1. The estimated value of W' of Chapter 4 is represented by the dot and a range from half that value to twice that value. The 95%-confidence intervals of W' are visualized by the crosses. Furthermore, both functions of $\tau_{W'}(t)$ of Equations (5.5) (old $\tau_{W'}$) and (5.6) (new $\tau_{W'}$). The figure shows that the function of \overline{CCP} is decreasing with respect to W' . This is explained by the fact that a higher W' indicates a larger anaerobic work capacity. In order to deplete this capacity, a cyclist would need to exceed his CP by a greater amount, hence a lower \overline{CCP} is induced. We notice that the value of \overline{CCP} has a negative linear relation with W' in the 95%-confidence intervals of \hat{W}' . Furthermore, we notice that the two functions of $\tau_{W'}(t)$ yield different values for CCP. Equation (5.5) yields a higher value of \overline{CCP} than Equation (5.6), especially during the sprint stage. During the time trial, the cyclist performs at a constant high power output, thus he spends almost no time in the restoration state ($P(t) < CP$). In the sprint stage, the cyclist performs a small burst of energy, but the rest of the race is performed at a relatively low power output. Therefore, the influence of the restoration rate is higher on the sprint than on the time trial, which is also apparent from the figure. From now on, this report uses the formula for $\tau_{W'}(t)$ of Equation (5.6), because in [3] it is claimed to be more accurate for elite cyclists.

Figure 6.4 shows the value of \overline{CCP} with respect to the value of W' of five subsequent days for the same cyclist. Day 1 is the time trial of Section 3.1. We notice that days 2,4 and 5 yield similar values for CCP and the negative linear relationship between \overline{CCP} and W' has the same gradient on these days. Day 1 stands out because it has a higher value of CCP. This is explained by the fact that this day was a time trial, which is a specialty of the cyclist. The gradient of day 1 is comparable to that of the other days. Day 3 stands out due to the low value of \overline{CCP} and larger gradient compared with the other days. This is because this day was a resting day during the Giro d'Italia. Therefore, the cyclist did not deplete his anaerobic work capacity during the rest day and thus did not depleted his anaerobic energy supply completely. This means that his power output was

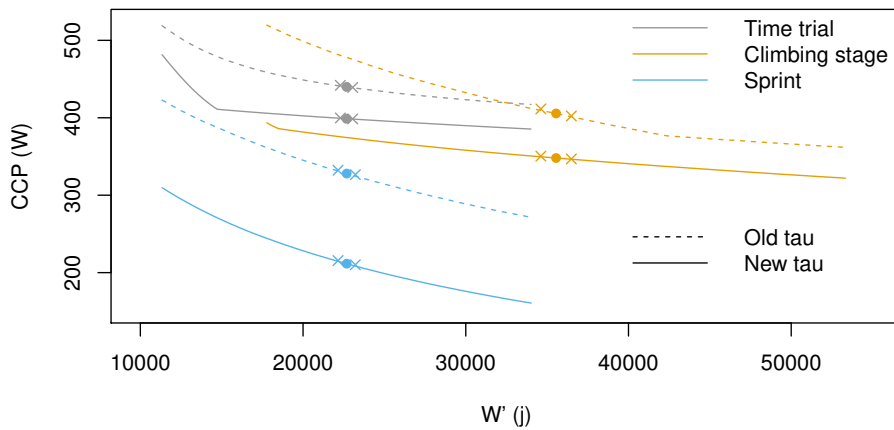


Figure 6.3: The sensitivity of \overline{CCP} with regard to the value of \hat{W}' and rate of reconstitution $\tau_{W'}(t)$ for the three exercises of Section 3.1. The dot represents the value of \hat{W}' of Chapter 3. The crosses visualize the 95%-confidence intervals of W' as stated in Section ??.

relatively low that day, thus under the assumption that he did deplete his anaerobic energy capacity, the \overline{CCP} is lower than expected.

The range of values that the \overline{CCP} attains during days 1,2,4, and 5, is about 45W. As we do not expect the CCP of a cyclist to fluctuate with this amount of power in four days, this figure also illustrates the inaccuracy of the CCP. This problem is addressed in Sections 6.6 and 6.7.

The fact that the gradient for days 1,2,4, and 5 is similar is both important and interesting. This indicates that if the estimate of \hat{W}' would not be correct, i.e. in reality the value of W' is a little smaller or bigger, that it would have the same effect on the value of CCP for each of these days.

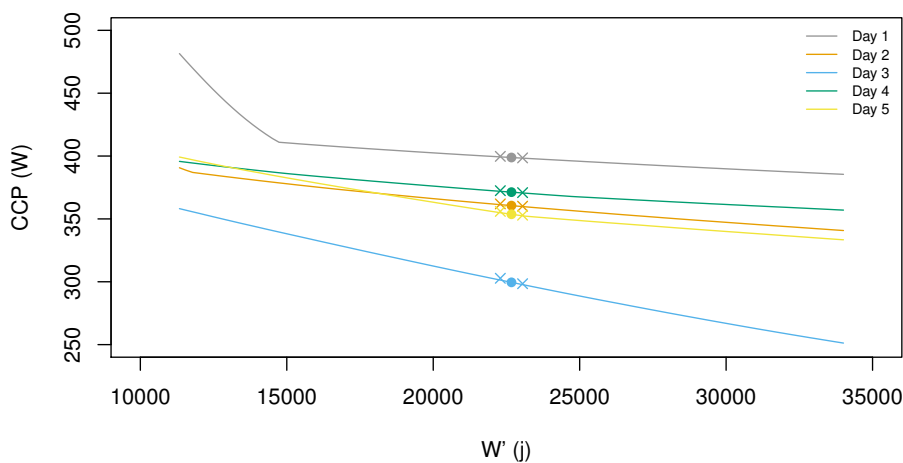


Figure 6.4: The sensitivity of CCP with regard to the value of \hat{W}' for the five subsequent exercises of cyclist 2. The dot represents the value of \hat{W}' of Chapter 3.

6.5. Main cause for volatility

Figures 6.3 and 6.4 indicate that the choices for W' and $\tau_{W'}(t)$ do not induce the volatility in the obtained CCP-values. Therefore, the probable main cause for volatility is that a cyclist's anaerobic work supply is not depleted each exercise.

An important observation is that the values of \overline{CCP}_t^i underestimate the actual, latent value of the CCP, i.e. $\overline{CCP}_t^i \leq CCP_t^i$. This is explained by the following argument. If a cyclist did deplete his or her anaerobic work supply during an exercise, i.e. the minimum of $W'_{\text{bal}}(t) = 0$, then $\overline{CCP}_t^i = CCP_t^i$. In cases a cyclist did not deplete his or her anaerobic work supply, i.e. $\min W'_{\text{bal}}(t) > 0$, but we do assume this inequality to be equal, then $\overline{CCP}_t^i < CCP_t^i$. This due to the fact that the function $f(CP) = \min_t \{W'_{\text{bal}}(t)|_{CP}\}$ is strictly increasing as shown in Lemma 6.2. Thus, if for the actual value of CCP, the cyclist did not go all out, i.e. $f(CCP) > 0$, then the value CCP for which $f(CCP) = 0$ satisfies $CCP \leq CCP$.

Therefore, we interpret the latent variable CCP_t^i as a stochastic variable \overline{CCP}_t^i and an error $\epsilon_t^i \geq 0$, i.e. $CCP_t^i = \overline{CCP}_t^i + \epsilon_t^i$. The fact that the error ϵ_t^i is larger or equal to 0, is due to the fact that $\overline{CCP} \leq CCP$.

In Sections 6.6 and 6.7 two methods are proposed to deal with the error ϵ_t^i and thus estimate the latent variable CCP_t^i from the calculated \overline{CCP}_t^i . In Section 6.6 it is investigated whether there is a relationship between two parameters that represent the intensity of an exercise and the minimum value of $W'_{\text{bal}}(t)$. If such a relationship exists, it would indirectly imply a relationship between these two parameters and ϵ_t^i . In Section 6.7 two smoothing methods are proposed to estimate CCP_t^i under the assumption of a bounded (total) variation of CCP_t^i .

6.6. Exercise intensity

As seen in Figure 6.4, on a day that a cyclist does deplete his or her anaerobic work supply, this has a considerable impact on the calculated value of CCP. This section researches a possible relation between the intensity of the exercise with the minimum value of $W'_{\text{bal}}(t)$. The added value of such a relationship would be significant. If we could predict the minimum value of $W'_{\text{bal}}(t)$ based on exercise data, we could calculate the value of the CCP based on that value of $\min_t \{W'_{\text{bal}}(t)\}$ instead of zero. This would improve the accuracy of the calculated value of the CCP. The intensity of the exercise is quantified by two different metrics; the rate of perceived exertion (RPE) and the maximum heart rate.

The methodology to find the relationship between the exercise intensity and minimum value of $W'_{\text{bal}}(t)$ is as follows. It is assumed that the performance level of a cyclist is almost constant, i.e. it does not have large daily variations. Therefore, the performance on a given day is quantified as the maximum cycled critical power of the past 30 days. Given this value of CCP for a given day, it is calculated what the minimum level of $W'_{\text{bal}}(t)$ is that day. These values are then compared with the values of the rate of perceived exertion (RPE) and the maximal heart rate on that day.

Figures 6.5 and 6.6 show heat plots of all six cyclists in which the minimum level of $W'_{\text{bal}}(t)$ reached is plotted against the maximum heart rate (Figure 6.5) and PRE (Figure 6.6) of a day. Table 6.1 shows the value of R^2 for linear models fitted with ordinary least squares. Although for some cyclists there is a weak linear relationship between either maximal heart rate and minimum $W'_{\text{bal}}(t)$ or RPE and minimum $W'_{\text{bal}}(t)$, for most cases the relationship is too weak in order for it to improve the accuracy of the calculated CCP significantly. Further research in factors that can predict the minimum value of $W'_{\text{bal}}(t)$ reached during a day, such as daily lactate measurements or new questionnaires, could be valuable in order to improve the accuracy of the CCP metric.

Table 6.1: The value of R^2 of OLS performed on $\min\{W'_{\text{bal}}\}$ versus heartrate and RPE.

	R^2 of $\min\{W'_{\text{bal}}\}$ versus	
	Heartrate	RPE
Cyclist 1	0.21	0.56
Cyclist 2	0.09	0.22
Cyclist 3	0.26	0.23
Cyclist 4	0.13	0.45
Cyclist 5	0.40	0.45
Cyclist 6	0.35	0.41

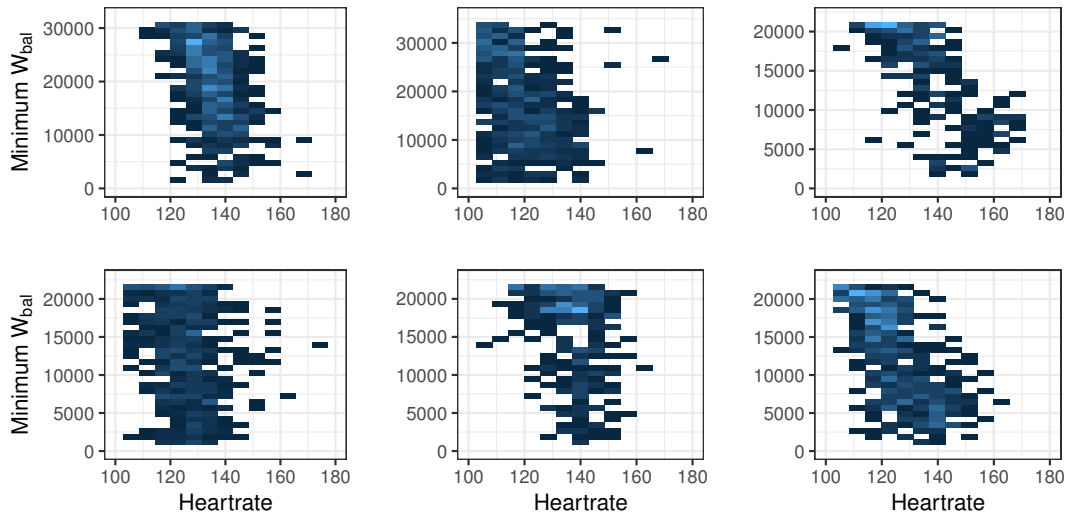


Figure 6.5: The minimum $W'_{\text{bal}}(t)$ reached plotted against the maximal heart rate for the six different cyclists. The color-scale indicates the number of data points in an area, where it is increasing from dark to light.

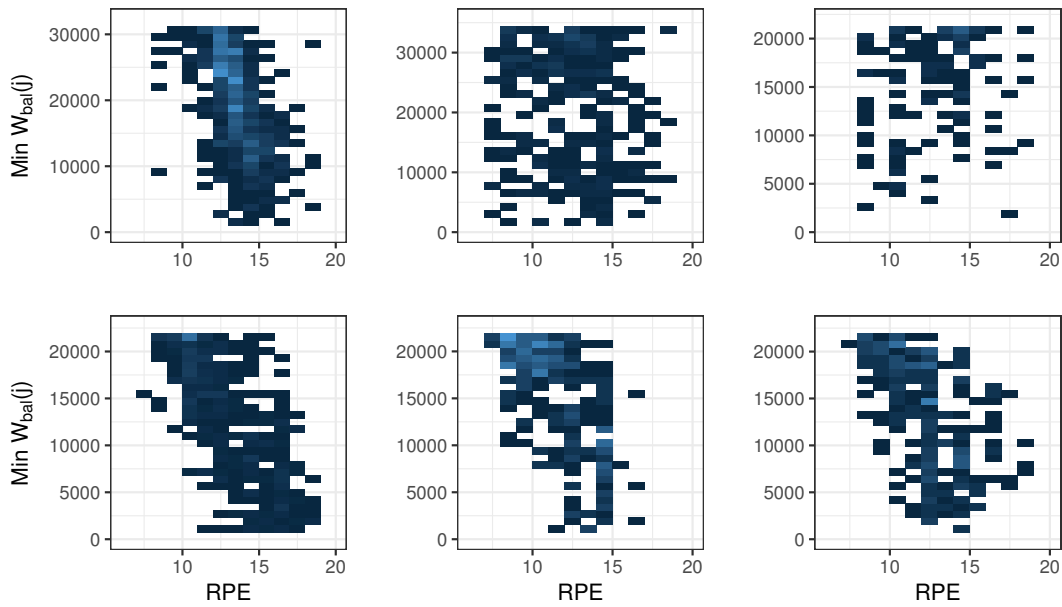


Figure 6.6: The minimum $W'_{\text{bal}}(i)$ reached plotted against the rate of perceived exertion for the six different cyclists. The color-scale indicates the number of data points in an area, where it is increasing from dark to light.

6.7. Smoothing the cycled critical power

In this section we take the obtained values of the CCP for all days into consideration. Under these circumstances we analyze the data and propose two mathematical methods to improve the accuracy of the values of the CCP; local maxima and curve fitting. In turn, two methods of curve fitting are proposed, the first imposes a constraint on the daily change in CCP, the second on the total variation in CCP.

Both methods, local maxima and curve fitting, use the fact that $\overline{\text{CCP}}_t^i \leq \text{CCP}_t^i$ and are constructed based on the assumption that the performance level has a bounded variation over time.

6.7.1. Local maxima

The method of local maxima is based on the assumption that a cyclist depletes his or anaerobic work supply every k days. Thus, the performance level of cyclist i on day t is estimated by the maximum of CCP over $\{t - k + 1, \dots, t - 1, t\}$.

$$\widehat{\text{CCP}}_t^i = \max_{t \in \{t-k+1, \dots, t-1, t\}} \overline{\text{CCP}}_t^i \quad (6.4)$$

Figure 6.7 shows the calculated cycled critical power of all exercises, divided into three categories; trainings, races, and time trials. In 2013 it was not yet recorded of which type an exercise was, so all exercises in 2013 are classified as a training. Furthermore, it shows the results of the local maxima method for three different values of k ; 7, 14, and 30, which represent time intervals of one week, two weeks, and a month. The figure clearly shows that $\widehat{\text{CCP}}_t^i \geq \overline{\text{CCP}}_t^i$ as imposed. Furthermore, the graph becomes smoother as k increases. Also, the values of $\overline{\text{CCP}}_t^i$ that are probably underestimating CCP_t^i do not have any influence on the value of $\widehat{\text{CCP}}_t^i$, because another value of $\overline{\text{CCP}}_t^i$ within k days has a higher value.

This method of smoothing the data has disadvantages as well. First of all, it completely ignores a large part of the data points by taking only a maximum. For example, if for a certain day the $\text{CCP} = 300$ and for the following $k - 1$ days the CCP is constant on a level $c < 300$, then $\widehat{\text{CCP}}$ is equal to 300 for these k days, for both $c = 1$ and $c = 299$. Thus, although the value of $\overline{\text{CCP}}_t^i$ underestimates CCP_t^i , all values of $\overline{\text{CCP}}_t^i$ do hold some valuable information that is neglected by taking local maxima. Another disadvantage of taking local maxima is that the performance parameter remains constant for time intervals of at most k days. Therefore, when modeling training attributes to the performance measure, small differences in the performance level are not easily detected. For optimizing training schedules, a more precise CCP on a more frequent basis is required.

6.7.2. Curve fitting

The second method that is proposed to improve the accuracy of the performance metric is a form of curve fitting. Two different ways of curve fitting are used; the first one assumes a bounded daily variation of CCP , the second method tries to find a curve $\widehat{\text{CCP}}_t$ that satisfies the lower bound of $\overline{\text{CCP}}_t$ while simultaneously minimizing the total variance and the total error of the function.

Bounded local variation.

This method of curve fitting is based on the assumption that the cycled critical power can change from one day to another by a maximum value M_d . Furthermore, the curve fitting method minimizes the total squared error of the estimate $\widehat{\text{CCP}}_t$ as in the system of Equations (6.5).

$$\begin{aligned} \min \quad & \sum_{i=1}^N \left(\widehat{\text{CCP}}_{t_i} - \overline{\text{CCP}}_{t_i} \right) \\ \text{s.t.} \quad & \widehat{\text{CCP}}_{t_i} \geq \overline{\text{CCP}}_{t_i} \quad \forall i \in [1, N] \\ & |\widehat{\text{CCP}}_{t_i} - \widehat{\text{CCP}}_{t_{i-1}}| \leq M_d \cdot (t_i - t_{i-1}) \quad \forall i \in [2, N] \end{aligned} \quad (6.5)$$

In order to solve this problem with the Simplex method, a widely used method to efficiently solve constrained minimization problems [16], we need to get rid of the absolute value signs. Notice that the absolute value $|x|$ can be written as $|x| = x^+ + x^-$, with $x^+, x^- \geq 0$ and $x = x^+ - x^-$. Therefore, we define two new variables d_i^+ and d_i^- . These variables denote the positive and negative part of the absolute value $|\widehat{\text{CCP}}_{t_{i+1}} - \widehat{\text{CCP}}_{t_i}|$, i.e. $d_i^+ + d_i^- = |\widehat{\text{CCP}}_{t_{i+1}} - \widehat{\text{CCP}}_{t_i}|$ with $d_i^+, d_i^- \geq 0$ and $d_i^+ - d_i^- = \widehat{\text{CCP}}_{t_{i+1}} - \widehat{\text{CCP}}_{t_i}$. With these new variables we rewrite System 6.5 as a linear system.

$$\begin{aligned} \min \quad & \sum_{i=1}^N \left(\widehat{\text{CCP}}_{t_i} - \overline{\text{CCP}}_{t_i} \right) \\ \text{s.t.} \quad & \widehat{\text{CCP}}_{t_i} \geq \overline{\text{CCP}}_{t_i} \quad \forall i \in [1, N] \\ & d_i^+ - d_i^- = \widehat{\text{CCP}}_{t_i} - \widehat{\text{CCP}}_{t_{i-1}} \quad \forall i \in [2, N] \\ & d_i^+ + d_i^- \leq M_d \cdot (t_i - t_{i-1}) \quad \forall i \in [2, N] \\ & d_i^+, d_i^- \geq 0 \quad \forall i \in [2, N] \end{aligned} \quad (6.6)$$

After transforming System (6.5) into System (6.6), it is now solvable by the Simplex method, which yields us the results for $M_d = 1, 3$, and 5 as shown in Figure 6.8. The green line in this figure represents the values of $\widehat{\text{CCP}}_{t_i}$.

The advantage of this method is that the parameter M_d is interpretable and can thus be chosen by experts and coaches in the field. The disadvantage of this method is the influence of M_d on the shape of the final curve. The curve, due to the variability in $\overline{\text{CCP}}_{t_i}$, has almost everywhere a gradient of $+M_d$ or $-M_d$. For

$M_d = 1$ we have that $|\widehat{\text{CCP}}_{t_i} - \widehat{\text{CCP}}_{t_{i-1}}| = M_d \cdot (t_i - t_{i-1})$ in 97% of the indices in the set $[1, N]$. For $M_d = 3$ this is 89% and for $M_d = 5$ this is 83%. In Figure 6.8 the values of $\widehat{\text{CCP}}_t$ are shown for $M_d = 1, 3,$ and 5 , in which this constant gradient is clearly visible.

Bounded total variation.

This method of curve fitting is based on the assumption that the total variation during the entire period is bounded by a value M_T . Mathematically speaking, it tries to find values for $\widehat{\text{CCP}}_t$ for every t , such that it is a solution to minimization problem (6.7).

$$\begin{aligned} \min \quad & \sum_{i=1}^N \left(\widehat{\text{CCP}}_{t_i} - \overline{\text{CCP}}_{t_i} \right) \\ \text{s.t.} \quad & \widehat{\text{CCP}}_{t_i} \geq \overline{\text{CCP}}_{t_i} \quad \forall i \in [1, N] \\ & \sum_{i=2}^N |\widehat{\text{CCP}}_{t_i} - \widehat{\text{CCP}}_{t_{i-1}}| \leq M_T \end{aligned} \quad (6.7)$$

Once more we encounter absolute values in the constraints, therefore we apply the same trick as for bounded local variation to rewrite the system into a linear system solvable with linear programming.

$$\begin{aligned} \min \quad & \sum_{i=1}^N \left(\widehat{\text{CCP}}_{t_i} - \overline{\text{CCP}}_{t_i} \right) \\ \text{s.t.} \quad & \widehat{\text{CCP}}_{t_i} \geq \overline{\text{CCP}}_{t_i} \quad \forall i \in [1, N] \\ & d_i^+ - d_i^- = \widehat{\text{CCP}}_{t_i} - \widehat{\text{CCP}}_{t_{i-1}} \quad \forall i \in [2, N] \\ & \sum_{i=2}^N d_i^+ + d_i^- \leq M_T \\ & d_i^+, d_i^- \geq 0 \end{aligned} \quad (6.8)$$

The results of solving this system are shown in Figure 6.9, where the values of $\widehat{\text{CCP}}_{t_i}$ are represented by the green line. In order to make Figures 6.8 and 6.9 comparable, we have chosen M_T to be equal to the values of M_d times the time span of the entire period. Thus, because the period over which the CCP is calculated is approximately 1500 days, the values of M_T in Figure 6.9 are 1500, 4500, and 7500. Because the gradient of the locally bounded curves almost always equal $\pm M_d$, the total variation of the two models will be roughly the same.

Although the total variation is indeed approximately equal for combinations of M_d and M_T , the curves are very different. Where the locally bounded curves look like piecewise linear functions with gradient $\pm M_d$, the totally bounded curves make larger jumps and have periods in which they are constant as well.

The advantages of curve smoothing in comparison with taking local maxima are that 1) it takes into account all data points, 2) it does not drop to a value of zero in a period in which no exercises have been performed, 3) it yields less constant parts, so the impact of exercise attributes is easier to fit, and 4) if the reliability of the value of $\overline{\text{CCP}}$ increases, the impact of the parameters M_d and M_T becomes smaller.

6.8. Conclusion

The biggest advantage of the concept of cycled critical power is that it is easily calculable on a daily basis on basis of objective data. This ensures that a daily metric of a cyclist's performance can be calculated, which can then be used as a predictor on which to optimize training parameters. The downside of the concept is the fact that it assumes that the anaerobic energy of a cyclist to be depleted during each exercise. This makes the cycled critical power an underestimation of the actual cycled critical power. Two methods might be useful to improve the accuracy of the cycled critical power. The first method is to identify parameters that can predict the minimum value of anaerobic work energy reached during an exercise. The second method is to use statistical or timeseries approaches to estimate the actual value of the daily critical power.

For the first method we concluded that both training intensity and maximum heartrate do not seem to be good predictors of the minimum value of anaerobic energy during a given exercise. Smooth curving has more potential: The method of local maxima to estimate the daily critical power has the downside that it yields constant periods of the performance level, which is impractical. The methods of locally and totally bounded variation seem to produce the most realistic estimators of the cycled critical power. This statement is hard to support, since no validation methods are available to show the actual accuracy. But, as can be seen

in Figures 6.8 and 6.9, the curves correctly identify the first two seasonal breaks in which a lower performance level is expected. The locally bounded variation method is easier to grasp for experts in the field, because a bound on daily variation is more tangible than a bound on total variation. Therefore, in the next chapter, where we identify the impact of training attributes on performance, we quantify the performance of a cyclist by applying locally bounded variation on the CCP with $M_d = 3$.

Figure 6.7: Local maxima method to smooth the calculated CCP data points for $k = 7, 14,$ and 30 .

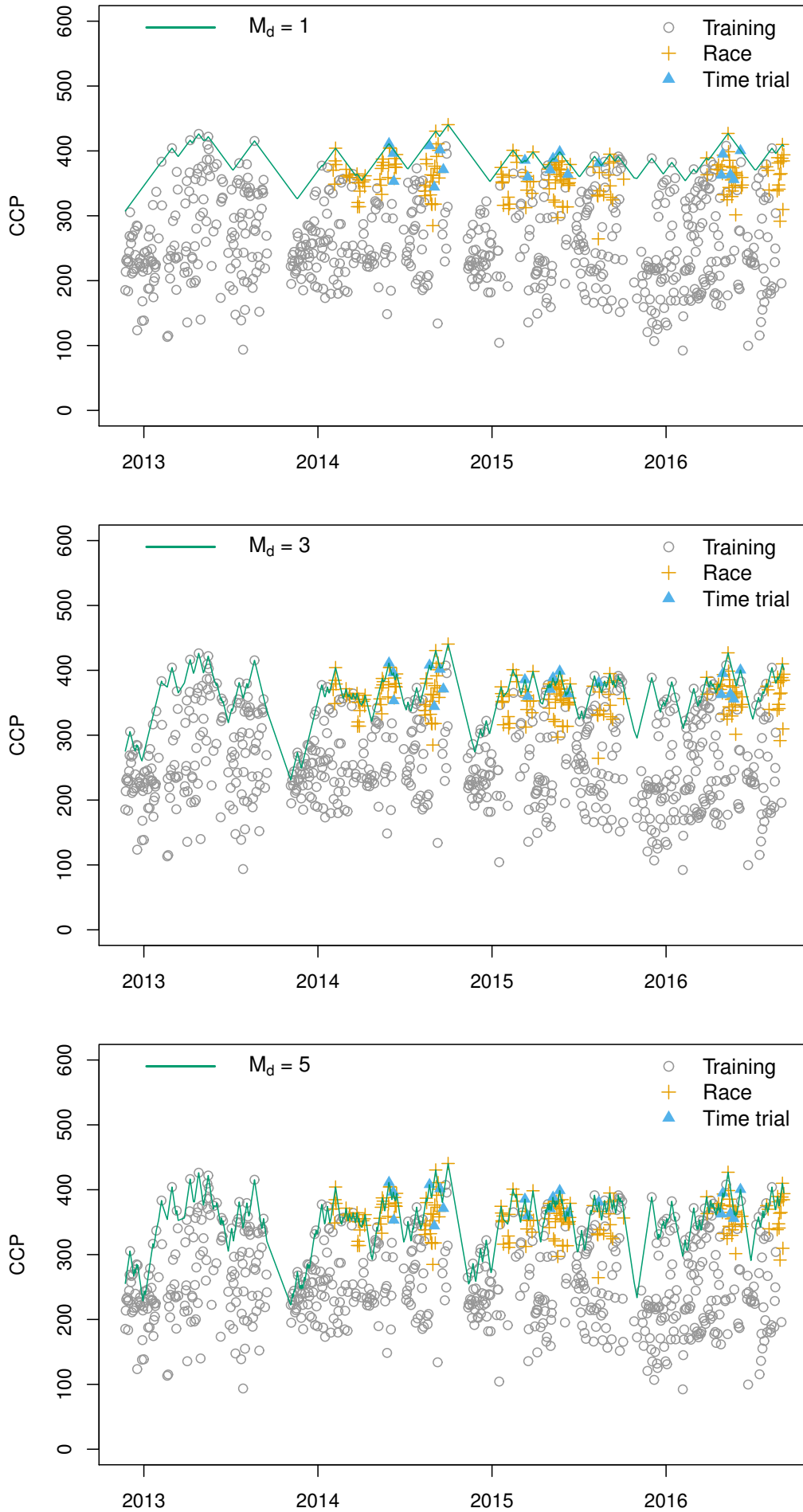


Figure 6.8: Curve fitting method to smooth the calculated CCP data points under the constraint of locally bounded variation for $M_d = 1, 3,$ and 5.

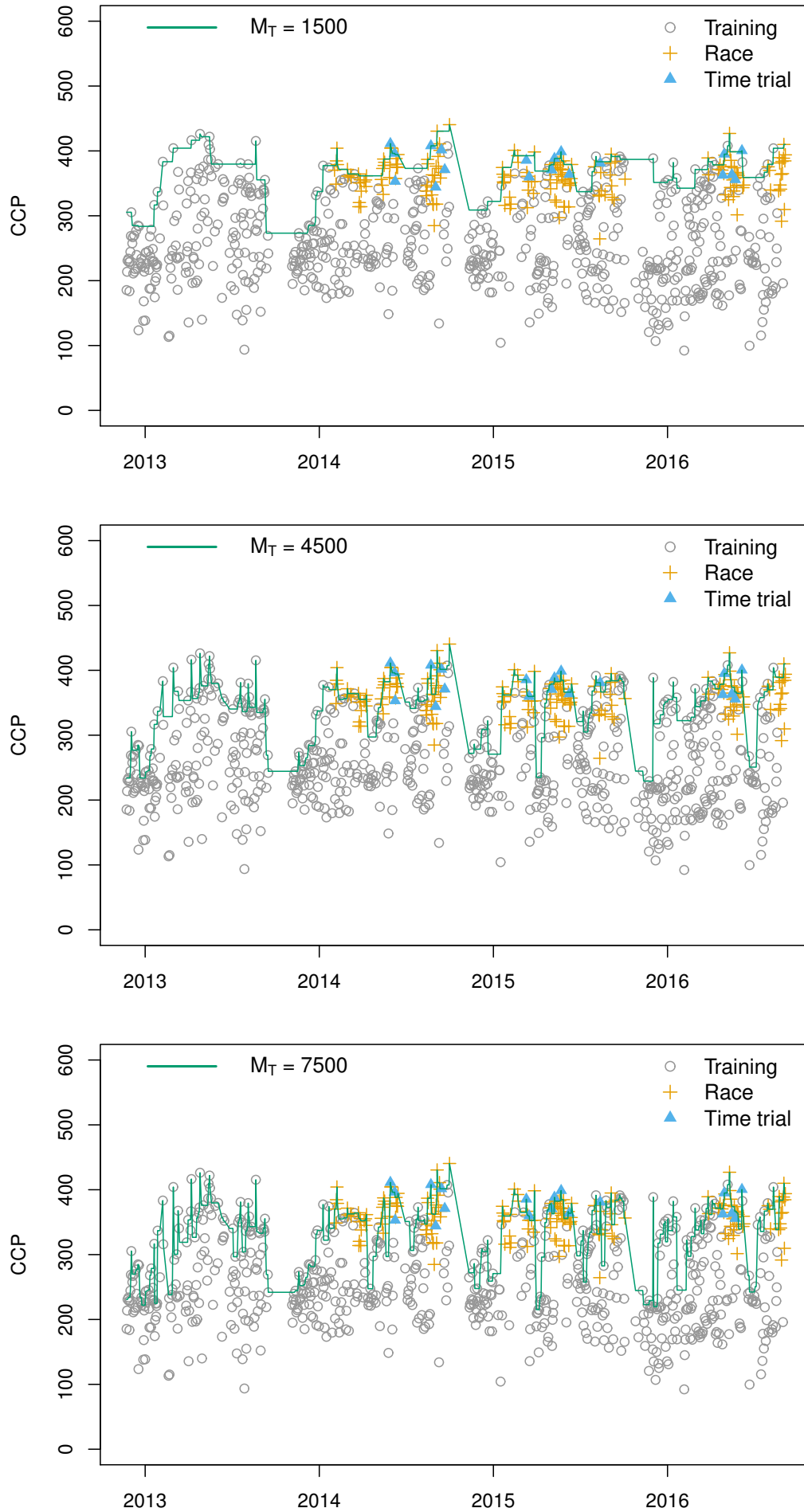


Figure 6.9: Curve fitting method to smooth the calculated CCP data points under the constraint of totally bounded variation for $M_T = 1500, 4500, \text{ and } 7500$.

7

Modeling performance

“All models are wrong, but some are useful” — G. Box, 1978

In the previous chapter, we developed a concept that represents a quantification of performance and fitted this to real data. This provided us with the independent variable we want to model in this chapter; the results from the locally bounded CCP algorithm with $M_d = 3$. In this chapter, we investigate if and how we can model and predict the CCP (i.e. the performance level) based on past training statistics. In other words, we investigate which training attributes influence the performance of a cyclist (the CCP) and in which degree. This is done by using the Fitness-Fatigue model [6], a model widely used in the physiology literature. This model describes the relationship between performance, fitness, and fatigue. The Fitness-Fatigue model has already been successfully applied in a variety of sports, such as running [15], ice skating [9], and triathlon [2]. In this chapter we investigate the influence of various training attributes on the value of CCP. The method is constructed such that extra attributes can easily be added to the analysis in future research.

The chapter starts by introducing the Fitness-Fatigue model in Section 7.1. It continues by stating the methods for parameter estimation in Section 7.2. In Section 7.3, the implementation of the algorithm is given. In Section 7.4, results of this model fitted to actual data are shown and discussed. The chapter ends with the main conclusions.

7.1. The fitness-fatigue model

The Fitness-Fatigue model was introduced in 1976 by Calvert et al. [6]. The purpose of the Fitness-Fatigue model is to model and predict the performance (in our case the CCP) of a cyclist based on past training attributes, such as Duration and Intensity. The model is based on a convolution function of training attributes to model the performance of an athlete. In the model there are M different daily training attributes, denoted with $Z_m(t)$, $1 \leq m \leq M$. In our case $M = 5$ such that we have the definition of $Z_m(t)$ as in Equation (7.1). In the remainder of this chapter, the time index t is defined as the number of days since the start of measurement.

$$Z_m(t) = \begin{cases} \text{Duration}(t) & m = 1 \\ \text{Intensity}(t) & m = 2 \\ \text{Subjective Load}(t) & m = 3 \\ \text{TSS}(t) & m = 4 \\ \text{Objective Load}(t) & m = 5 \end{cases} \quad (7.1)$$

In this definition, the *Duration* is the number of hours exercised on day t , the *Intensity* is the value between 6-20 denoted by the cyclist after the exercise, as introduced in Chapter 3, the *Subjective Load* is the product of Intensity and Duration, the *TSS* is such as explained in Chapter 2 and *Objective Load* is the amount of energy in kJ expended during the exercise due to the cycling (so no internal expanded energy).

These values are linearly integrated into one summarizing value $x(t)$ that quantifies the training on day t . In other words, $x(t)$ is a linear combination of $Z_m(t)$, $1 \leq m \leq M$ such as stated in Equation (7.2).

$$x(t) = \sum_{m=1}^M \alpha_m Z_m(t) \quad (7.2)$$

The values α_m are referred to as the relative training parameters and determine the relative importance of the different training attributes on the performance of a cyclist.

The Fitness-Fatigue model utilizes the summarized training value $x(t)$ to model and predict the performance of a cyclist. It is based on the assumption that performance is influenced by the training attributes of Equation (7.1). The model predicts the performance level by a convolution function over all past summarized training values, in which the influence of an exercise depends on the amount of time elapsed since that exercise. The function that models the impact of time on the effect of an exercise is called the kernel function of the convolution and denoted with h . This entails that $h(i)$ models the impact of an exercise i days earlier on the performance of a rider. Mathematically, this is represented in Equation (7.3).

$$y(t) = \sum_{i=1}^{\infty} h(i) \cdot x(t-i) \quad (7.3)$$

Calvert et al. [6] observed that the influence of an exercise on performance decays exponentially over time, so the kernel function is based on the exponential decay function, shown in the Equation (7.4). In this equation λ is the parameter that describes the rate of decay. However, in this context it is more convenient to talk about the inverse $\tau = 1/\lambda$ whose units are in days.

$$h_e(i) = e^{-\lambda i}, \quad i \geq 0 \quad (7.4)$$

The kernel function h of Calvert et al. [6] incorporates two parts; a positive effect on the performance due to improved muscle resistance, and a negative effect due to fatigue. The positive part itself consists of a subtraction of two negative exponential functions that represent respectively the benefit of exercising and the delay in which these benefits occur due to physiological processes. The positive effects of the exercise are modeled such as in Equation (7.5).

$$h_+(i) = e^{-\lambda_{\text{fit}} i}, \quad i \geq 0 \quad (7.5)$$

In reality the improved effect on resistance of exercise is delayed by some days due to physiological processes. Therefore, another exponential is introduced with parameter λ_{del} that represents this delay. The positive part of the kernel thus becomes as in Equation (7.6).

$$h_+(i) = e^{-\lambda_{\text{fit}} i} - e^{-\lambda_{\text{del}} i}, \quad i > 0 \quad (7.6)$$

The fatigue part of the kernel is negative, because it has a negative effect on performance. Furthermore, it is multiplied by a parameter K which represents the respective impact of fatigue relative to improved fitness. The fatigue part of the kernel is Equation (7.7).

$$h_-(i) = -K e^{-\lambda_{\text{fat}} i} \quad (7.7)$$

The final kernel $h(i)$ is the sum of $h_+(i)$ and $h_-(i)$, as stated in Equation (7.8).

$$h(i) = \left(\left(e^{-\lambda_{\text{fit}} i} - e^{-\lambda_{\text{del}} i} \right) - K \cdot e^{-\lambda_{\text{fat}} i} \right) \quad (7.8)$$

such that the mathematical model becomes as in Equation (7.9). The idea is that the effect of fatigue is larger in the beginning but decays quicker than the positive effect on muscle resistance. This means that the effect of an exercise on the performance is negative in the beginning and positive afterwards.

$$y(t) = \sum_{i=1}^{\infty} \left(\left(e^{-\lambda_{\text{fit}} i} - e^{-\lambda_{\text{del}} i} \right) - K \cdot e^{-\lambda_{\text{fat}} i} \right) \cdot x(t-i) \quad (7.9)$$

Finally, one last addition is added to the model. A constant value C that represents the hypothetical performance level of an untrained cyclist. Hence, the final Fitness-Fatigue model for a cyclist becomes as shown in Equation (7.10).

$$y(t) = C + \sum_{i=1}^{\infty} x(t-i) \cdot \left(\left(e^{-\lambda_{\text{fit}} i} - e^{-\lambda_{\text{del}} i} \right) - K \cdot e^{-\lambda_{\text{fat}} i} \right) \quad (7.10)$$

7.1.1. Interpretation of kernel parameters

The values λ_{fit} , λ_{del} , and λ_{fat} determine the speed of decay of the corresponding exponential function. For the purpose of parameter interpretation, a transformation $\tau = 1/\lambda$ is used, which has the more convenient unit of days. An exponential decay function such as in Equation (7.4) has a half time of $-\ln(1/2) \cdot \tau \approx 0.7\tau$, i.e. if the impact of an exercise on that same day is indexed with 1, 0.7τ days later the impact is indexed with 0.5. Vice versa, after τ days, the impact is indexed with $1/e \approx 0.37$. Thus, if the initial impact of fitness and delay is indexed with 100% and the initial impact of fatigue is indexed with $100\%K$, the kernel parameters separately can be interpreted as follows:

τ_{fit}	After $0.7\tau_{\text{fit}}$ days, the impact on fitness is approximately 50%	After τ_{fit} days, the impact on fitness is approximately 37%.
τ_{del}	After $0.7\tau_{\text{fit}}$ days, the impact on the delay of fitness is approximately 50%	After τ_{del} days, the impact on the delay of fitness is approximately 37%.
τ_{fat}	After $0.7\tau_{\text{fat}}$ days, the impact on fatigue is approximately $50\%K$	After τ_{fat} days, the impact on fatigue is approximately $37\%K$.

In the study of Calvert et al. [6] values for τ_{fit} , τ_{del} , τ_{fat} , and K are estimated based on a study on multiple athletes. These values are expected to be athlete specific. Therefore, they need to be estimated for each cyclist individually. In [6], the parameter values as in Equation (??) were deduced from data

$$\tau_{\text{fit}} = 50 \text{ days} \quad \tau_{\text{del}} = 5 \text{ days} \quad \tau_{\text{fat}} = 15 \text{ days} \quad K = 2.0 \quad (7.11)$$

In Figure 7.1 both the fitness and fatigue part of the kernel are plotted together with the kernel itself over a time span of 60 days and with the values of the kernel parameters as stated in Equation (7.11). As we can see, the initial effect of the training is negative, due to the fatigue, but after approximately 17 days the net effect becomes positive.

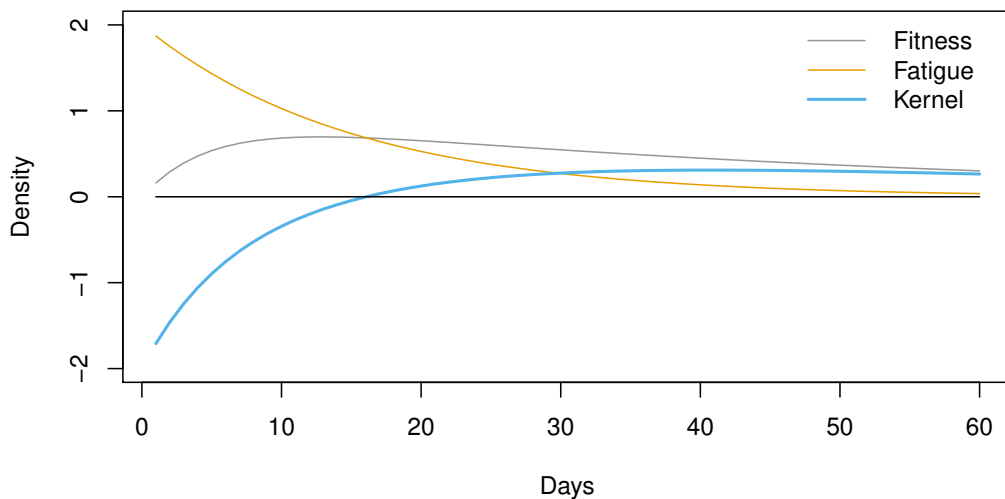


Figure 7.1: The positive part of the kernel $h_+(i)$, the negative part of the kernel $h_-(i)$ and the kernel itself of the fitness-fatigue model with values as stated in Equation (7.11).

7.2. Estimating the training parameters

Now that we have a model to predict the performance of a cyclist, we need to estimate the individual parameters of the model. First of all, we rewrite the model so it is easier to estimate the parameters. Subsequently, we state how we estimate the two different parameter sets.

Now the summarized training value $x(t)$ of Equation (7.2) can be substituted in the Fitness-Fatigue model of Equation (7.10), yielding Equation (7.12).

$$y(t) = C + \sum_{i=1}^{\infty} \sum_{m=1}^M \alpha_m Z_m(t-i) \cdot \left(\left(e^{-\lambda_{\text{fit}} \cdot i} - e^{-\lambda_{\text{del}} \cdot i} \right) - K \cdot e^{-\lambda_{\text{fat}} \cdot i} \right) \quad (7.12)$$

Summing i till infinity is unrealistic, because for every cyclist there has not been an infinite number of exercises. Furthermore, because of the exponential decay of the kernel function, a cut-off can be justified. Therefore, we bound the first summation as far as we have data. This has the negative effect that for the first days, the effect of training on performance is based on a small sample. Therefore, when evaluating the parameters, we do not take the first year of data points in consideration. Using the notion that the sum over i is bounded, we can switch the summation of Equation (7.12) as in Equation 7.13.

$$y(t) = C + \sum_{m=1}^M \alpha_m \sum_{i=1}^I Z_m(t-i) \cdot \left(\left(e^{-\lambda_{\text{fit}} \cdot i} - e^{-\lambda_{\text{del}} \cdot i} \right) - K \cdot e^{-\lambda_{\text{fat}} \cdot i} \right) \quad (7.13)$$

This objective of this model is to predict the performance of a cyclist. Therefore, we use the CCP that was calculated in the previous chapter, using the locally bounded variation with $M_d = 3$ as a response variable on which to optimize the training parameters.

Two different sets of training parameters have to be estimated. The first set consists of the kernel parameters τ_{fit} , τ_{del} , τ_{fat} , and K . These parameters yield information about the optimal training schedule, as explained in Subsection 7.1.1. The second set consists of the values α_m , the relative training parameters, that determine which training parameters are more important to monitor than others.

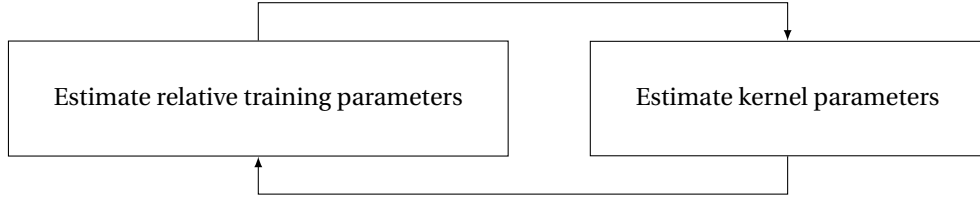


Figure 7.2: Iterative process to optimize both the relative training parameters as the kernel parameters.

7.2.1. Goodness of fit

The estimation of the parameters is done by an optimization algorithm that maximizes the goodness of fit over the parameter space in each iteration. The R^2 -value of the ordinary least squares relation between $y(t)$ and CCP(t) is used to evaluate the goodness of fit of the prediction $y(t)$. This value indicates how accurately we can model the performance of a cyclist given his or her training attributes.

7.2.2. Relative training parameters

For given values of the parameters λ_{fit} , λ_{del} , λ_{fat} , and K , we can calculate the inner sum of Equation (7.13) and denote this with $V_m(t)$, such that we can rewrite Equation (7.13) as in Equation (7.14).

$$y(t) = C + \sum_{m=1}^M \alpha_m V_m(t) \quad (7.14)$$

Determining the values of C and α_m is done by the LASSO-method [23]. This method is preferred over other regressions methods since it is an efficient method that simultaneously performs regularization and feature selection, thus minimizing the number of training attributes incorporated in the final model. The LASSO-method standardizes the values of $V_m(t)$ for all m , such that the values of α_m can be compared among each other. It finds the values of C and α_m , $m = 1, \dots, M$ such that

$$\min_{C, \alpha_m} \left\{ \frac{1}{N} \sum_{n=1}^N \left(y(i) - C - \sum_{m=1}^M \alpha_m V_m(i) \right)^2 + \gamma \sum_{m=1}^M |\alpha_m| \right\} \quad (7.15)$$

Here γ is a free parameter that needs to be specified beforehand to determine the amount of regularization; a higher value of γ leads to less freedom for the parameters. The advantage of using the L_1 -norm for the penalty is that it yields a subset selection based on the values of m such that $\alpha_m \neq 0$. This subset can be interpreted as being sufficient to predict the performance of the cyclist. Increasing the value of γ forces more values of α_m to be zero, as to prevent overfitting and making the final model more usable in practice. In Subsection 7.4.3 an analysis is performed of the influence of the value of γ .

The optimal value of γ is chosen by cross-validation, which calculates the mean cross-validated error for every value of γ . The value of γ is selected such that it minimizes this mean cross-validated error.

7.2.3. Kernel parameters

After the LASSO-method is used to estimate the values for C and α_m , these values are held fixed and the values for λ_{fit} , λ_{del} , λ_{fat} , and K are estimated such that the objective value is optimized. Knobbe et al. [9] showed that the relationship of R^2 as a function of each of the kernel parameters separately is concave. Therefore, a hill climbing algorithm is used to find local optimal values for the kernel parameters. This algorithm iteratively increases and decreases the values of τ_{fit} , τ_{fat} , τ_{del} and K by respectively 1, 0.5, 1 and 0.1, then it evaluates which direction yields the largest improvement in R^2 , after which the estimate is replaced by the corresponding point. If no more improvements are possible, the algorithm is converged and terminates. The step-values 1, 0.5, 1 and 0.1 are chosen as small as possible, while still being interpretable. For example, for fitness and fatigue, a step of one day is chosen, because exercises are scheduled daily. In order to be able to interpret the kernel parameters, all values are bounded below by 0, i.e. the hill climb algorithm will not evaluate negative values for the kernel parameters.

7.3. Implementation

In this section the implementation of the algorithm that estimates the training parameters is introduced. The analysis is performed step by step as to gradually build up to the final model. In the first steps, some parameters are held fixed, while others are being estimated. In the final step, all parameters are estimated simultaneously. The implementation of the algorithm is illustrated with the data of cyclist 2.

7.3.1. Step by step analysis of training parameter estimation

In the results section, Section (7.4), we perform the different analyses in order to build up to the final results. Below, the different steps of the analyses are listed.

1. The first step of the analysis is to evaluate which predictor has the highest predictive value. Therefore, we restrict C to be equal to the value found in Chapter 4 (348 W) and the parameters τ_{fit} , τ_{del} , τ_{fat} and K are set as in Equation (7.11). Then, iteratively for each m , α_m is set to 1 and $\alpha_n = 0$ for $n \neq m$. In this way, we can see which of the training attributes is the best predictor of performance on its own.
2. The second step differs from the first by optimizing the values of τ_{fit} , τ_{del} , τ_{fat} and K by the hill climb algorithm as explained in Subsection 7.2.3. This way, we can analyze what the impact is over time for the different training attributes.
3. In the third step, we keep the kernel parameters fixed as in Equation (7.11) and use the LASSO-method to estimate the values of the α_m . Furthermore, we investigate the influence of the regularization penalty value γ . This way, for the given kernel parameters, we can analyze the impact of each training attribute.
4. In the fourth and final step, both the relative training parameters and kernel parameters are estimated by the algorithm visualized in Figure 7.2. Both parameter sets are estimated independently with the other set held fixed, until the algorithm is converged. It starts by using the kernel parameters as stated in Equation (7.11) and estimating the relative training parameters.

7.4. Results

This section presents the results of the above mentioned step-by-step analysis. The first four subsections cover the results of the four steps stated in Subsection 7.3.1. Afterwards, Subsection 7.4.5 states the results of the final step for all cyclists.

7.4.1. The first step - Best predictor

In this step we analyze the results of the predictive value of each single training attribute for the standard kernel parameters of Equation (7.11). Table 7.1 contains the values of all fitted parameters for cyclist 2, together with the R^2 -value of the linear relationship between the predicted and actual performance value. As we can see, all single training attributes lead to low R^2 -values ranging from 0.00 for TSS to 0.11 for intensity. Therefore, the predictive value of a single training attribute with the standard kernel parameters is low. Nonetheless, intensity does have a higher R^2 -value than the other training attributes, which indicates that for cyclist 2 it is the most accurate predictor for these fixed kernel parameters.

Table 7.1: The R^2 -value for cyclist 2 with fixed training parameters. The values printed in italics are fixed.

Parameter	Relative training parameters						Kernel parameters				R^2
	C	α_1	α_2	α_3	α_4	α_5	τ_{fit}	τ_{del}	τ_{fat}	K	
	348	<i>1.00</i>	<i>0.00</i>	<i>0.00</i>	<i>0.00</i>	<i>0.00</i>	50	5	15	2.0	0.02
	348	<i>0.00</i>	<i>1.00</i>	<i>0.00</i>	<i>0.00</i>	<i>0.00</i>	50	5	15	2.0	0.11
	348	<i>0.00</i>	<i>0.00</i>	<i>1.00</i>	<i>0.00</i>	<i>0.00</i>	50	5	15	2.0	0.04
	348	<i>0.00</i>	<i>0.00</i>	<i>0.00</i>	<i>1.00</i>	<i>0.00</i>	50	5	15	2.0	0.00
	348	<i>0.00</i>	<i>0.00</i>	<i>0.00</i>	<i>0.00</i>	<i>1.00</i>	50	5	15	2.0	0.02

7.4.2. The second step - Impact over time

In this step we try to improve the R^2 -value of the previous step by optimizing the kernel parameters for each single training attribute by the hill climb algorithm proposed in Subsection 7.2.3. Furthermore, we show that the value of R^2 in this case is indeed a concave function of the single kernel parameters.

Table 7.2 contains the results of this step of the analysis. The first noticeable fact is that the R^2 has increased to values between 0.36 and 0.45, where the best predictive training attribute is Duration. Figure 7.3 visualizes the actual performance (CCP) and the predicted performance when using solely the training attribute Duration with kernel parameters as in the first row of Table 7.2. This figure shows that the prediction in the first year is inaccurate, but that is due to the fact that the first year is not included when calculating the R^2 -value. In the subsequent 3 years, the Fitness Fatigue model does seem to predict the general trend of the performance level quite accurately, as is illustrated by the R^2 value of 0.45.

The estimated kernel parameters also contain interesting information. The values of τ_{fit} fall in the range from 22 to 49, which might indicate that the time period after which extra fitness is achieved differs per training attribute. For $\alpha_4 = 1$ we have that $\tau_{\text{fit}} = \tau_{\text{fat}}$ and $K > 1.0$. Therefore, $h(i) < 0$ for all i , due to the fact that fatigue exceeds extra fitness over time. This is unrealistic, since it would indicate that the cyclist should not train at all to reach his optimal performance.

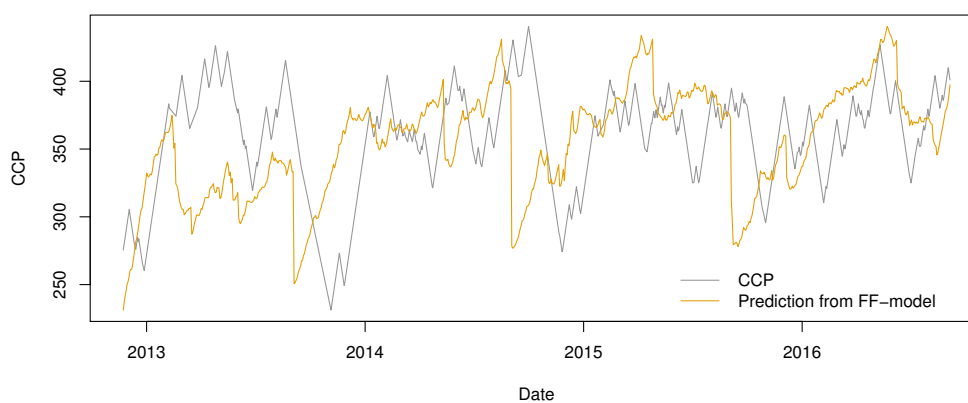


Figure 7.3: The prediction of the FF-model for cyclist 2 when solely duration is used as training attribute with kernel parameters $\tau_{\text{fit}} = 41$, $\tau_{\text{del}} = 0.5$, $\tau_{\text{fat}} = 1$, and $K = 2.0$

In Figure 7.4 the value of R^2 between $y(t)$ and $CCP(t)$ is plotted against the different one-dimensional kernel parameters. We notice that we indeed found a local optimum, because all plots show concave behavior. Furthermore, it is interesting to note that for certain parameters, a change in that parameter does not

Table 7.2: The R^2 -value for cyclist 2 with fixed relative training parameters and free kernel parameters. The values printed in italics are fixed.

Parameter	Relative training parameters					Kernel parameters				R^2	
	C	α_1	α_2	α_3	α_4	α_5	τ_{fit}	τ_{del}	τ_{fat}		K
	<i>348</i>	<i>1.00</i>	<i>0.00</i>	<i>0.00</i>	<i>0.00</i>	<i>0.00</i>	29	0.5	11	0.4	0.45
	<i>348</i>	<i>0.00</i>	<i>1.00</i>	<i>0.00</i>	<i>0.00</i>	<i>0.00</i>	49	5	3	1.8	0.36
	<i>348</i>	<i>0.00</i>	<i>0.00</i>	<i>1.00</i>	<i>0.00</i>	<i>0.00</i>	22	10.5	8	0.2	0.36
	<i>348</i>	<i>0.00</i>	<i>0.00</i>	<i>0.00</i>	<i>1.00</i>	<i>0.00</i>	36	18	36	1.3	0.42
	<i>348</i>	<i>0.00</i>	<i>0.00</i>	<i>0.00</i>	<i>0.00</i>	<i>1.00</i>	28	0.5	11	0.4	0.43

influence the value of R^2 greatly. For example, values of τ_{fit} between 20 and 50 all lead to R^2 values greater than 0.40 and for τ_{fat} all values between 0 and 30 even lead to values above 0.44. On the other hand, changing the value of K from 0.4 to 1.5 reduces the R^2 value by 0.2 points. This indicates that for the values of τ_{fit} and τ_{fat} , that are the most interesting from a practical point of view, a large range of values is possible that does not influence the value of R^2 by more than 0.1.

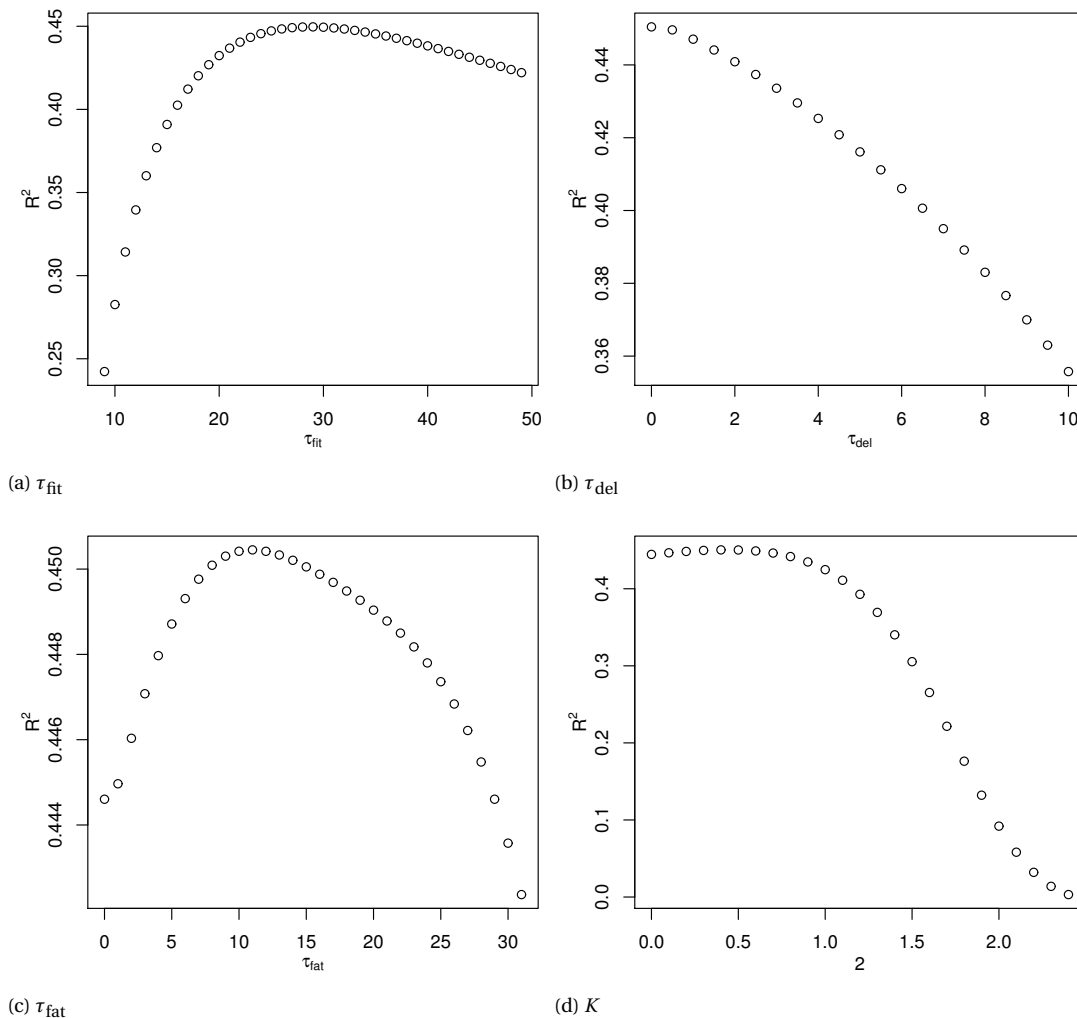


Figure 7.4: The value of R^2 plotted against the values of the kernel parameters to show that the kernel values indeed represent a local maximum.

7.4.3. The third step - Attribute selection

In this step we fix the kernel parameters of Equation (7.11) and estimate the values of C and the α_m to assess the impact of each individual training attribute. During the analysis, the LASSO-method exhibited some unexpected behavior; the total error term as in Equation (7.15) did not decrease as γ decreased. This is probably caused by highly correlated predictors. For more information on this behavior, see Appendix B. In order to overcome this unexpected and unwanted behavior of the LASSO-parameters, the training attribute Objective Load is removed from the analysis, thus we continue with first four training attributes, i.e. Duration, Intensity, Subjective Load and TSS.

In Figure 7.5 the values of the different α_m are plotted against the value of $\log \gamma$. This graph shows that the value of α_1 , corresponding to the training attribute Duration, dominates the other α values. This indicates that, for this cyclist, duration is the training attribute that has the most impact on performance among the investigated training attributes for this given set of kernel parameters. Furthermore, it is interesting to see that the values of α_3 and α_4 , corresponding to Subjective Load and TSS, are both negative and relative small in absolute value (< 0.1). This indicates that for this cyclist, the impact of these attributes is negative and small compared with Duration and Intensity. These are also the values to be restricted to zero first when increasing the value of γ .

In Figure 7.6 we see the results of the cross validation for the different values of γ . The conclusion in this case is that the optimal value of γ is such that all four parameters α_m are present and thus non-zero. These results are confirmed in Table 7.3, which contains the values of C and the α_m for the given kernel parameters and $\gamma = 0.11$, the value that minimizes the mean cross-validated error.

The value of R^2 is higher than the R^2 -values obtained in the first step, thus combining training attributes instead of picking a specific one is an improvement of the model. However, the value of R^2 is lower than in the previous step, thus optimizing the training attributes for fixed kernel parameters has not improved the accuracy in comparison with fixed training attributes and free kernel parameters. The absolute value of the α_m is largest for $m = 1$ and $m = 2$, which indicates that the training attributes Duration and Intensity have the largest impact on performance. Furthermore, α_3 and α_4 , corresponding to Subjective Load and TSS, are negative, indicating that these training attributes have negative influence on the performance for this given set of kernel parameters.

Table 7.3: The R^2 -value for cyclist 2 with free relative training parameters and fixed kernel parameters. The values printed in italics are fixed.

Parameter	Relative training parameters						Kernel parameters				R^2
	C	α_1	α_2	α_3	α_4	α_5	τ_{fit}	τ_{del}	τ_{fat}	K	
Value	336	2.47	0.38	-0.09	-0.04	<i>0.00</i>	<i>50</i>	<i>5</i>	<i>15</i>	<i>2</i>	0.34

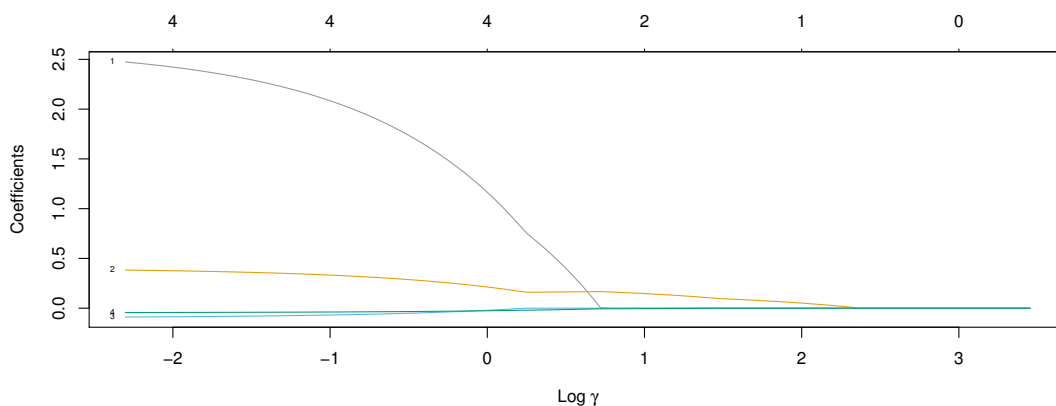


Figure 7.5: The values of α_m plotted against the log-value of γ for cyclist 2 and fixed kernel parameters.

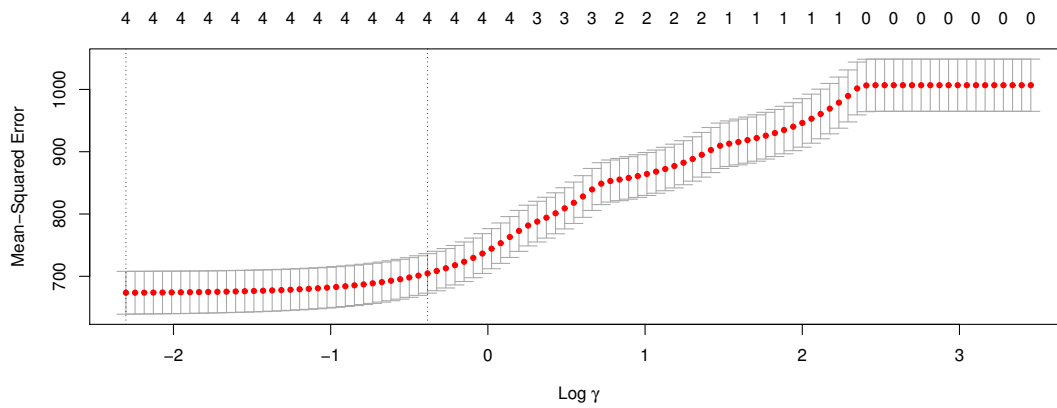


Figure 7.6: Cross-validation for the values of γ for cyclist 2 and fixed kernel parameters.

7.4.4. The fourth step - Estimating both parameter sets simultaneously.

In the fourth and final step we optimize both the kernel parameters as the relative training parameters iteratively as visualized in Figure 7.2. Table 7.4 contains the results of this analysis. Comparing the results of this step with those of the previous, we see that the accuracy has improved from $R^2 = 0.34$ to 0.45. This is mostly due to changes in the value of τ_{fat} , while the other parameters are relatively unaltered.

However, optimizing both the kernel parameters and the relative training parameters yields the same value of R^2 as when we only optimize the kernel parameters for certain training attributes, see Table 7.2. This is an interesting observation, since it indicates that combining multiple training attributes does not necessarily lead to a higher value of R^2 .

Table 7.4: The results of the analysis of step 4 for cyclist 2

Parameter	Relative training parameters					Kernel parameters				R^2	
	C	α_1	α_2	α_3	α_4	α_5	τ_{fit}	τ_{del}	τ_{fat}		K
Value	252	1.11	0.11	-0.02	-0.01	0.00	56	4.5	1.0	1.9	0.45

Figure 7.7 visualizes the prediction of step four for cyclist 2.

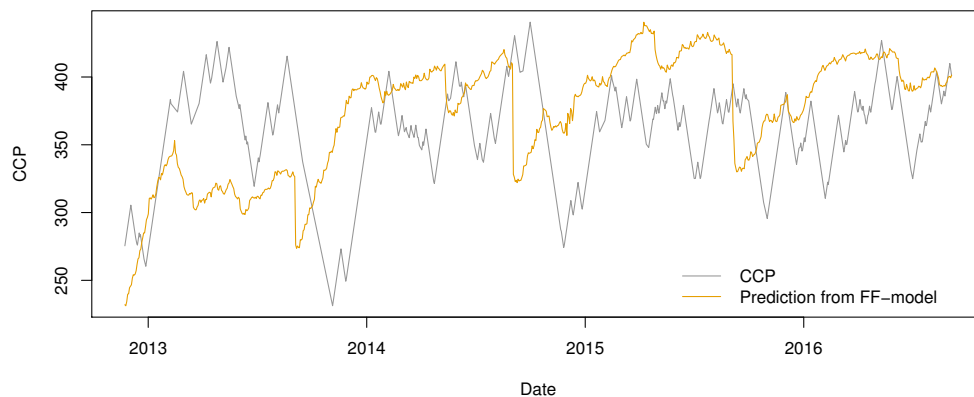


Figure 7.7: The value of CCP over time plotted together with the predicted value of CCP as by the model of Equation (7.10), using the parameters shown in Table 7.4.

7.4.5. Fourth step for all cyclists

In Table 7.5 the results of the final analysis for all cyclists are stated. As we can see in the table, the algorithm results in different parameters and goodness-of-fit measures for all cyclists. The values of R^2 fall between 0.37 and 0.56, with the exception of cyclist 4. These values are comparable to the results of Knobbe et al. [9] where the model was used for ice skaters and R^2 -values in the range of 0.27 – 0.59 are found, but lower than in the study of two amateur runners in [15], where R^2 -values of 0.71 and 0.96 are found. These results lead to the

conclusion that the Fitness-Fatigue model can indeed be applied to elite cyclists in a comparable degree as it can to ice skaters. The fact that the R^2 -values of the two amateur runners is higher, can be explained by the number of data points (≈ 20) on which the model is applied and by the fact that both runners were untrained before the experiments.

Looking at the relative training parameters, it is interesting to note that different attributes have different effects on the cyclists. For example, cyclist 1 receives a negative influence of long trainings, while for cyclist 2 long training are beneficial, and for the other four cyclists the influence is zero. The kernel parameters also differ per cyclist. For example, the values of τ_{fit} fall within a range of 23 to 79.

Table 7.5: The estimated values of the training parameters for cyclist 2

Parameter	Relative training parameters					Kernel parameters				R^2	
	C	α_1	α_2	α_3	α_4	α_5	τ_{fit}	τ_{del}	τ_{fat}		K
Cyclist 1	220	-0.79	0.00	0.04	-0.02	0.00	70	5	35	2.5	0.56
Cyclist 2	252	1.11	0.11	-0.02	-0.01	0.00	56	4.5	1.0	1.9	0.45
Cyclist 3	392	0.00	-0.07	0.07	-0.03	0.00	79	1	27	1.9	0.55
Cyclist 4	371	0.00	-0.07	0.06	-0.02	0.00	54	5	19	2	0.13
Cyclist 5	346	0.00	-0.23	-0.01	-0.01	0.00	62	16.5	19	0.9	0.42
Cyclist 6	173	0.00	0.00	0.03	0.03	0.00	23	5.5	1	2	0.37

In Appendix C Figures are place in which the model prediction is plotted for all six cyclists. These figures also visually indicate that for certain cyclists (1 and 6), the Fitness-Fatigue model seems to yield accurate predictions, whereas for other cyclists (4 and 5) it does not seem to provide accurate predictions

7.5. Conclusion

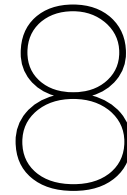
Several conclusions can be drawn from the results section. Do note that all these conclusions are based on the assumption that the CCP value of the previous chapter is an accurate measure of performance.

Table 7.5 indicates that the Fitness-Fatigue model behaves differently for each individual cyclist. For five out of six cyclists, the model predicts performance with R^2 -values between 0.37 and 0.56. Therefore, it depends on (the data of) the cyclist, whether or not the Fitness-Fatigue will be able to help him or her in determining his optimal training schedule.

Furthermore, Table 7.5 also shows estimated kernel parameters that differ among cyclists. Although this is as expected, each cyclist improves in a different way, some estimated values seem unrealistic, such as a τ_{fat} of 1, indicating there is barely an impact of fatigue. Thus, despite reasonable R^2 -values for some cyclists, the values of the kernel parameters lead to believe that not all sets of estimated parameters are realistic, and thus not yield useful information.

Nonetheless, cyclists 1 and 3 have R^2 -values of 0.56 and 0.55 respectively and have reasonable estimated kernel parameters. In those cases, the Fitness-Fatigue model does lead to interesting and useful information for constructing the optimal training schedule. A coach or a cyclist could then use the Fitness-Fatigue model to check whether his or her constructed training schedule achieves the goals of the cyclist, or to use the values of the estimated parameters to help him or her construct the optimal training schedule.

The reason why the Fitness-Fatigue model leads to accurate and realistic predictions for some cyclists, but not for others could be explained by multiple causes. It could be caused by the absence of a sufficient amount of data, by inaccuracy in the performance metric, or by a combination of both causes.



Conclusion and future work

"Mathematics is the most exact science, and its conclusions are capable of absolute proof. But this is so only because mathematics does not attempt to draw absolute conclusions. All mathematical truths are relative, conditional." - C.P. Steinmetz, 1923

8.1. Conclusion

Let us return to the main research goal we stated in the introduction:

"Adapt the Fitness-Fatigue model such that it can be used by elite cyclists to accurately model and predict their performance."

The results of this report indicate that the Fitness-Fatigue model indeed has the potential to be a valuable addition to the toolset available to cyclists to optimize training schedules. In this report, this is illustrated by preliminary analysis in two main subjects: quantifying the performance of a cyclist and estimating the parameters of the Fitness-Fatigue model; the two current major challenges of sport analytics in cycling.

The first of these challenges is objectively quantifying the performance of a cyclist over a given period. The cycled critical power (CCP) is a metric that addresses this issue by modeling the energy systems of the body and estimating the performance level of that cyclist over the given period. This performance level can subsequently be used to analyze the influence of training attributes. The advantages of the CCP compared to other performance metrics are that it is easily calculable on a daily basis and that no extra physical effort is required for its calculations. The most significant drawback is that the calculated CCP is only accurate on days that a cyclist's anaerobic work supply has depleted. In the next section, some possibilities are discussed that could improve the accuracy of the CCP.

The second major challenge is the individualization of the training schedule to a cyclist's specific needs. Existing literature [2], [9], [15] already shows that the Fitness-Fatigue model is a good predictor of performance when an accurate performance metric is used. Furthermore, these researches yield individual parameters that provide practical information for an individual's training schedule. The Fitness-Fatigue model also leads to accurate and realistic predictions of the performance for some cyclists. However, for other cyclists the prediction is inaccurate or the estimated parameters are not all within the expected range. This could be caused by the absence of sufficient data, inaccuracy in the performance metric, or a combination of both.

Taking these two considerations into account, the Fitness-Fatigue model is likely to be valuable in the future construction of training schedules for all elite cyclists under the condition that the CCP is improved or another accurate performance measure is developed.

It is once more the 28th of May 2017. Tom Dumoulin is warming up for a time trial, perhaps the most important time trial of his entire career. It is the final stage of the 100th edition of the Giro d'Italia. Tom is in third place, but time trials are his specialty. Furthermore, he has been training according to a training schedule constructed with the support of the Fitness-Fatigue model. This way he is certain that his training load has been optimal over the previous weeks and that he is in the best shape he can be. He dominates the time trial and ends up winning the Giro d'Italia 2017!



Figure 8.1: Tom Dumoulin with the cup of the Giro d'Italia 2017

8.2. Future research

As stated in the previous section, the potential for the Fitness-Fatigue model to be used in the future as a tool for cyclists and coaches is present, but further research is required. The proposed future research is divided in two parts; improving the performance metric (CCP) and improving the application of the Fitness-Fatigue model.

8.2.1. Improving the CCP

The most promising steps that can be undertaken to improve the accuracy of the CCP do not fall within the field of sport analytics, but within the fields of biology and kinesiology.

In order to make the CCP more accurate on days in which the cyclist's anaerobic work supply did not deplete, the minimum level of anaerobic energy in the body on such a day could be investigated; as well as how that level could be predicted. If, for example, we could predict the minimum level of anaerobic energy based on the subjective intensity of an exercise, the algorithm to calculate the CCP could take this information into account in order to come up with a more accurate estimation of the CCP. This way, the CCP would yield more information on days in which the cyclist's anaerobic energy supply did not deplete.

The accuracy of the CCP on days that the cyclist's anaerobic energy supply depleted can also be improved. This could be done by further researching and evaluating the equations used to model the dynamics of the anaerobic energy supply. Furthermore, a method to estimate the value of $\tau_{W'}(t)$ could be developed for individual cyclists; as this value is probably not uniform for all cyclists.

The last proposed research topic is how the dynamics of W' over time can be taken into account when quantifying the performance. As we have stated before, for some cyclists, such as sprinters, the value of W' is more important, but the concept of CCP assumes it to be a fixed value. For these cyclists it is crucial to find a performance metric or to develop the CCP in order to have a daily estimate of the anaerobic energy supply as well.

8.2.2. Improving the Fitness-Fatigue model

The practical application of the Fitness-Fatigue model could be improved by further investigating the interpretation and estimation of the model parameters.

The values of both the relative training parameters and kernel parameters are difficult to interpret for non-mathematicians; hindering the practical application. Therefore, research that investigates the optimal training schedule, given the estimated values of the Fitness-Fatigue model and certain goals in a season, could assist coaches by providing ready-to-use training schedules

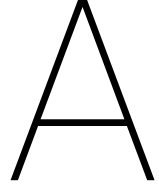
Furthermore, the method of finding the values of these parameters could be improved. As stated, the hill climb algorithm to optimize the kernel parameters leads to a local optimum. Whether this is also the global optimum or whether there is another, more efficient, way to find the global optimum could be investigated. Estimating the relative training parameters by the LASSO-method also leads to an unwanted situation, so research that investigates how to estimate the relative training parameters would also yield valuable information. Lastly, the iterative combination of the hill climb and LASSO-method should be critically examined.

Three final suggestions that might improve the applicability of the Fitness-Fatigue model are the following. Firstly, the estimation of the model could only be applied to days in which the cyclist's anaerobic energy supply depleted. For example during races. That way, the number of total validation points is reduced, but the remaining validation points are more accurate. Secondly, in the Fitness-Fatigue model it is assumed that every training attribute has the same kernel parameters, i.e. the effect of every training attribute is equal over time. It is known that long duration training is more influential for a longer period of time than high intensity trainings, whereas high intensity training has more influence just before a race. Therefore, it would be interesting to investigate an extension of the Fitness-Fatigue model where the kernel parameters are allowed to differ for different training attributes. Lastly, other type of exercises that cyclist perform such as going to the gym or swimming, could also be incorporated into the Fitness-Fatigue model.

Bibliography

- [1] H. Allen and A. Coggan. *Training and racing with a power meter*. VeloPress, 2012.
- [2] E.W. Banister, J.B. Carter, and P.C. Zarkadas. “Training theory and taper: validation in triathlon athletes”. In: *European journal of applied physiology and occupational physiology* 79.2 (1999), pp. 182–191.
- [3] J.C. Bartram et al. “Accuracy of W’ recovery kinetics in high performance cyclists - modelling intermittent work capacity.” In: *International Journal of Sports Physiology and Performance* (2017).
- [4] H.C. Bergstrom et al. “Differences among estimates of critical power and anaerobic work capacity derived from five mathematical models and the three-minute all-out test”. In: *The Journal of Strength & Conditioning Research* 28.3 (2014), pp. 592–600.
- [5] A. Björck. *Numerical methods for least squares problems*. SIAM, 1996.
- [6] T.W. Calvert et al. “A systems model of the effects of training on physical performance”. In: *IEEE Transactions on Systems, Man, and Cybernetics* 2 (1976), pp. 94–102.
- [7] P.B. Gastin and D.L. Lawson. “Variable resistance all-out test to generate accumulated oxygen deficit and predict anaerobic capacity”. In: *European journal of applied physiology and occupational physiology* 69.4 (1994), pp. 331–336.
- [8] M. Hebiri and J. Lederer. “How correlations influence lasso prediction”. In: *IEEE Transactions on Information Theory* 59.3 (2013), pp. 1846–1854.
- [9] A. Knobbe et al. “Sports analytics for professional speed skating”. In: *Data Mining and Knowledge Discovery* (2017), pp. 1–31.
- [10] M. Liversedge. *W’bal optimization by a mathematician!* 2014. URL: <http://markliversedge.blogspot.nl/2014/10/wbal-optimisation-by-mathematician.html> (visited on 04/17/2017).
- [11] J.I. Medbo et al. “Anaerobic capacity determined by maximal accumulated O₂ deficit”. In: *Journal of Applied Physiology* 64.1 (1988), pp. 50–60.
- [12] H. Monod and J. Scherrer. “Capacity for static work in a synergistic muscular group in man”. In: *Comptes rendus des séances de la Société de biologie et de ses filiales* 151.7 (1957), pp. 1358–1362.
- [13] T. Moritani et al. “Critical power as a measure of physical work capacity and anaerobic threshold”. In: *Ergonomics* 24 5 (1981), pp. 339–350.
- [14] R.H. Morton. “A 3-parameter critical power model”. In: *Ergonomics* 39.4 (1996), pp. 611–619.
- [15] R.H. Morton, J.R. Fitz-Clarke, and E.W. Banister. “Modeling human performance in running”. In: *Journal of applied physiology* 69.3 (1990), pp. 1171–1177.
- [16] J.A. Nelder and R. Mead. “A simplex method for function minimization”. In: *The computer journal* 7.4 (1965), pp. 308–313.
- [17] L. Passfield et al. “Knowledge is power: Issues of measuring training and performance in cycling”. In: *Journal of sports sciences* 35.14 (2017), pp. 1426–1434.
- [18] M. Post-Vreugdenhil. “The detection of changes in the performance of a pro-cyclist”. B.S. Thesis. Delft university of technology, 2016.
- [19] P. F. Skiba et al. “Effect of Work and Recovery durations on W’ reconstitution during intermittent exercise”. In: *Medicine & Science in sports & exercise* (2013).
- [20] P. F. Skiba et al. “validation of a novel intermittent W’ model for cycling using field data”. In: *International journal of sport physiology and performance* (2014).
- [21] P.F. Skiba et al. “Modeling the expenditure and reconstitution of work capacity above critical power.” In: *Medicine and science in sports and exercise* 44.8 (2012), pp. 1526–1532.

-
- [22] L. Steinberg. *Changing the game: the rise of sport analytics*. 2015. URL: <https://www.forbes.com/sites/leighsteinberg/2015/08/18/changing-the-game-the-rise-of-sports-analytics/2/#62077158a1b5>.
- [23] R. Tibshirani. "Regression shrinkage and selection via the lasso". In: *Journal of the Royal Statistical Society. Series B (Methodological)* (1996), pp. 267–288.
- [24] M.C. Tsai. "Revisiting the power-duration relationship and developing alternative protocols to estimate critical power parameters". PhD thesis. University of Toronto, 2015.
- [25] A. Vanhatalo, J.H. Doust, and M. Burnley. "Determination of critical power using a 3-min all-out cycling test". In: *Medicine and science in sports and exercise* 39.3 (2007), p. 548.



Proofs of lemmas and theorem of chapter 6.

A.1. Proof of Lemma 6.1

Lemma A.1. *The function $f : \mathbb{R} \rightarrow \mathbb{R}$ with $f(CP) = \min_t (W'_{\text{bal}}(t)|_{CP})$ is monotone.*

Proof. Suppose that we have arbitrary $W' > 0$, $P(t) \geq 0$ for $t \in [0, T]$ and the formulas $h_1(x)$ and $h_2(x)$ that satisfy $h_j \geq 0$ and $h_j(0) = 0$ for $j = 1, 2$, $0 < \frac{dh_1}{dx} < M$, and $0 \leq \frac{dh_2}{dx} < M$ as in Definition 6.1. Now we take an arbitrary CP_1 and CP_2 such that $CP_1 < CP_2$. We want to show that $f(CP_1) \leq f(CP_2)$, i.e. $\min_{t \in [0, T]} \{W'_{\text{bal}}(t)|_{CP_1}\} \leq \min_{t \in [0, T]} \{W'_{\text{bal}}(t)|_{CP_2}\}$. In order to show this, we show by induction that for all $t \in [0, T]$: $W'_{\text{bal}}(t)|_{CP_1} \leq W'_{\text{bal}}(t)|_{CP_2}$.

For $t = 0$ we have that $W'_{\text{bal}}(0)|_{CP_1} = W' = W'_{\text{bal}}(0)|_{CP_2}$.

Now assume that $W'_{\text{bal}}(t_{i-1})|_{CP_1} \leq W'_{\text{bal}}(t_{i-1})|_{CP_2}$. Then, depending on $P(t_{i-1})$, we have three cases to investigate:

1. $\mathbf{P}(t_{i-1}) \leq \mathbf{CP}_1 < \mathbf{CP}_2$. In this case we have

$$\begin{aligned} W'_{\text{bal}}(t_i)|_{CP_1} &= W'_{\text{bal}}(t_{i-1})|_{CP_1} + h_2(CP_1 - P(t_{i-1})) \\ W'_{\text{bal}}(t_i)|_{CP_2} &= W'_{\text{bal}}(t_{i-1})|_{CP_2} + h_2(CP_2 - P(t_{i-1})) \end{aligned}$$

The fact that $CP_2 > CP_1$ implies that $CP_2 - P(t_{i-1}) > CP_1 - P(t_{i-1})$, and because h_2 has a positive first derivative we have that $h_2(CP_2 - P(t_{i-1})) \geq h_2(CP_1 - P(t_{i-1}))$. Together with the induction hypothesis yields that $W'_{\text{bal}}(t)|_{CP_1} \leq W'_{\text{bal}}(t)|_{CP_2}$

2. $\mathbf{CP}_1 < \mathbf{P}(t_{i-1}) < \mathbf{CP}_2$. Now we have that

$$\begin{aligned} W'_{\text{bal}}(t_i)|_{CP_1} &= W'_{\text{bal}}(t_{i-1})|_{CP_1} - h_1(P(t_{i-1}) - CP_1) \\ W'_{\text{bal}}(t_i)|_{CP_2} &= W'_{\text{bal}}(t_{i-1})|_{CP_2} + h_2(CP_2 - P(t_{i-1})) \end{aligned}$$

and due to the induction hypothesis and the fact that $h_1(P(t_{i-1}) - CP_1) > 0$ and $h_2(CP_2 - P(t_{i-1})) \geq 0$, we can once more conclude that $W'_{\text{bal}}(t)|_{CP_1} \leq W'_{\text{bal}}(t)|_{CP_2}$.

3. $\mathbf{CP}_1 < \mathbf{CP}_2 \leq \mathbf{P}(t_{i-1})$. In the last case we have that

$$\begin{aligned} W'_{\text{bal}}(t_i)|_{CP_1} &= W'_{\text{bal}}(t_{i-1})|_{CP_1} - h_1(P(t_{i-1}) - CP_1) \\ W'_{\text{bal}}(t_i)|_{CP_2} &= W'_{\text{bal}}(t_{i-1})|_{CP_2} - h_1(P(t_{i-1}) - CP_2) \end{aligned}$$

The fact that $CP_2 > CP_1$ implies that $P(t_{i-1}) - CP_2 < P(t_{i-1}) - CP_1$, and because h_1 has a positive first derivative we have that $h_1(P(t_{i-1}) - CP_2) < h_1(P(t_{i-1}) - CP_1)$. Together with the induction hypothesis yields once more that $W'_{\text{bal}}(t)|_{CP_1} \leq W'_{\text{bal}}(t)|_{CP_2}$

We have shown by induction that for all $t \in [0, T] : W'_{\text{bal}}(t)|_{CP_1} \leq W'_{\text{bal}}(t)|_{CP_2}$ which implies that $\min_{t \in [0, T]} \{W'_{\text{bal}}(t)|_{CP_1}\} \leq \min_{t \in [0, T]} \{W'_{\text{bal}}(t)|_{CP_2}\}$.

Thus we can conclude that for all $CP_1 < CP_2 : f(CP_1) \leq f(CP_2)$. In other words, $f(CP)$ is a monotonic function. \square

A.2. Proof of Lemma 6.2

Lemma A.2. *The function $f : \mathbb{R} \rightarrow \mathbb{R}$ with $f(CP) = \min_t (W'_{\text{bal}}(t)|_{CP})$ is strictly increasing for $CP < \max_{t \in [0, T]} \{P(t)\}$*

Proof. We already know from the previous lemma that $f(CP)$ is a monotonically increasing function. This time we take arbitrary $CP_1 < CP_2 < \max_{t \in [0, T]} \{P(t)\}$.

Denote with $t^* = \operatorname{argmin}_t \{P(t)\} = t_{i^*}$ for some $i^* \in [1, N]$. Now note that at time t_{i^*+1} we have that $W'_{\text{bal}}(t_{i^*+1}) < W'$, because $W'_{\text{bal}}(t_{i^*}) \leq W'$, $P(t_{i^*}) > CP$ and $\frac{dh_1}{dx} > 0$.

Denote $I^* = \{i \in [1, N] : W'_{\text{bal}}(t_i)|_{CP_1} = \min_{t \in [0, T]} \{W'_{\text{bal}}(t)|_{CP_1}\}$. Notice that $1 \notin I^*$ due to the last argument which yields that $\min\{W'_{\text{bal}}(t)\} < W'$.

Take an arbitrary $i \in I^*$ and note that $W'_{\text{bal}}(t_{i-1})|_{CP_1} \leq W'_{\text{bal}}(t_{i-1})|_{CP_2}$. Furthermore, note that because for all $i \in I^*$ the value of $W_{\text{bal}}(t)$ is minimal at t_i and thus we have that $P(t_{i-1}) < CP_1 < CP_2$.

Therefore, we have

$$\begin{aligned} W'_{\text{bal}}(t_i)|_{CP_1} &= W'_{\text{bal}}(t_{i-1})|_{CP_1} - h_1(P(t_{i-1}) - CP_1) \\ W'_{\text{bal}}(t_i)|_{CP_2} &= W'_{\text{bal}}(t_{i-1})|_{CP_2} - h_1(P(t_{i-1}) - CP_2) \end{aligned}$$

Following the claims of the previous proof, we can once more state that $P(t_{i-1}) - CP_1 > P(t_{i-1}) - CP_2$ and because h_1 has a strictly positive derivative we conclude $h_1(P(t_{i-1}) - CP_1) > h_1(P(t_{i-1}) - CP_2)$. Now that yields that for all $i \in I^* : W'_{\text{bal}}(t_i)|_{CP_1} < W'_{\text{bal}}(t_i)|_{CP_2}$. Thus, due to the construction of I and the knowledge that $f(CP)$ is a monotonically increasing function, we conclude that $f(CP_1) < f(CP_2)$. \square

A.3. Proof of Lemma 6.3

Lemma A.3. *The function $f : \mathbb{R} \rightarrow \mathbb{R}$ with $f(CP) = \min_t (W'_{\text{bal}}(t)|_{CP})$ is continuous.*

Proof. Suppose that we have arbitrary $W' > 0$, $P(t) \geq 0$ for $t \in [0, T]$ and the formulas $h_1(x)$ and $h_2(x)$ that satisfy $h_j \geq 0$ for $j = 1, 2$, and $0 < \frac{dh_1}{dx} < M$, and $0 \leq \frac{dh_2}{dx} < M$ as in Definition 6.1.

Denote $I^* = \{i \in [1, N] : W'_{\text{bal}}(t_i) = \min_{t \in [0, T]} \{W'_{\text{bal}}(t)\}$ and take $i^* = \min I^*$.

Now denote with $I_x^+ := \{i \in [1, i^*] : P(t_i) > x\}$, $I_x^- := \{i \in [1, i^*]\}$ and $I_x^0 := \{i \in [1, i^*] : P(t_i) = x\}$.

Take an arbitrary $c \in \mathbb{R}$ and pick δ_1 such that $I_{c+\delta_1}^+ = I_{c-\delta_1}^+$ and $I_{c+\delta_1}^- = I_{c-\delta_1}^-$. This is possible because the set $\{P(t_i) : i \in [1, i^*]\}$ is finite. Furthermore, pick $\delta_2 = \frac{\epsilon}{T \cdot M}$ in which M is the bound on the derivatives of $h_1(x)$ and $h_2(x)$. Finally, take $\delta < \min\{\delta_1, \delta_2\}$.

Now, under the hypothesis that $|x - c| < \delta$, we show that $|f(x) - f(c)| < \epsilon$. Without loss of generality we assume that $x > c$, such that we can use the monotonicity of $f(CP)$.

$$\begin{aligned} |f(x) - f(c)| &= f(x) - f(c) \\ &= \min_t \{W'_{\text{bal}}(t)|_x\} - \min_t \{W'_{\text{bal}}(t)|_c\} \\ &\leq W' + \sum_{t_i: i-1 \in I_c^+} h_2(x - P(t_i)) - \sum_{t_i: i-1 \in I_c^-} h_1(P(t_i) - x) - W' - \sum_{t_i: i-1 \in I_c^+} h_2(c - P(t_i)) + \sum_{t_i: i-1 \in I_c^-} h_1(P(t_i) - c) \\ &= \sum_{t_i: i-1 \in I_c^+} [h_2(x - P(t_i)) - h_2(c - P(t_i))] - \sum_{t_i: i-1 \in I_c^-} [h_1(P(t_i) - x) - h_1(P(t_i) - c)] \\ &\leq h \cdot |I_c^-| \cdot |x - c| \cdot M - h \cdot |I_c^-| \cdot |x - c| \cdot M \\ &\leq |T| \cdot |x - c| \cdot M \\ &< |T| \cdot M \cdot \delta \\ &\leq \epsilon \end{aligned}$$

\square

A.4. Proof of Theorem 6.1

Theorem A.1. *The definition of CCP is well defined, i.e. there is a unique value CCP for which $f(CCP) = \min_{t \in [0, T]} \{W'_{bal}(t)|_{CCP}\} = 0$.*

Proof. Lemma 6.3 yields that the function $f(CP)$ is continuous. Furthermore, we know that $f(\max_{t \in [0, T]} \{P(t)\}) \geq W' > 0$.

For a value of $CP < 0$, it yields that $P(t) > CP$ for all $t \in [0, T]$, because $P(t) \geq 0$. Therefore, for $CP < 0$, we have $f(CP) = W' - \sum_{i=1}^N h_1(P(t_{i-1}) - CP) \geq W' - \sum_{i=1}^N h_1(-CP)$. Now because the first derivate of h_1 is strictly positive, we can choose CP so small such that $\sum_{i=1}^N h_1(-CP) > W'$ and thus such that $f(CP) < 0$.

Because $f(CP)$ is continuous, $f(\max_{t \in [0, T]} \{P(t)\}) > 0$ and for a small enough CP we have that $f(CP) < 0$, we know that $f(CP)$ attains the value 0 at least once.

Furthermore, Lemma 6.2 yields that $f(CP)$ is strictly increasing for $CP < \max_{t \in [0, T]} \{P(t)\}$, which yields that $f(CP)$ reaches each value exactly once, i.e. there is a unique value CCP such that $f(CCP) = 0$. \square

B

Behaviour of LASSO-parameters.

As stated in Chapter 7, the LASSO-parameters behaved unexpectedly when five different training attributes were taken into account in the analysis. This is visualized in the Figure B.1, where the values of α_m are visualized for different values of γ . Remember that these are the values of α_m satisfying equation:

$$\min_{C, \alpha_m} \left\{ \frac{1}{N} \sum_{n=1}^N \left(y(i) - C - \sum_{m=1}^M \alpha_m V(i) \right)^2 + \gamma \sum_{m=1}^M |\alpha_m| \right\} \quad (\text{B.1})$$

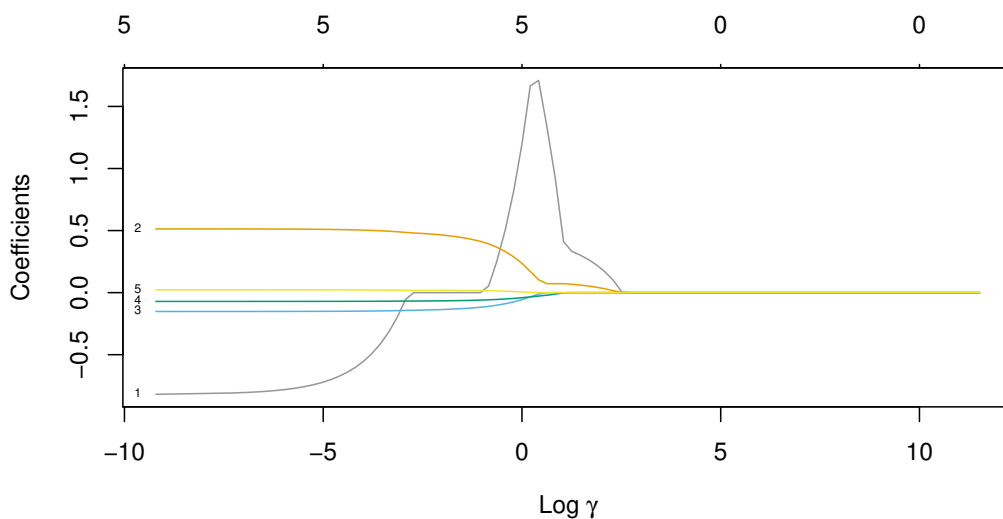


Figure B.1: The values of α_m plotted against the log-value of γ for cyclist 2 and fixed kernel parameters.

The unexpected behaviour is the fact that the value of $\alpha_1 = 0$ for $\gamma \in [0.07, 0.35]$, but $\alpha_1 \neq 0$ for $\gamma \in [0.36, 12]$. This is unexpected because for a higher γ , the absolute value of α_1 is penalized harder, thus for an increasing γ we would expect α_1 to remain zero after it has been set to zero. Only when other values of $|\alpha_m|$ are dropping, could a rise in α_1 be plausible, but if we look at Figure B.2, we can see that $\sum_{m=1}^M |\alpha_m|$ is increasing.

This is illogical, because if we would take the values of α_m for $\gamma = 0.35$ and used those to estimate the CCP for $\gamma = 12$, the total MSE would remain equal, while the total penalty would be less than what the LASSO-method yields.

So apparently, something is going wrong. The calculations were performed with two different R-packages, `glmnet` and `ncvreg`, but both yielded the exact same results. A recent study [8] has stated that, although a lot of applications of the LASSO use correlated predictors, the influence of correlation is still unknown. In this study they research the influence of correlated predictors on the prediction and conclude that this influence is

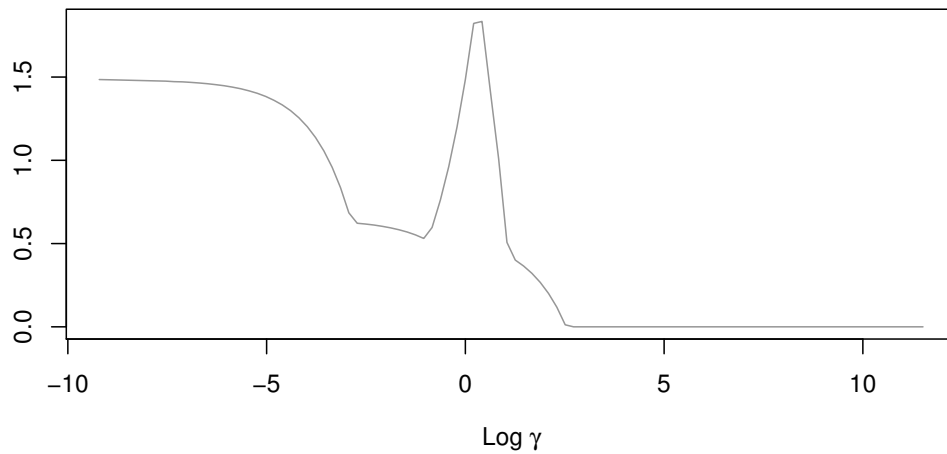


Figure B.2: The sum of the absolute values of α_m plotted against the log-value of γ for cyclist 2 and fixed kernel parameters.

negligible. In Figure B.3 we can see that the correlations between the predictors are high, especially between kJ and TSS, and kJ and duration.

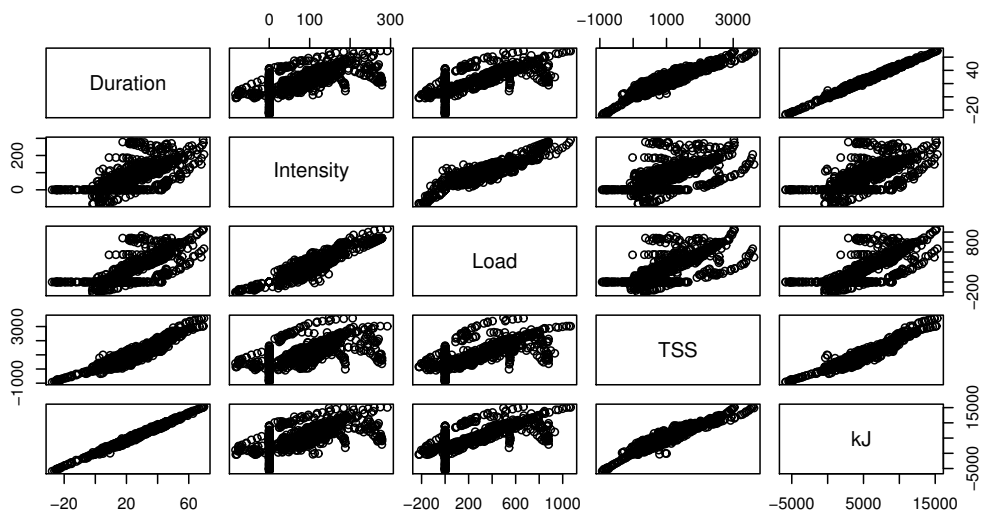


Figure B.3: Correlations between the different values of $V_m(t)$ for the fixed kernel parameters

In light of this, we expect that the correlations among the predictors result in the unexpected behaviour of the LASSO-parameters, probably due to numerical instability in the algorithm, but unfortunately we did not have the time to further investigate what exactly is going wrong.

C

Figures of final model.

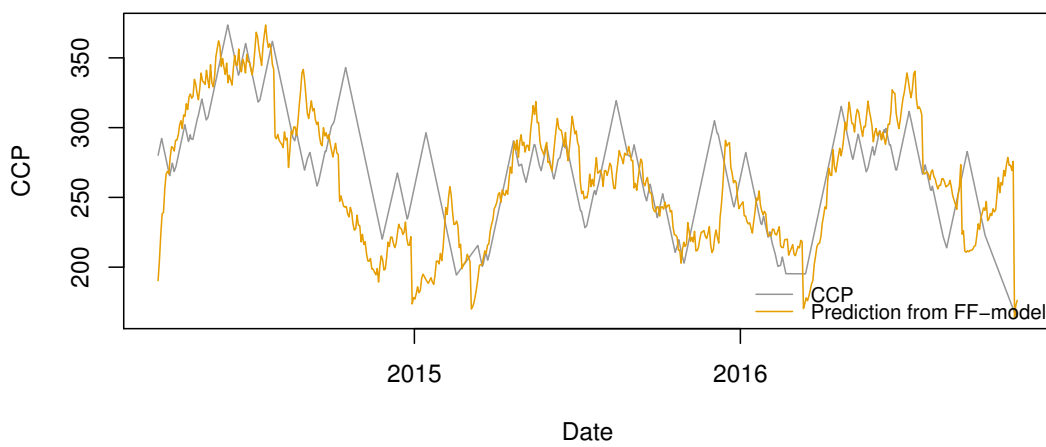


Figure C.1: Cyclist 1 - The value of CCP over time plotted together with the predicted value of CCP as by the Fitness-Fatigue model, using the parameters shown in Table 7.5.

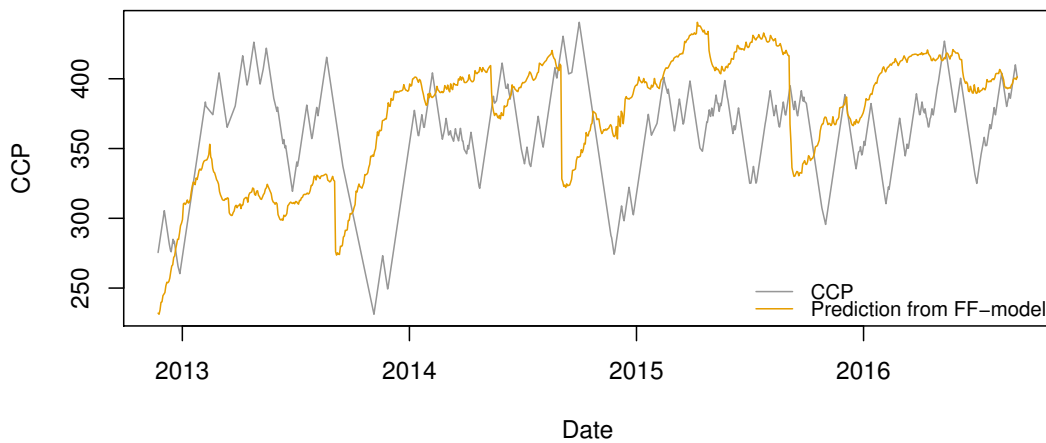


Figure C.2: Cyclist 2 - The value of CCP over time plotted together with the predicted value of CCP as by the Fitness-Fatigue model, using the parameters shown in Table 7.5.

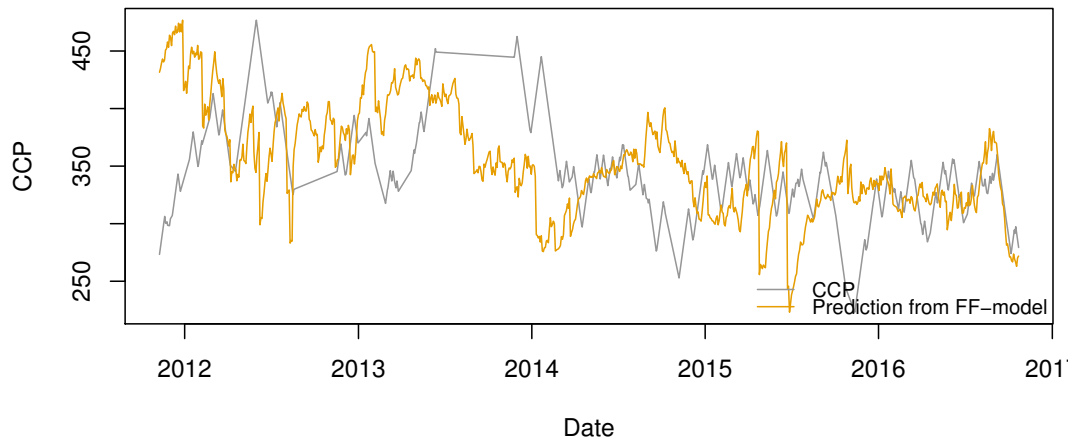


Figure C.3: Cyclist 3 - The value of CCP over time plotted together with the predicted value of CCP as by the Fitness-Fatigue model, using the parameters shown in Table 7.5.

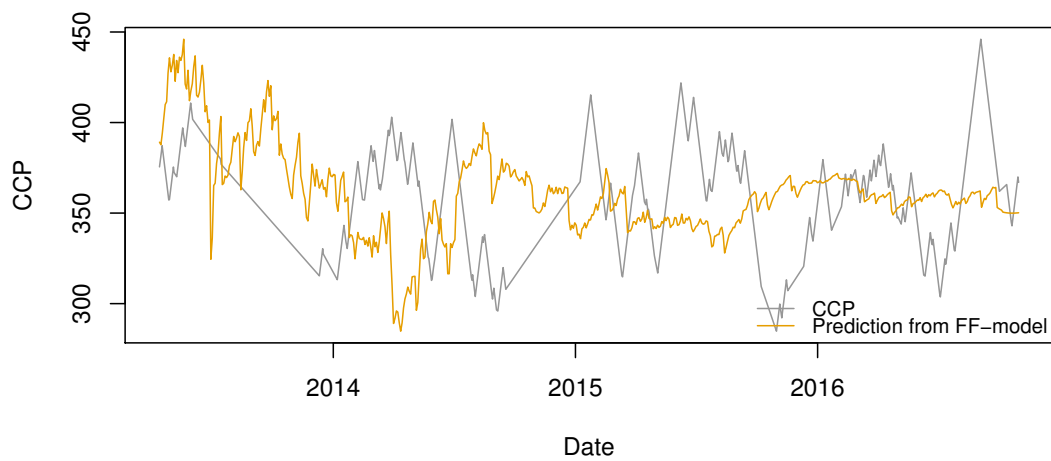


Figure C.4: Cyclist 4 - The value of CCP over time plotted together with the predicted value of CCP as by the Fitness-Fatigue model, using the parameters shown in Table 7.5.

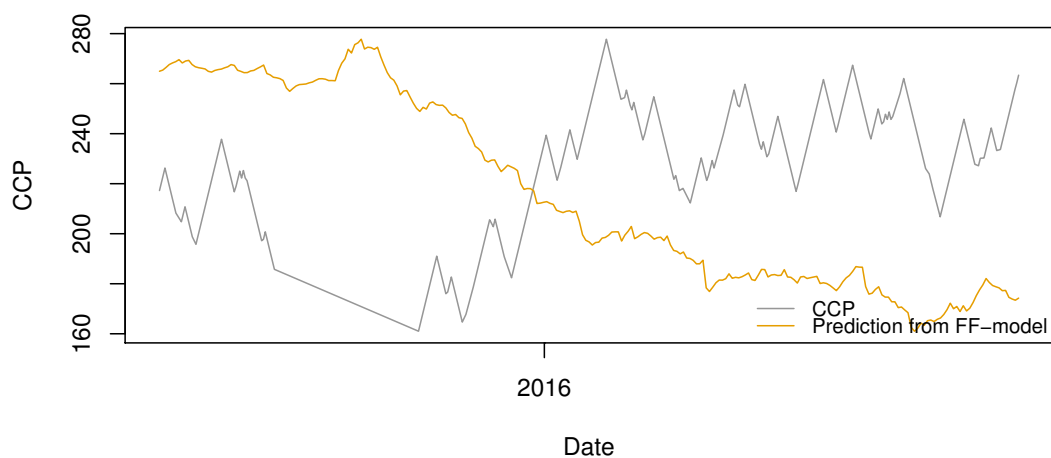


Figure C.5: Cyclist 5 - The value of CCP over time plotted together with the predicted value of CCP as by the Fitness-Fatigue model, using the parameters shown in Table 7.5.

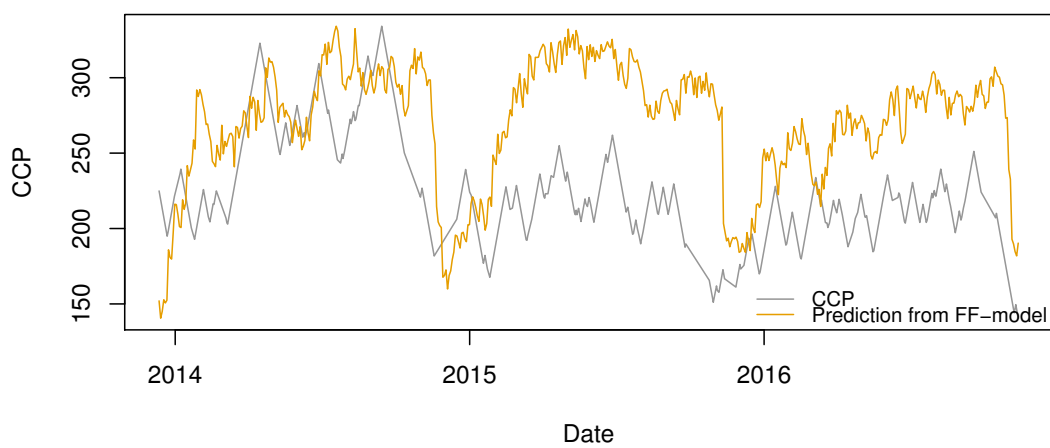


Figure C.6: Cyclist 6 - The value of CCP over time plotted together with the predicted value of CCP as by the Fitness-Fatigue model, using the parameters shown in Table 7.5.